



Recent progress on flexible and stretchable piezoresistive strain sensors: From design to application



Lingyan Duan^a, Dagmar R. D'hooge^{b,c,*}, Ludwig Cardon^{a,*}

^a Centre for Polymer and Material Technologies, Department of Materials, Textiles and Chemical Engineering, Ghent University, Technologiepark 130, B-9052 Zwijnaarde (Ghent), Belgium

^b Laboratory for Chemical Technology, Department of Materials, Textiles and Chemical Engineering, Ghent University, Technologiepark 125, B-9052 Zwijnaarde (Ghent), Belgium

^c Centre for Textile Science and Engineering, Department of Materials, Textiles and Chemical Engineering, Ghent University, Technologiepark 70A, B-9052 Zwijnaarde (Ghent), Belgium

ARTICLE INFO

Keywords:

Flexible and stretchable sensors
Sensing mechanism
Geometric engineering
Conductive polymer composites
Performance optimization
Structural design

ABSTRACT

Flexible and stretchable piezoresistive strain sensors which can translate mechanical stimuli (strain changes) into electrical signals (resistance changes) provide a simple and feasible detection tool in the field of health/damage monitoring, human motion detection, personal healthcare, human-machine interfaces, and electronic skin. Herein a detailed overview is presented on both strategies for sensing performance improvement and progress to medium or large-scale fabrication. A broad range of matrices/substrates and incorporated nanomaterials is covered and attention is paid to the current state-of-the-art of feasible but low-cost manufacturing methods. The sensor design parameters include sensitivity (gauge factor), stretchability, linearity, hysteresis, biocompatibility, and self-healing potential. Starting from fundamental sensing mechanisms, *i.e.* the tunneling effect, the disconnection mechanism, and the crack propagation mechanism, examples are provided from lab to application scale.

1. Introduction

Flexible and stretchable sensor devices have attracted tremendous attention in recent years, due to their various promising applications, including structural health and damage monitoring [1–5], human motion detection [6,7], personal healthcare [6,8–13], human-machine interfaces [14–17], electronic skin [18–20], and soft robotics [21]. A further distinction can be made between piezoresistive [22], capacitive [23], piezoelectric [24], field effect transistor [25], fiber Bragg gratings (FBGs) [26], Raman shift [27], liquid metal [28], and triboelectric [29] based sensor devices, showcasing the versatility and relevance of the sensor research field.

One of the strengths of flexible and stretchable sensor devices is the feasibility to address both low and high strain levels [30]. For applications aiming at large deformation or intimate integration with irregular surfaces, the conventional metal sensors, which sustain only maximum strains of *ca.* 5% [31], and inorganic semiconductor materials are limited by their intrinsic brittle and rigid nature, low sensitivity, low fatigue life, environmental dependence, and poor biocompatibility.

Specifically conductive polymer composite (CPC) based sensors have been developed in the last decades [32–37]. Very promising are piezoresistive CPC based strain sensors, since they exhibit great merits such as a rather simple fabrication process, a rather

* Corresponding authors at: Laboratory for Chemical Technology, Department of Materials, Textiles and Chemical Engineering, Ghent University, Technologiepark 125, B-9052 Zwijnaarde (Ghent), Belgium (D.R. D'hooge).

E-mail addresses: dagmar.dhooge@ugent.be (D.R. D'hooge), ludwig.cardon@ugent.be (L. Cardon).

<https://doi.org/10.1016/j.pmatsci.2019.100617>

Received 16 January 2018; Received in revised form 10 November 2019; Accepted 10 November 2019

Available online 11 November 2019

0079-6425/ © 2019 Elsevier Ltd. All rights reserved.

Nomenclature			
<i>Roman symbols</i>			
A	cross-sectional area (m ²)	FGS	fragmentized graphene sponges
L	length (m)	FSG	fish-scale-like graphene
m/m	mass ratio (-)	GF	gauge factor (-)
R	electrical resistance (Ω)	GWF	graphene woven fabric
<i>Greek symbols</i>		IL	ionic liquid
ε	strain (-)	ILBW	ionic-liquid-based wavy
ρ	electrical resistivity (Ω·m)	MWCNTs	multi-walled carbon nanotubes
τ	time constant (s)	LPG	laser patterned graphene
ν	Poisson's ratio (-)	NaCl	sodium chloride
<i>Abbreviations</i>		NR	natural rubber
AFM	atomic force microscope	OBC	olefin block copolymer
AgNPs	silver nanoparticles	PANI	polyaniline
AgNWs	silver nanowires	PDMS	polydimethylsiloxane
[BMIM][BF ₄]	1-butyl-3-methylimidazolium tetrafluoroborate	PEDOT:PSS	poly(3,4-ethylenedioxythiophene): poly(styrene sulfonate)
CB	carbon black	POE	polyolefin elastomer
CNTs	carbon nanotubes	PP	polypropylene
CPCs	conductive polymer composites	PPy	polypyrrole
CSF	carbonized silk fabric	PVC	poly (vinyl chloride)
CuNWs	copper nanowires	PVDF	poly (vinylidene fluoride)
DI	deionized water	rGO	reduced graphene oxide
EG	ethylene glycol	SBCs	styrenic block copolymers
FBGs	fiber Bragg gratings	SBR	styrene-butadiene rubber
FDM	fused deposition modelling	SBS	poly(styrene- <i>block</i> -butadiene- <i>block</i> -styrene)
		SEBS	styrene-ethylene/butylene-styrene triblock copolymer
		SEM	scanning electron microscopy
		SPX	spandex
		SWCNTs	single-walled carbon nanotubes
		TPU	thermoplastic polyurethane
		TPV	thermoplastic vulcanizate

uncomplicated sensor configuration, a relatively simple read-out system, a potential high flexibility and stretchability, and acceptable dynamic properties. The other strain sensor types mentioned are still faced with numerous challenges such as sophisticated measurement equipment, low resolution, and poor to intermediate dynamic performance. In view of the above statements, the present contribution is only focused on flexible and stretchable CPC based piezoresistive strain sensors.

In piezoresistive CPC based strain sensors, the change of electrical parameters under deformation is monitored as a signal for environmental mechanical stimuli. One of the most critical aspects for sensor design is the choice of suitable materials for the fabrication of flexible strain sensors that meet the sensing, mechanical and structural requirements imposed by a particular application. For numerous CPCs with incorporated conductive fillers or devices embedded with conductive thin film layers, the polymer matrices/substrates and/or encapsulation materials are the stretchable component. However, these piezoresistive materials are still facing some challenges, including unsuitability for small strain monitoring due to rather low sensitivity [38–40], degradation of sensing performance by fatigue, and plastic deformation of the polymer substrate. Other aspects are inevitable resistance hysteresis between the loading and unloading curves ascribed to the intrinsic viscoelastic nature of the polymer matrix, internal friction of the composites, and unstable mechanical integrity during large cyclic deformation, which inhibits long-term use.

As flexible support materials the most commonly employed polymers are rubbers/elastomers, such as silicone-based rubber (e.g. polydimethylsiloxane (PDMS) [41–44] and Ecoflex (SMOOTH-ON) [39,45]), thermoplastic polyurethane (TPU) elastomer [38,46–49], styrenic block copolymers (SBCs) [50–56], natural rubber (NR) [57–59], styrene-butadiene rubber (SBR) [58,60], and polyolefin elastomer (POE) [61,62]. Polypropylene (PP) [63,64], polyvinylidene fluoride (PVDF) [65,66], and epoxy [67–71] have also been considered. The conductive materials typically contain carbon-based micro/nano-phases (e.g. carbon nanotubes (CNTs) [46,47], carbon black (CB) [46,62], and graphene [47,59,72]), metal nanowires [40,73,74], nanoparticles [50,55], nanosheets [75], conductive polymers (e.g. polypyrrole (PPy) [76], polyaniline (PANI) [74,77], and poly(3,4-ethylenedioxythiophene): poly(styrene sulfonate) (PEDOT:PSS) [73]), ionic liquid (IL) [78,79], and liquid metals [80]. Hybrid materials such as multi-walled carbon nanotubes (MWCNTs)/CB hybrid fillers [46,65], MWCNTs/graphene bifillers [47], silver nanowire/graphene hybrid particles [40], and silver nanoparticle (AgNP)/single-walled carbon nanotubes (SWCNTs) composite [81] have also been employed. Alternatively, the device stretchability is achieved by geometric engineering of the conductive materials with special structures such as the wrinkled [82,83], thickness-gradient [41], double helical [84], buckled [85,86], wavy [87], accordion [88], coiled [89], serpentine pattern [90], nanomesh [91], network [92], and island-bridge structure [93] accommodating the strain.

Ideally, the stretchability requirements can be quite varied so that the sensing device application range becomes broad. For

sensing devices integrated directly onto joint skins [94,95] or embedded into clothing or textiles [96,97] for movement and load measurements, high strain implementations are typically requested. In contrast for applications such as tiny skin motion detection (e.g. phonation [98] and facial expression [15]) or personal healthcare with subtle strain induced by respiration [99] and heartbeat [100], small but repetitive strain cycles or moderate one-time strains tolerances are required [37]. Essentially, the stretchability relies on the robustness of the conductive network that provides electronic transmission paths and the stretchable limitations of the loaded materials [101].

For the actual application, the flexible strain sensors need also to be assembled in a highly-integrated system composed of several artificial intelligence modules, including power supply, signal detection, data processing, analysis, transmission, and display modules [102]. Undoubtedly, numerous challenging issues related to reliability, reproducibility, robustness, long-term monitoring capability, and the complexity to achieve fully-integrated sensor systems for highly accurate detection still exist. A strong multidisciplinary character is thus obtained, requiring combined knowledge from for instance materials science, electronics, measurement methods, mechanics, system and chemical engineering. As an essential part, the fabrication processes are supposed to be cost-effective and scalable. However, most current fabrication techniques are still premature and the most as-prepared flexible sensors are still in their prototype stage [102].

The present contribution provides a detailed overview of recent advances for research on flexible and stretchable (piezoresistive)

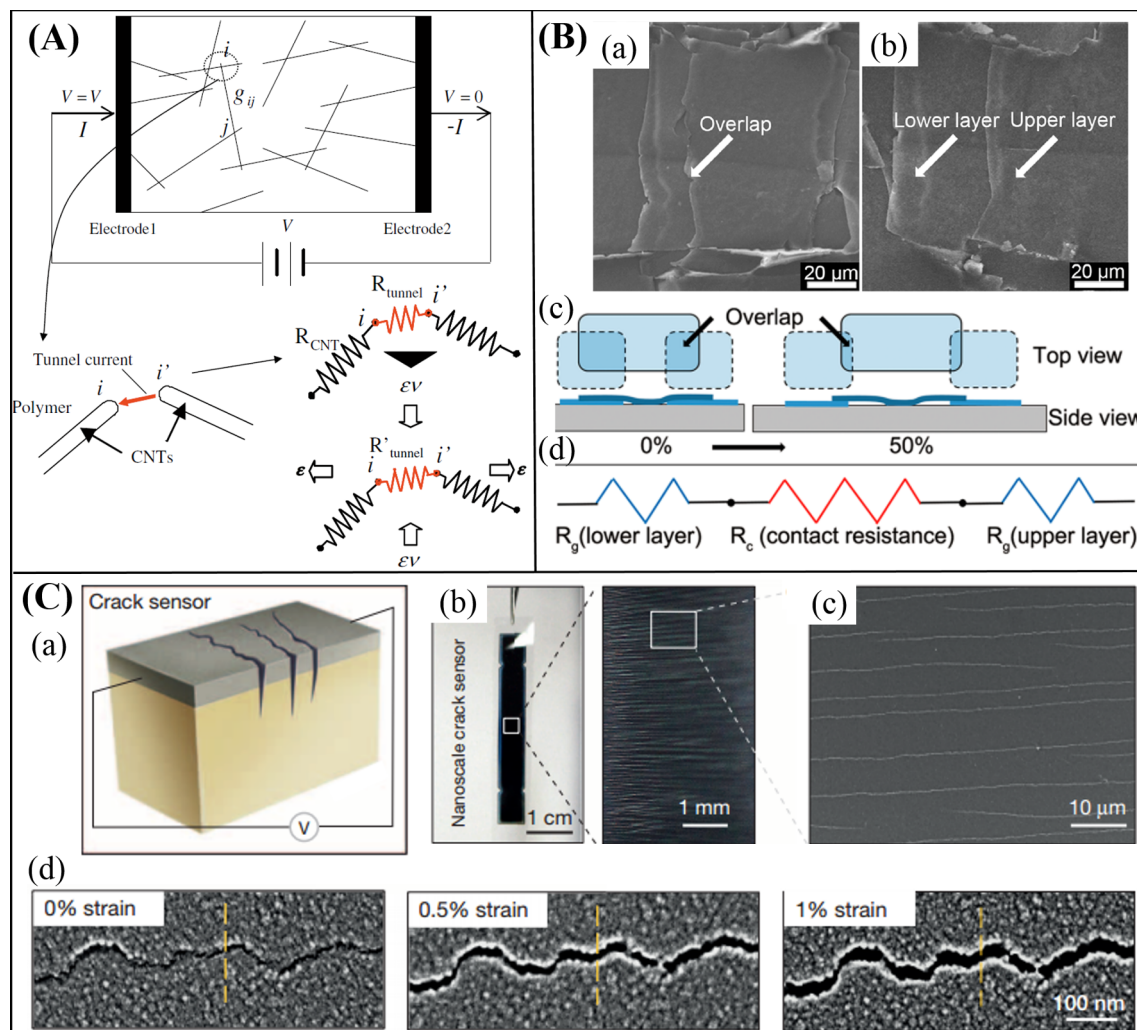


Fig. 1. Strain sensing mechanisms: (A) Schematic view of CNT conductive network including tunneling effect/mechanism [106]. (B) Disconnection mechanism with (a) SEM image of a fish-scale-like graphene-based (FSG) strain sensor at 0% strain; the white arrows indicate two overlapping rGO slices; (b) SEM image of a FSG strain sensor at 50% strain; (c) schematic illustration of the reduction of overlapped area of fish-scale-like graphene-based strain sensor upon stretching; (d) schematic illustration of the resistance model of a sensing unit [7]. (C) Crack propagation mechanism with (a) illustration of crack-based ultrasensitive strain sensor; (b) left, image of the spider-inspired sensor with a cracked layer; right, enlarged image of the cracks in the surface; (c) SEM image of the boxed region of the right-hand image in (b); (d) SEM images of the zip-like crack junctions for different applied strains [111].

strain sensors, with emphasis on both strategies for sensing performance improvement and progress to medium or large-scale fabrication. It should be stressed that the relevance and novelty of the review relates to this combined description of these two research achievements.

Attention is focused on the sensing mechanism, sensing performance, and the related optimization or design strategies. Building blocks and their assembled structures are covered and comparisons of recently reported results to effectively guide the selection of appropriate materials and structure design are incorporated. Feasible low-cost manufacturing methods to implement scale-up, promising applications and application sensing platforms are also covered in detail. Finally, challenges and perspectives for future research in view of industrial realization are presented.

2. Fundamental sensing mechanisms

Generally, the sensing function of a sensor material or its working principle originates from the variation of resistance R under deformation. The resistance is given by $\rho l/A$, with ρ , l , and A the (electrical) resistivity, length, and cross-sectional area. The relative change in resistance $\Delta R/R$ is expressed as $(1 + 2\nu)\varepsilon + \Delta\rho/\rho$, with ν and ε Poisson's ratio and strain [103].

Change in the resistance of materials caused by structural deformation is known as piezoresistivity. In principle, the geometry changes caused by structural deformation of the bulk material and the piezoresistivity of the conductive materials themselves contribute to the observed change of the CPC resistance [104]. However, the impact of stress induced deformation of nanomaterials [105] can be negligible with respect to the macroscale composite strain upon stretching. The latter is ascribed to the poor stress transfer [32] due to the typically large elastic mismatch and weak interfacial adhesion strength between them [104]. In other words, the effect of the piezoresistivity of conductive nanomaterials on the total resistance change in CPCs strain sensors can be marginal [32,104,105].

Conductive filler networks within an insulated polymer matrix are proposed to be obtained not only by the perfectly contacted inter-fillers, but also by neighboring fillers within a certain cut-off distance to allow electrons to path through polymer thin layers and form quantum tunneling junctions [104,106] (Fig. 1A). Upon stretching, the increase of resistance is ascribed to several aspects, including the breakup of the conductive pathway or the loss of contact between neighboring fillers, and the increase in the inter-filler distance. The dominant working principle in the case of CPCs strain sensors arises here from the change in the tunneling resistance [106]. This sensing mechanism is therefore elaborated as a tunneling effect [104].

In addition, the disconnection mechanism has been put forward [104]. This sensing principle is elaborated for thin films made of a nanomaterial conductive network (e.g. silver nanowires (AgNWs) [107] and graphene [7]), in which electrons can pass through overlapping nanomaterials within the percolation network. If stretching is applied, the electrical connection or the overlapping area of adjacent nanomaterials decreases (Fig. 1B), leading to the increase of contact resistance [7]. The decrease of the overlapping area is caused by the slippage of adjacent nanomaterials, mainly due to the low friction between overlapping nanomaterials [7], weak interfacial binding, and large stiffness mismatch between the conductive nanomaterials and stretchable polymers [7,104,107]. For few strain sensors with special connection characteristics such as reversibly interlocked microdome [108], interlocked nanofibers [109], or gecko-inspired microstructure [110], the change in effective contact areas or sites of the microstructure essentially contributes to the change of resistance, rather than the disconnection between overlapped conductive nanomaterials [104,108–110].

For strain sensors with brittle nanomaterial thin films coated on flexible substrates, nano/micro cracks intend to initiate at the stress concentrated areas to release the accommodated stress. If strain is applied, the rapid separation of adjacent crack junctions (Fig. 1C) critically limits the electrical conduction through the thin film [104,111], which then substantially promotes the significant increase of resistance. Meanwhile, the crack-based strain sensors are based on reversible disconnection and reconnection of cracks [40,98,104,112,113]. This crack propagation mechanism [104] has been increasingly employed to develop ultrahigh sensitive and stretchable strain sensors [39,40,81,98,111,112,114,115], as explained in detail below. The crack configuration, length, width, density, cracked-area [39], and the depth [112] are critical factors that influence the final sensing performance and working range.

3. Sensor design parameters

To allow for sensor design control over several parameters is needed. In this section, a detailed discussion is included related to the key design variables with main focus on the sensitivity (or gauge factor) and stretchability. In addition, the discussion is complemented with novel design variables (e.g. biocompatibility) that emerged during the last decades. Finally, attention is paid to the multisensitive design in view of recent developments.

3.1. Sensitivity or gauge factor

The sensitivity or gauge factor (GF) reflects the capacity of active materials for appropriate responses to external mechanical stimuli. It is considered as the most important design parameter, especially for subtle displacement or structural damage detection. For resistive-type of strain sensors, the sensitivity/GF is quantified as the instant ratio of the relative change in electrical resistance to the applied strain [41,78,102,104,116]. Note that the strain range for which the GF is determined needs to be specified to avoid a biased interpretation. However, in some studies this information is lacking and/or a single point GF is only specified.

The GF value varies greatly, depending on the active materials, assembled structures, and the piezoresistive mechanism. The sensitivity is also very dependent on the applied strain, as non-linear behavior is frequently obtained [58] (cf. Section 3.3). It is important to point out that GFs have been calculated in a discrete strain interval in most research studies to facilitate the comparison

of the samples although there is strictly a non-linear tendency [117].

With CPCs the performance depends on the type, content, dispersion, and morphology of the fillers, and the interaction between fillers and polymer matrix. CPCs with a filler concentration near the electrical percolation threshold generally show the largest variation in electrical resistance, whereas operation very close to the percolation threshold has a detrimental impact on device-to-device reproducibility [118]. The key point for sensitivity improvement typically based on the tunneling effect is to increase the tunneling resistance or the proportion of the tunneling resistance with respect to the total resistance, hence, not the total resistance itself [65,106].

The sensitivity has been tuned by conductive network morphological control strategies [119]. For example, Ke et al. [65] achieved tunable electrical conductivity and strain sensitivity by changing the mass ratio of CNTs to CB ($m_{\text{CNTs}}/m_{\text{CB}}$), which resulted in a change of the conductive network structure in PVDF/MWCNTs/CB composites. Lower $m_{\text{CNTs}}/m_{\text{CB}}$ ratios contributed to higher sensitivity upon comparison at similar electrical resistivity or same total filler content. For a hybrid filler system with lower CNT contents, the conductive network consists of a special structure with CNT acting as backbone for conductive pathways and parts of CB particles located between the gaps of neighboring CNTs. Such a conductive assembly is more susceptible to tensile strain than those consisting of only CNTs. During stretching, the bridging effect of CB is weakened and the distance between CB particles and CNTs is increased. This induced increase in the tunneling resistance and thus alters the GF at low strain levels.

Besides, strain sensitivity can be controlled by adopting processing procedures, as for instance explored in the research of Ma et al. [120] by comparing one-step and two-step processing methods for conductive elastomeric materials based on MWCNTs filled thermoplastic vulcanizate (TPV). Although a comparable initial conductivity is obtained, the one-step-TPV shows a high GF of ca. 10^3 at a strain of 100%, while the resistance for the two-step TPV composite is independent with strain, even at a strain of 200%. This superior behavior has been ascribed to the much higher destruction rate of the more disordered MWCNTs conductive network in one-step-TPV. In addition, strong interfacial binding between elastic nanomaterials (e.g. CNT [46,121] and graphene [122]) and polymers also gives higher strain sensitivity.

A very effective way to achieve a high sensitivity is to allow for substantial connection or structural changes even under small strain. Within this respect crack-assisted resistive strain sensors have been aimed at [39,40,81,98,111,112,114,115], inspired by the crack-shaped slit organs of spiders [111]. For example, Liao et al. [115] recently developed an ultrasensitive and stretchable microcrack-assisted resistive strain sensor by using silver nanowires on patterned PDMS. The remarkable sensitivity (GF of 1.5×10^5 within 60% strain range) was attributed to the introduction of a patterned surface microstructure, consisting of regular and remarkably uniform parallel concave lines and square plat arrays in the patterned PDMS substrate. The parallel concave lines interweaved with each other and the features could be replicated and identified with high quality. Notably, many microcracks have been observed inside parallel concave lines and square plats [115]. Similarly, an ultrasensitive cracking-assisted strain sensor fabricated by Chen et al. [40] exhibits a GF as high as 2×10^5 (strain between 0 and 0.3%), 10^3 (strain between 0.3 and 0.5%), and 4×10^3 (strain between 0.8 and 1%). This work illustrates a strategy to fabricate an ultrahigh sensitive strain sensor for subtle deformation detection applications such as heartbeat monitoring, pulse beat detection, and sound signal recognition. Furthermore, it has been indicated that fragmented SWCNT paper embedded in PDMS can sustain its sensitivity even at very high strain levels. A (single point) GF of over 10^7 is obtained at 50% strain [114]. Generally, the cracks are generated by pre-stretching [39,40,98,114,115] (Fig. 2A), thermal solvent evaporation, and thermally induced stress during a cooling step [81] (Fig. 2B) or bending [112] (Fig. 2C). More information related to cracking-assisted nanofabrication techniques can be found in the review of Kim et al. [123].

In addition to crack-assisted strain sensors, bio-inspired interlocked microstructure geometries [108,109,124,125] (Fig. 3A), whisker structures [126,127] (Fig. 3B), silk [128,129] (Fig. 3C) and cotton fabric [130] molded structures, and 2D/3D micro/nanostructures [110,131–133] (Fig. 3D) have also been employed to improve the performance of sensors [131–133] as well as to introduce multiple sensing capabilities [108,109,126,127]. For instance, inspired by the interlocked epidermal-dermal layers in human skin, the PDMS/MWCNTs tactile sensor developed by Park et al. [108] showed high sensitivity in distinguishing various mechanical stimuli, considering opposing conductive interlocked microdome arrays (Fig. 3A). The high sensitivity has been attributed to the considerable increase in the resistance resulting from the large decrease of contact area between the microdomes [108]. Similarly, bioinspired e-whisker arrays (Fig. 3B) with good strain sensitivity (GF of 3.4×10^5), fast response (50 ms), and high durability/stability have been developed by Hua et al. [127] via pencil-drawn paper. The e-whisker array sensor demonstrates good performances on strain monitoring, 3D spatial mapping, and detailed localization of objects, orientation, and shape reconstruction [127].

3.2. Stretchability

In the traditional field, such as structural health monitoring, relatively low stretchability below 1% is sufficient. However, for flexible and stretchable electronic devices that need to be bonded to substrates with complex topography without becoming wrinkled, a higher stretchability (e.g. $> 50\%$, for skin-attachable and wearable strain sensors [134]) and thus a wider working range is required. Essentially, the stretchability of the sensing device relies on the robustness of the conductive network that preserves the interconnectedness under global strain. The stretchability has been enhanced by means of either adopting stretchable materials (first approach) or structural conversion (second approach).

The first approach relies on the exploration of intrinsic stretchable materials as the elastic polymer matrix. Several kinds of active component, especially 1-dimensional (1D) [134] or 2D nanomaterials [39,135] with high-aspect-ratio such as CNTs [46,47,51,55,136], metallic nanowires [73,107], and graphene [58,72] or graphite [39], have therefore been mixed into an elastomeric matrix [46,47,51,58,72]. They also have been integrated within [50,107,136] or on the top [39,107] of elastomeric

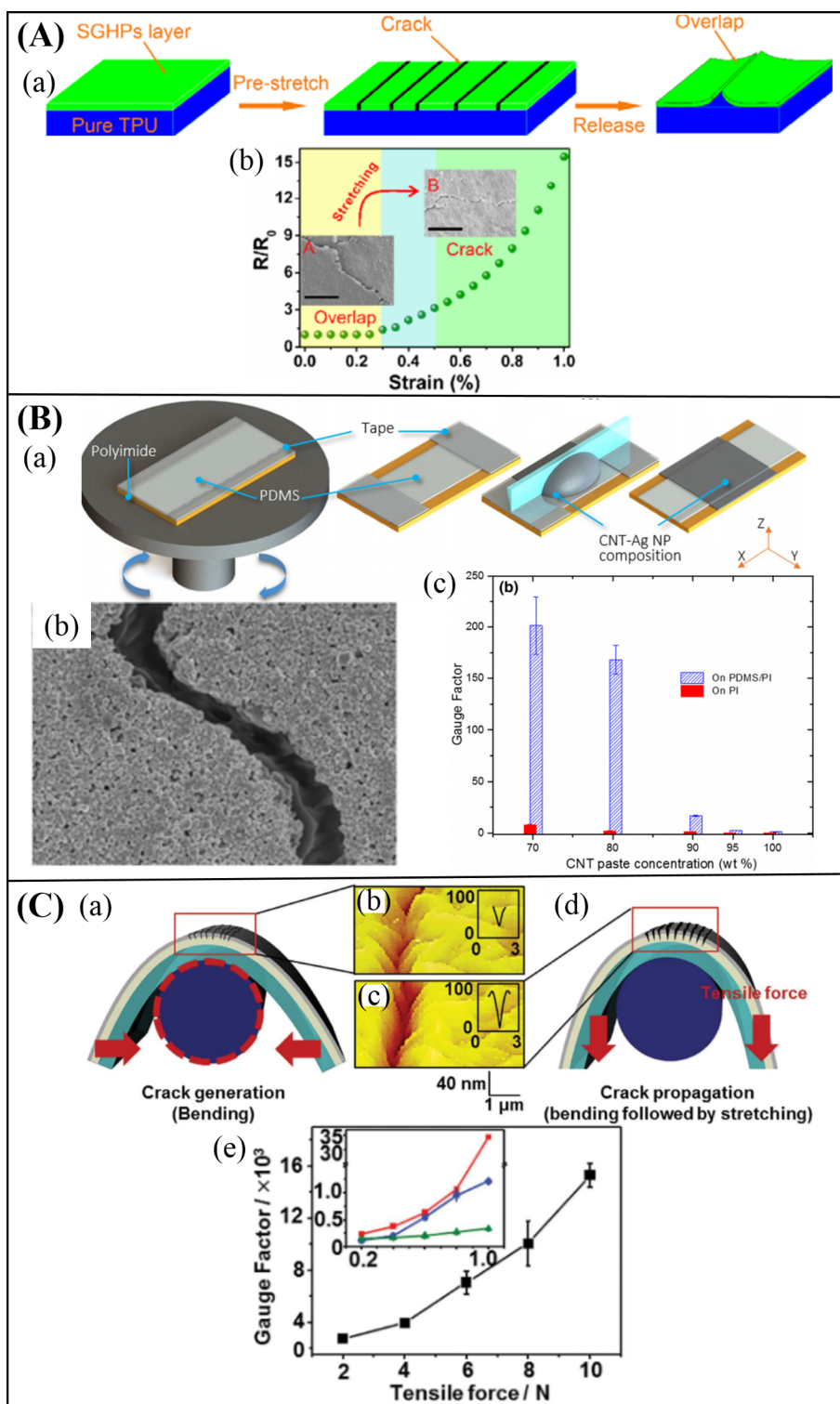


Fig. 2. Crack generation methods. (A) Pre-stretching with (a) schematic illustration of pre-stretching and releasing process of strain sensors based on silver nanowires/graphene hybrid particles/TPU composite; (b) resistance change upon stretching for the strain sensor under pre-stretch of 10% strain. Insets are the SEM images during stretching [40]. (B) Thermal solvent evaporation and thermally induced stress during cooling steps with (a) schematic of CNT-AgNP thin film fabrication process; (b) SEM image of CNT-AgNP thin film with CNT loading at 70 wt%, the scale bar is 3 μm ; (c) gauge factors of CNT-AgNP sensor at different CNT paste concentration with and without PDMS [81]. (C) Bending with (a) schematic of initial crack generation by bending; (b-c) the 3D profiles and depths measured by AFM in bent cracks from (a) and propagated cracks from (d); (d) crack propagation by additionally applied stretching; (e) gauge factor at 2% strain obtained by the sensors [112].

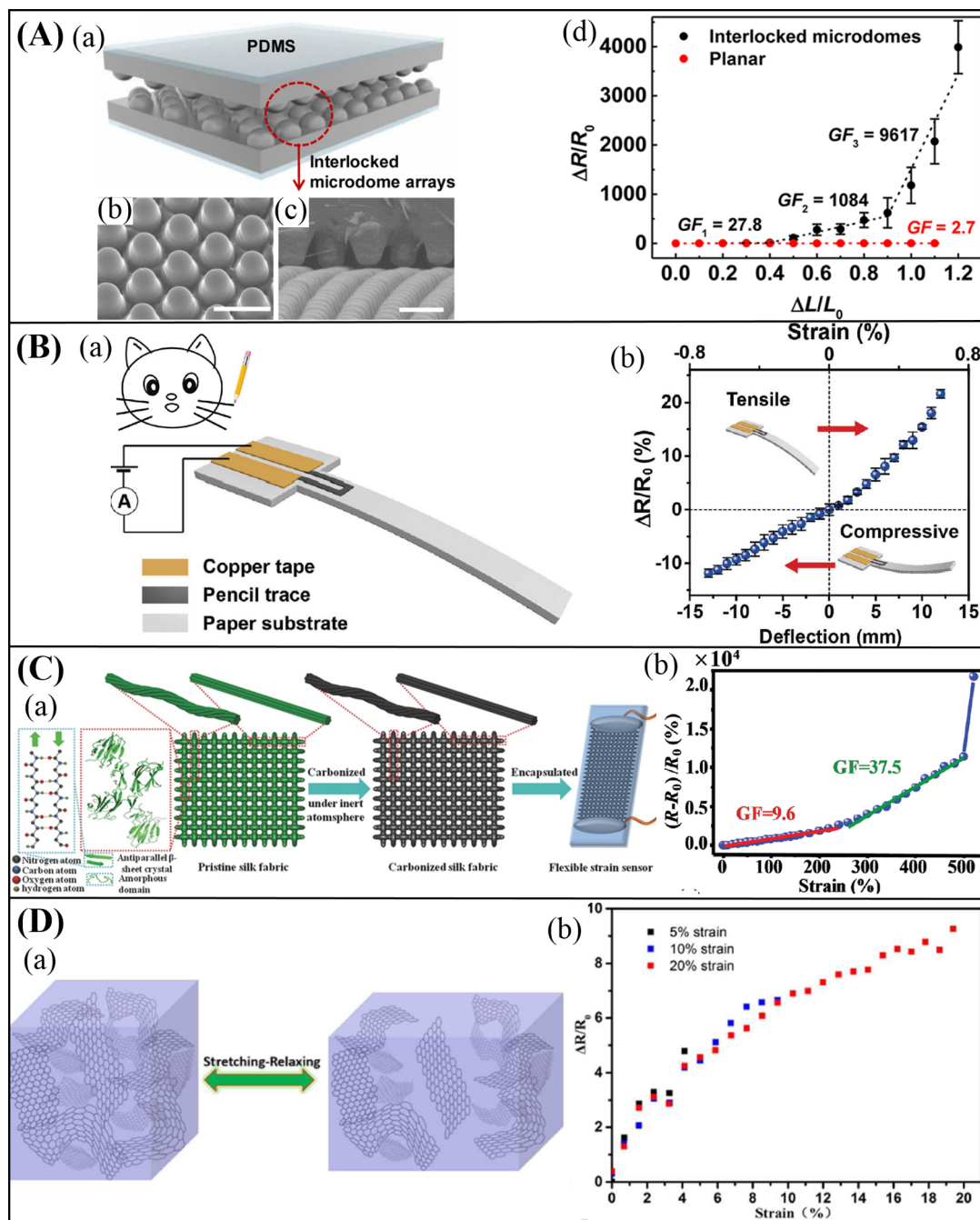


Fig. 3. Strain sensors with some special structural design. (A) Interlocked microstructure with (a) schematic of CNT-PDMS composite film with interlocked microdome array; (b) tilted SEM image of a composite film with microdome arrays; (c) cross-sectional SEM image of an interlocked composite film; (d) stretch-sensing capabilities comparison of interlocked microdome arrays and planar films [108]. (B) Whisker structure with (a) schematic illustration of cat's whisker and device schematic of pencil-drawn e-whisker; (b) normalized resistance change as functions of applied strain (top x-axis) [127]. (C) Carbonized silk fabric (CSF) with (a) illustration of the hierarchical structures and the fabrication process of CSF strain sensors; (b) resistance variation versus applied strain [128]. (D) 3D microstructure with (a) schematic illustration of structural change of the 3D graphene foam composite under stretching and releasing; (b) relative resistance variation of the strain sensor under stretching [131].

substrates, and some are in the form of intentionally fractured [39,50,58,136] conductive thin films. Note that the matrix for this approach can also be thermoplastic [65,121], although only in limited cases in which comparable sensitivity is shown and the stretchability and resilience satisfy the working requirement. The first approach is typically simple and cost-effective, leads to high yields, and allows easy handling [137], while a multistep process is needed for the construction of intentionally fractured conductive

thin films [39,50,58,136]. In addition, a strong binding of the sensing component with the polymer matrix/substrate is beneficial for achieving high stretchability [45].

The second approach is based on structural design through geometric engineering rather than by exploiting intrinsic material properties. The structural configurations for rigid materials on an elastomeric substrate are divided into out-of-plane and in-plane structures. Three-dimensional wavy [87], wrinkled [82], double helical [84], coiled [89] shapes are examples of out-of-plane structures, whereas buckled structure [85], serpentine pattern [138], and mesh-like geometries [139,140] belong to in-plane design. The latter design is proposed to effectively accommodate much larger applied strain and eliminate the concern of breaking under external scratching [18]. However, compared to the first approach, the second approach is low-yield, high cost and involves a complicated multistep fabrication process such as lithography, transfer, and vacuum deposition [102]. Additional information about functional materials and strategies based on in-plane structures can be found in following reviews [14,141]. For a detailed description of geometric engineering processes of flexible electronic devices, the reader is referred to the following review [44].

For the vast majority of strain sensors, a trade-off relationship between “high sensitivity” and “high stretchability” is concluded [41,44,102,104]. Monitoring a wide range of deformation requires that the active material can keep its structural connections at high strains, while detection of subtle displacement demands the microstructure of the sensing material to change dramatically even under small strain [41]. Rational structure design and control of the connection types of sensing materials are requested to ensure both high sensitivity and high stretchability [39,41,50,115,142]. For example, a sensor based on a thickness-gradient SWCNT film on a PDMS substrate (Fig. 4A) was developed by Liu et al. [41] by employing a self-pinning method. The developed material possesses a GF as high as 1.61×10^2 ($\epsilon < 2\%$), 9.8 (Avg., $2\% < \epsilon < 15\%$), and 5.8×10^{-1} ($\epsilon > 15\%$) and can withstand uniaxial strain of more than 150% [41]. Close inspection of these GF values shows that the deficiency is although the decrease of the sensitivity from 1.61×10^2 to 5.8×10^{-1} if the strain is up to 15%.

Another example is the work of Amjadi et al. [39] who developed an ultrasensitive and highly stretchable strain sensor based on graphite thin films with parallel microcracks coated on top of Ecoflex (Fig. 4B). The sensors made of graphite thin films with short microcracks possess high GFs (maximum value of 5.2×10^2 at 50% strain) and stretchability ($\epsilon \geq 50\%$), while sensors with long microcracks show ultrahigh sensitivity (maximum value of 1.1×10^4 at 50% strain) with limited stretchability ($\epsilon \leq 50\%$) [39]. Furthermore, the combination of microcracks and the disconnection sensing mechanism was recently utilized by Zhao et al. [50]. These authors developed a high performance strain sensing platform with slit- and scale-like structures (Fig. 4C) through embedding fragmented graphene sponges (FGS) in a poly(styrene-*block*-butadiene-*block*-styrene) (SBS) matrix, followed by an iterative process of silver precursor absorption and reduction. The microcrack configuration of the silver layer and the more effective contact area and sponge structure of the FGS conductive block contributed to high GF ($\sim 10^7$ at 120% strain) and stretchability (up to 120%) simultaneously, as well as a fast response and an excellent reliability and stability. An elaborate control of the fabrication process for micro/nano crack and/or specific architecture construction is although required. The uniformity and repeatability need also still to be further guaranteed. A more convenient method has been recently developed by Tao et al. [142] via one-step laser patterning. The strain sensor was produced by embedding laser-patterned graphene in Ecoflex (Fig. 4D). The strain sensor exhibited excellent repeatability, self-adapted and tunable sensing performance with a GF up to 4.6×10^2 with the strain up to 35% and a GF of 2.7×10^2 with strain up to 100%. The sensing performance adapting to both subtle and large occasions can be tuned by adjusting the graphene mesh density.

3.3. Linearity

Linearity refers to a directly proportional relationship between the electrical signal and the applied strain. The magnitude of linearity can be evaluated with the coefficient of determination (R^2) measured by a linear regression. A larger value of R^2 signifies a stronger linear relationship [143]. In general, a nonlinear relationship is active for resistive-type strain sensors, which hinders the intuitive reflection of the accurate strain and the use of a simple calibration process [104].

The most prevalent explanation is that the nonlinearity is ascribed to the microstructural changes of the sensing component upon undergoing a shift from a homogeneous to a heterogeneous morphology upon stretching [23,44,102,104,107,144]. For instance, Amjadi et al. [107] reported a strain sensor based on AgNW/PDMS. The change of the topology of the percolating network with emerging bottleneck locations that critically limit the electrical current resulted in a nonlinear sensing response for the low density AgNW sensor. In contrast, a highly linear behavior was observed for the high density AgNW strain sensor due to the dense and robust network with no bottleneck locations observed even at high strains up to 100%. A similar strain sensor based on a CNT percolation network sandwiched between two Ecoflex layers was also produced by the same research group [45]. With a high dense network formed, the strain sensor simultaneously possessed super stretchability of $\sim 500\%$, high linearity ($R^2 > 0.95$), very high reliability, and fast response speed. Besides high network density, a significant contribution originated from the strong binding between CNTs and Ecoflex and the excellent elastic behavior of the CNTs so that the slippage of CNTs inside the Ecoflex matrix was less probable [45]. It should be noted that the linear responses described above are relative to the stretching amplitudes.

A crucial parameter for the (non-)linear behavior in CPC strain sensors is the filler content. For a filler content close to percolation threshold, there are not enough conductive particles to create contact paths or the concentration is negligible so that the conductivity is achieved by the tunneling effect [117,145]. The resistance then grows exponentially with the distance between adjacent particles [117], and the number of filler particles involved in the percolation network is greatly reduced upon stretching [146]. Consequently, nonlinear strain response and great increase of resistance are observed [147,148]. At concentrations well above the percolation threshold, the resistance change depends on the structural changes with the variation of the dominating mechanism of conductivity in distinct strain domains. The conductivity is then also less influenced by smaller strain as explained in detail in Selvan et al. [145]. The

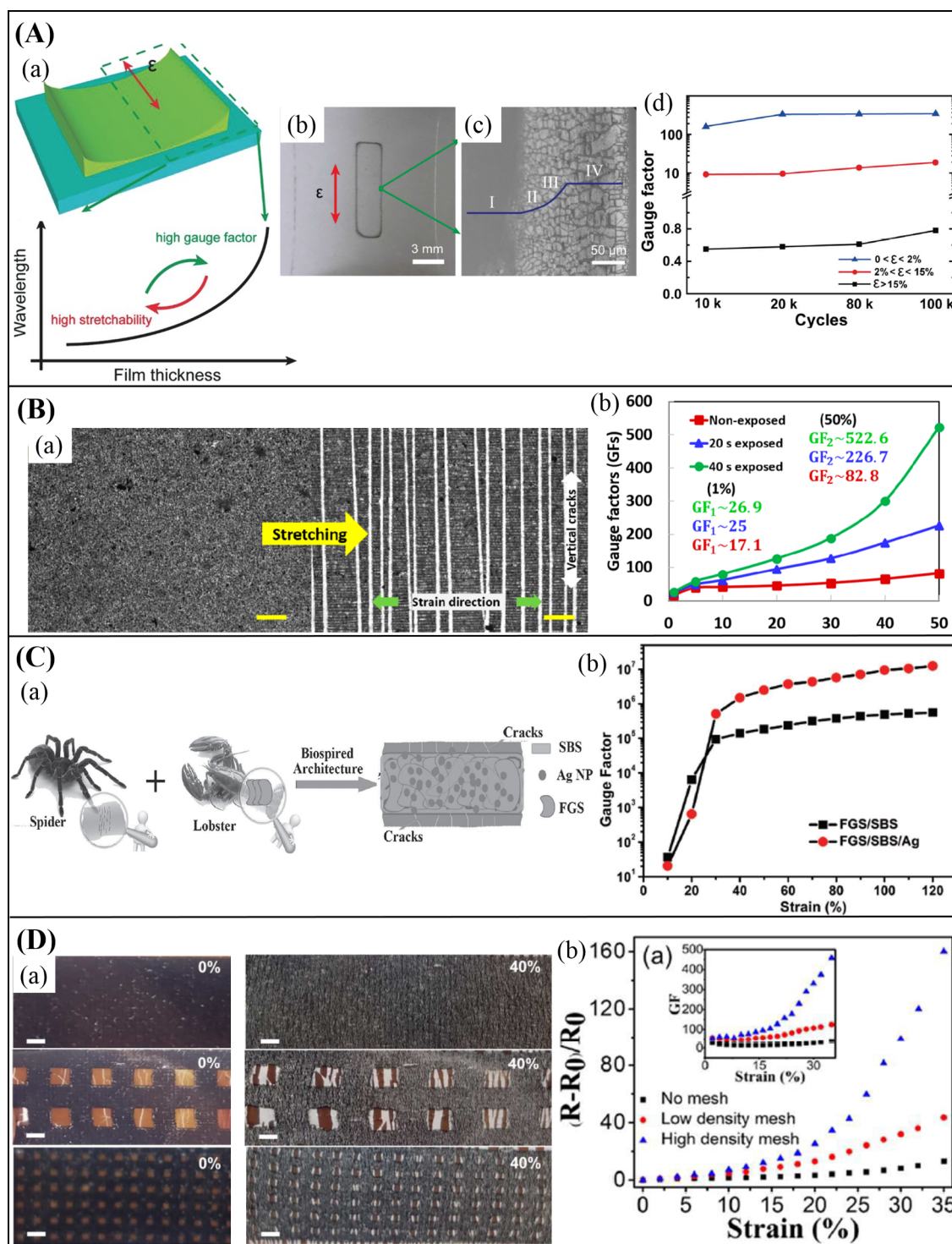


Fig. 4. Strategies to achieve high GFs and stretchability simultaneously. (A) Thickness-gradient film with (a) schematic illustration of thickness-gradient structure that help to achieve both high GF and high stretchability; the microscope image of (b) film sample under 60% strain, the black ring shows the thick part and (c) the ring region in (b); (d) the GFs of the sensor at different strains and cycles [41]. (B) Parallel microcracks based strain sensor with (a) optical microscope images of the graphite thin film before and after microcrack generation; parallel microcrack opening in perpendicular direction of strain; (b) GFs as a function of the applied strain [39]. (C) Slit- and scale-like structures with (a) concept of slit- and scale-like architectures, slit-like structure provides sensitivity, while shell-like structure provides stretchability and sensitivity; (b) GF versus strain for FGS/SBS and FGS/SBS/Ag composites [50]. (D) Mesh-like geometry with (a) optical images of laser patterned graphene (LPG) strain sensors with different mesh densities under different strains; (b) relative resistance variation versus strain of the strain sensors with different mesh densities [142].

resistance change induced due to contact is the dominant mechanism under the initial strain, leading to a linear response, and the higher the contribution of contact conductive paths the better the linearity is [110]. After a certain strain, the gaps between adjacent particles widen on stretching, and tunneling behavior between neighboring fillers dominates the resistance change [147]. Further increasing the strain to moderate levels, the variation in resistance is determined by a gradual disconnection in the percolation network [149]. The tunneling effect and the loss of conductive paths therefore result in an exponential non-linear growth of resistance.

In addition, the (non-)linearity may also be influenced by the substrate property. For example, Yang et al. [150] recently developed a highly sensitive strain sensor with graphene woven fabrics (GWFs) on PDMS substrate. By tuning the ratios of base to cross-linker from 20:1 to 8:1, the Young's modulus of the substrate PDMS increased from hundreds of kPa to a few MPa, and R^2 was improved from 0.91 to 0.98. Buckle-delamination in GWFs was formed upon using a stiff substrate. The delamination converted graphene became bended for the subsequent tensile tests, which transferred the crack dominant transduction principle to a geometry dominant one, thus leading to improved linearity [150].

In summary, the piezoresistive linearity is relevant to the change of the dominant conductivity mechanism corresponding to specific strain domains [117,145,147,149], which is influenced by the variation of network morphology under stretching [107,145]. The network morphology variation inherently relies on the mechanical stability of the percolation network [151], thus, high dense, stable and robust network structures give rise to a higher linearity [133,151].

However, similar to sensitivity and stretchability, there also exists a trade-off relationship between high sensitivity and high linearity. Notably some researches achieved high strain sensitivity and linearity simultaneously. For instance, the sensitivity and linearity of strain sensors based on polymer composites with CNTs can be improved simultaneously by considering hybrid sensing nanomaterials [104,152]. In the work of Benchirouf et al. [152], reduced graphene oxide (rGO) and MWCNTs nanocomposite films on a flexible substrate exhibited a GF of 8.5 with a high linearity (R^2 of 0.98). The change of the number of tunneling contacts formed between the rGO and MWCNTs within the conductive network significantly changed the total thin film resistance under strain, contributing to a higher sensitivity [152]. Recently, by constructing well-controlled cracks in SWCNTs paper via laser engraving and roll-to-roll pressing, Xin et al. [153] developed high performance strain sensors with high sensitivity, high stretchability (with a GF over 4.2×10^4 at 150% strain), and high linearity (0.98 from 0% to 15% strain, and 0.96 from 22% to 150% strain), which were ascribed to the dense and well-controlled network cracks. The microstructure of the cracks underwent a homogeneous propagation response. However, the fragmentation process requires elaborate control and its adaptability to other cost-effective nanomaterial-based structures still requires further exploration.

On an overall basis, a trade-off relationship between “high sensitivity”, “high stretchability” and “sufficient linearity” is often proposed [45,104,107]. Highly sensitive strain sensors typically respond to the applied strain with a high nonlinearity and low stretchability [104]. It is therefore still a great challenge to develop strain sensors with simultaneously ultrahigh sensitivity, stretchability, and excellent linearity.

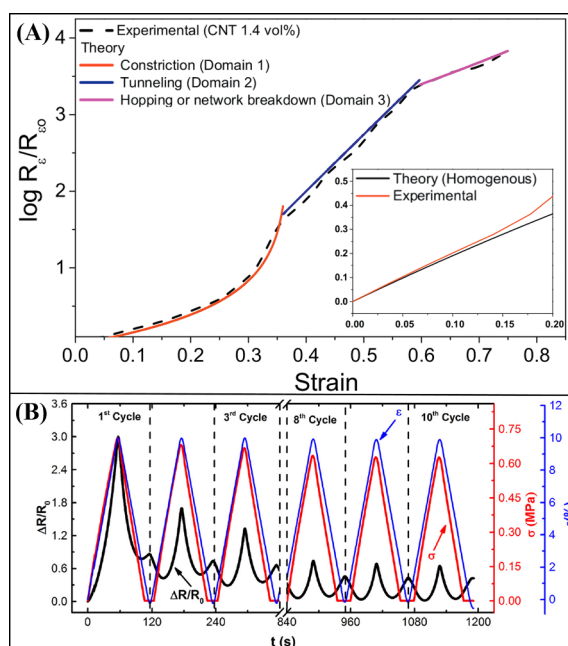


Fig. 5. (A) Comparison of the developed theory with the experiment results for the explanation of non-linear electrical response of NR/MWCNTs composites [145]. (B) Hysteresis of MWCNT/segmented polyurethane (SPU) composite strain sensor under cyclic stretching [154].

3.4. Hysteresis, response time and dynamic durability

The physical robustness and sensing reliability of strain sensors are quite crucial if dynamic forces are applied. As for this aspect, hysteresis, response time, and dynamic durability are three key parameters. Inconsistent or non-monotonic piezoresistive variation is referred as hysteresis. This is commonly depicted as double peaks for a single loading-unloading cycle [154] (Fig. 5B), displaying a negative piezoresistive effect implying an inverse relationship between resistance and strain [47,51,154]. The response time determines how quickly the strain sensor responds to the applied strain with accurate and steady indication. A 90% time constant ($\tau_{90\%}$) is commonly used as the standard response time for stretchable sensors [104,107]. In addition, dynamic durability demonstrates the endurance of strain sensors to long-term cyclic loading-unloading profiles with stable and reproducible resistive response and mechanical integrity.

In general, the hysteretic behavior and response delay exist in all polymer based strain sensors. They are still not fully understood and often explained by the competition of network breakdown and reformation during cyclic loading [69,154–156]. Several factors, including the intrinsic viscoelastic nature of polymers, the viscoelastic characteristics of conductive fillers and retarded reaggregation between filler-filler bonds/interactions in a relaxed state, poor interfacial adhesion, and imperfect recovery of conduction paths due to ubiquitous friction between the solid-state sensing element and the elastomeric molecules [45,78,104,107] are assumed to contribute to the hysteretic behavior. Friction is assumed to cause disparate time scales in detachment and slippage among filler particles, which leads to the delay in settling down of the fillers in the polymer matrix and inhibits the recovery of the percolation network [104,148]. A larger interfacial area of conductive fillers and polymer prolongs the time delay [157].

For strain sensors with randomly incorporated nanocomposites [45], strong binding between the elastomeric nanomaterials and the polymer matrix helps to minimize the hysteresis effect and promotes a faster response. Under such circumstances less slipping and detachment between fillers occurs and the sensing elements rapidly go back to the initial state upon releasing [45]. Conversely, very weak interfacial adhesion between rigid nanomaterials (e.g. metal nanowires) and polymers is expected for the full recovery of the conductive network after the release of strain [104].

The use of an ultra-soft polymer matrix provides a lower force for the quick establishment of the percolation network [45]. Besides, the electrical conductivity becomes considerably more frequency dependent at higher strains [114]. The response time of structure-based strain sensors (e.g. crack/gap-based strain sensors) is faster, due to the quick and easy reconnection-disconnection transformation [158]. To ensure accurate and deterministic deformation detection, it is recommended to adopt polymers with smaller viscoelastic properties or to suppress the viscoelastic effect of the elastomeric polymer matrix/substrate itself. For example, Choi et al. [78] developed a highly stretchable and “hysteresis-free” strain sensor by introducing the IL of ethylene glycol (EG) and sodium chloride (NaCl) with limitless deformability and a less hysteretic wavy structure of the fluidic channel (Fig. 6A). The resistance relaxation of the sensor was nearly negligible even under 250% strain. This is thought to be derived from the suppressed viscoelastic relaxation by the wavy structure of the elastomeric channel. Microfluidic strain sensors (Fig. 6B) show lower hysteresis and would allow accurate sensing up the strain limits set by the encapsulating elastomer due to the high deformability of liquids. On the other hand, some drawbacks such as leakage, electric circuit integration, and low GF limit their practical application [79].

Notably (buckled) sheath-core structured fiber/yarn/textile strain sensors (Fig. 6C) have attracted increasing interest due to the substantial contributions to high stretchability [85], “hysteresis free” nature [159], and fast strain response [82] by overcoming the viscoelastic delay of the polymer composites [82]. Generally, the piezoresistive fibers/yarns are fabricated by integrating conductive functional materials as sheaths through methods of coating [143,160,161], ink writing [82], and continuous wrapping [159] on the surface of (stretched) fiber/yarns as core.

In addition, it is evident that the hysteretic behavior depends on the integrity and robustness of the conductive network morphology, as well as the strain amplitude [102,107]. For instance, the “shoulder peak” for 15 and 30% strain for CNT/TPU composites strain sensor is much more obvious than for 5% strain [47]. The weak destruction of the entangled CNT network induced by small strain is easy to recover after releasing, while the competition between the destruction and establishment of the conductive network under large strain is remarkable. A single-peak response pattern is obtained for 5% strain amplitude for the stable CNT/graphene synergistic network, but it is easy to be destroyed if subjected to larger strain amplitudes. As the morphology of the conductive network almost remained unchanged under small strain, good reversibility and repeatability were thus then observed [47]. Similarly, the evenly distributed and densely packed CNTs conductive network in SBS underwent almost no evident changes, thus, more stable and consistent dynamic sensing performance under the strain amplitude of 10–50% was achieved [51].

Furthermore, compared with strain sensors made of nanomaterial fillers inside a polymer matrix, stretchable strain sensors based on disconnection gaps [157] (Fig. 6D) and the micro/nanoscale cracks (Fig. 6E) propagation mechanism [115,140] possess good hysteresis performance. The bundles between gaps [157] or the lateral compression effect on the nanostructure connection around the crack edges benefited the approximately complete recovery of the electrical resistance, if the applied strain was released [39,158]. Whether constructing a super dense and robust conductive network or engineering structure-based morphology, the influence of the local weak destruction is not significant enough to retard the recovery of the conductive network, showing no or negligible hysteresis. As such, the “integral size or unit” of the sensing element is much more crucial for the overall performances as the “apparent enlarged” sensing unit is less influenced by the viscoelastic nature of polymers. Eventually, the integrity of the conductive network morphology is greatly preserved upon releasing.

A declining trend of the relative change in resistance with increasing stretching/releasing cycle number and afterwards saturation is often observed. Such phenomenon is explained by the formation of additional conductive pathways through breakdown and subsequent formation of interface between matrix and filler [162]. However, a growing tendency with increasing cycles has also been observed [163], this is because the breakdown of conductive networks can be more predominant than the formation of conductive

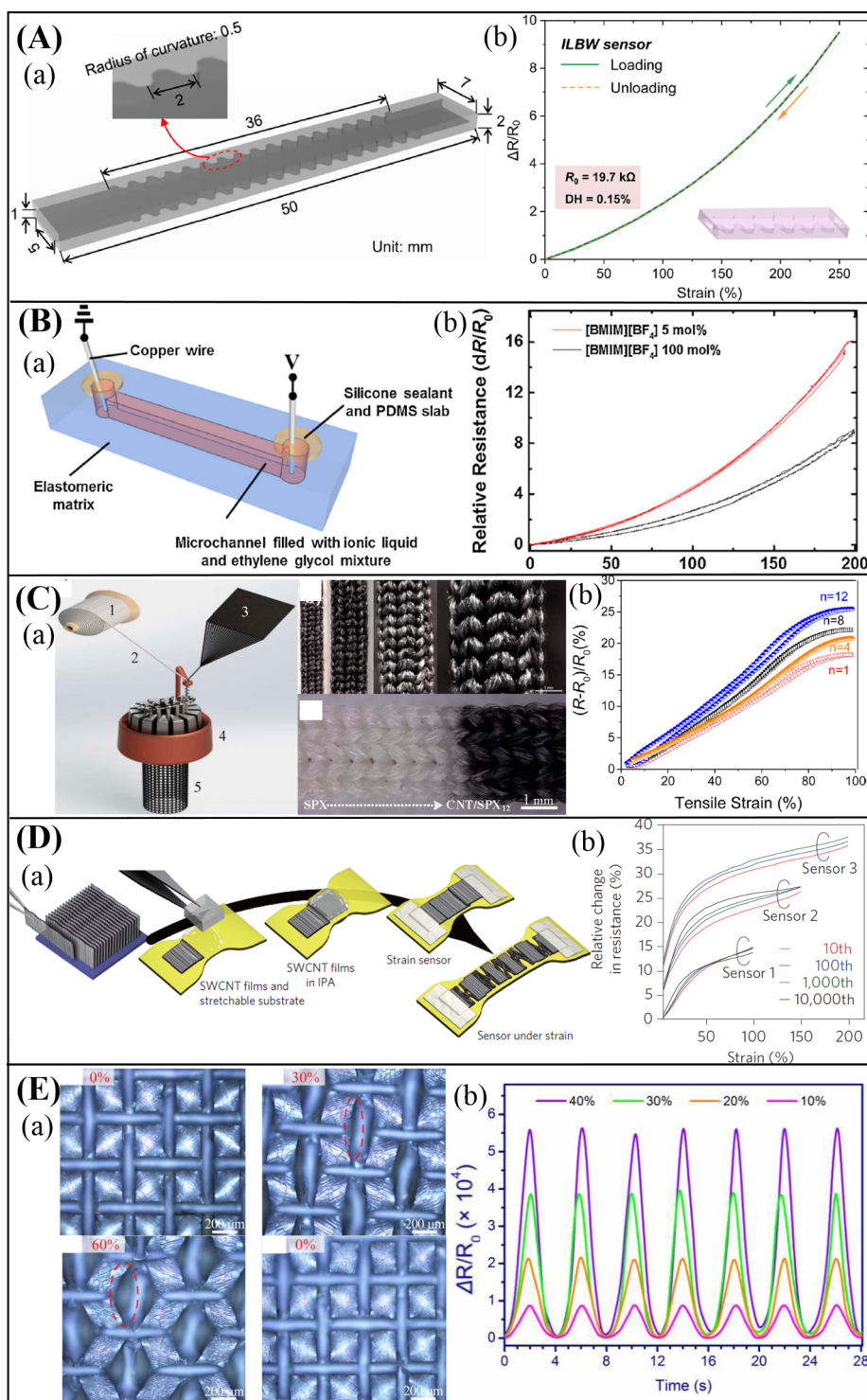


Fig. 6. Some strategies to achieve low hysteresis or hysteresis-free strain sensors. (A) Ionic-liquid-based wavy (ILBW) sensor with (a) geometrical dimensions of the ILBW strain sensor; (b) hysteresis-free curve of the ILBW strain sensor [78]. (B) Microfluidic strain sensor with (a) schematic illustration of a linear microchannel embedded strain sensor in PDMS matrix; (b) relative electrical resistance variation of the microfluidic strain sensors [79]. (C) Sheath-core conductive yarns with (a) schematic of the producing process of strain sensor based on knitted CNT-Sheath/Spandex-Core (CNT/SPX) elastomeric yarns, and photograph of the CNT/SPX structures; (b) change in normalized electrical resistance versus applied strain during loading and unloading for CNT/SPX_n textiles [159]. (D) Strain sensor with bridging bundle gaps with (a) key steps in fabricating the SWCNT strain sensor; (b) relative change in resistance versus strain for multiple-cycle tests [157]. (E) Microcrack-assisted strain sensor with (a) structure and morphology of the strain sensor under stable strains; (b) multicycle stretching tests of the strain sensor with AgNW spin-coated on patterned PDMS substrate [115].

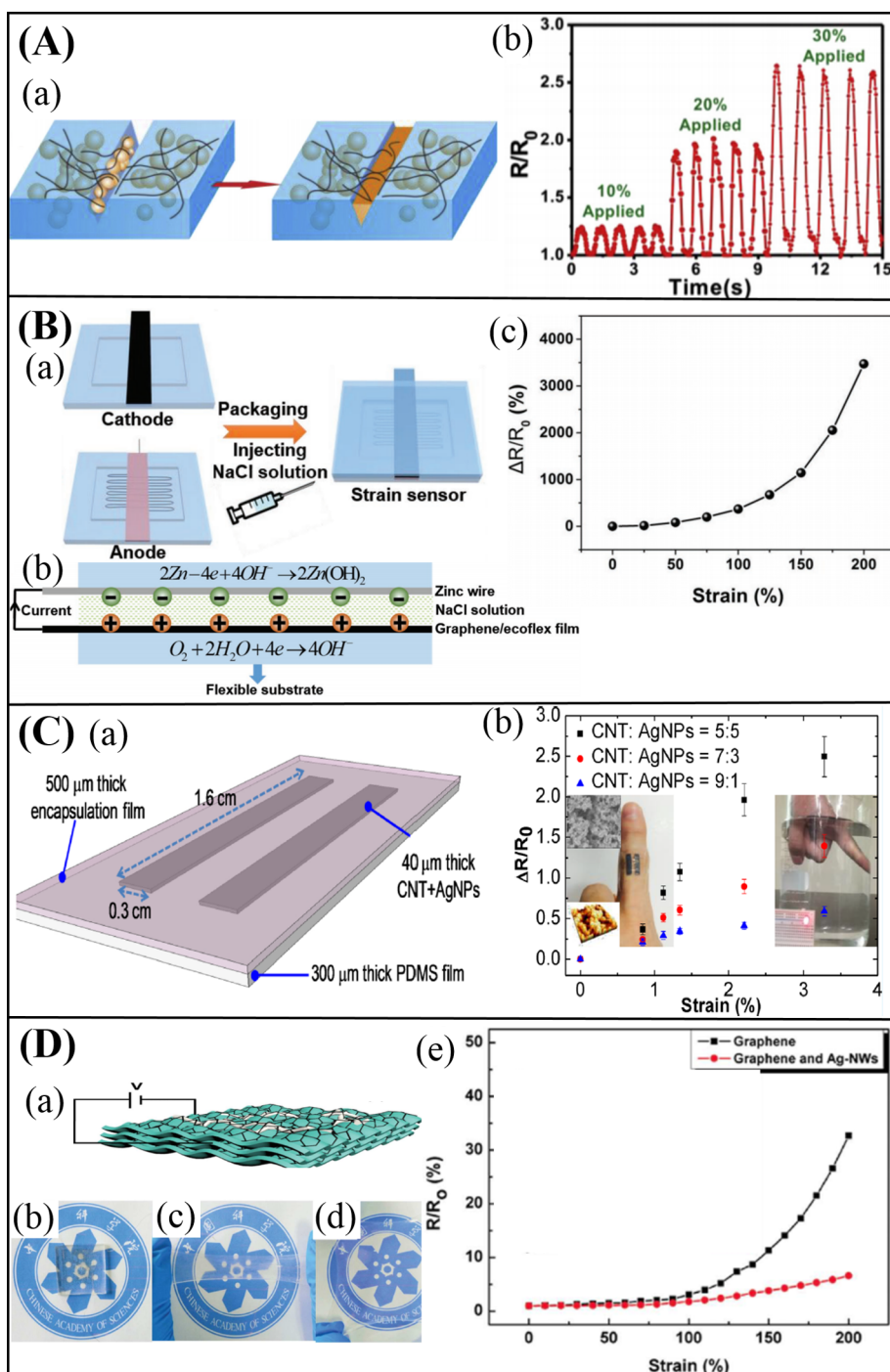


Fig. 7. Strain sensors with novel features. (A) Self-healing strain sensor with (a) schematic of the healing procedure of the strain sensor; (b) dynamic stretch-release cycles response of the strain sensor [164]. (B) Self-powered strain sensor platform with (a) schematic diagram of the partial fabrication process of the sensing device; (b) a schematic of the energy generation mechanism and electrical performances of the device without any strain; (c) the relative change in resistance versus strain curves [165]. (C) Waterproof strain sensor with (a) schematic architecture of the E-bandage for wearable strain sensors; (b) relative resistance change as a function of bending strain [168]. (D) Transparent strain sensor with (a) schematic of the strain sensor and the setup for charge injection; (b-d) photographs of the strain sensor under stretching up to 200%, showing increased transparency as it gets stretched; (e) relative resistance variation under stretching [171].

network in tension, which leads to their irreversible displacement under strain [163]. In addition, the degradation of the performance of strain sensors has been attributed to the fatigue and plastic deformation of substrates under large strain, and buckling and fracture of sensing nanomaterials [104,107].

In general and in line with the discussions above, the simultaneous achievement of high sensitivity, high stretchability, fast response, low hysteresis, and long-term stability in a simple and cost-effective way is still a great challenge, especially for personalized healthcare applications in which tiny strain changes on the surface of human skin need to be captured. Frequently, it is shown that strain sensors with stretchability over 100% strain and high sensitivity (GFs) over 50 are still challenging [104]. Each kind of material has its unique electrical, mechanical and other properties. More importantly, the assembled structures associated with processing strategies are more decisive for the final sensing performances, and special structure designs may help to create a unique function that their counterparts do not possess, especially when conventional sensing elements based on non-structured composite materials suffer from issues such as low sensitivity, slow response, and large hysteresis. Therefore, proper selection of materials, rational structure design and control of the connection types of sensing materials are effective routes to realize balanced performances for a specific application.

3.5. Additional novel design partners

Next to the above covered crucial performance parameters, more recent research has demonstrated that several novel design partners such as self-healing, self-powering, self-cleaning, transparency, biocompatibility, and biodegradability need to be considered as well to ensure a better application adaptability.

Foreseeably, the sensing performance and service lifetime of flexible strain sensors declines once they are exposed to abnormal working conditions and even fail due to irreversible mechanical cracks or damages. Inspired by self-healing phenomenon of the human skin, increasing efforts have been made to endow the flexible strain sensors with self-healing capacity to extend their lifetime [164]. In general, self-healing of polymeric materials is achieved through extrinsic and intrinsic strategies. Extrinsic self-healing is based on the leakage of a pre-embedded healing agent or catalyst from cracked microcapsules or a vascular network but is incapable of multiple healing. On the other hand, intrinsic self-healing is driven by reversible bonds, metal-ligand interactions, and conductive network reforming after melting and diffusion [164] (Fig. 7A). Due to the reversible nature it is applicable for multiple self-healing. However, there are still great challenges for simple and (economically) feasible fabrication strategies and more importantly to keep the strain sensors with high recovery efficiency even after multiple healing.

Another valuable design parameter attracting growing attention is self-powering [165] (Fig. 7B), as the external power supply is an indispensable part for most sensor systems. To reduce the power consumption, a promising method is to combine the power generator and storage device with electromechanical strain sensors [73,110]. The emerging development of energy-harvesting technologies such as piezoelectric, triboelectric, pyroelectric, thermoelectric and energy-storage devices such as flexible batteries and super capacitors makes it more feasible for the fabrication of all-in-one electronics. For example, the first contact-mode triboelectric self-powered strain sensor was fabricated by Zhang et al. [166] by using an auxetic polyurethane foam, conductive fabric, and polytetrafluoroethylene. The auxetic foam expands once being stretched and through contact with a friction layer allows to generate electricity. This sensor possesses the highest sensitivity of all triboelectric nanogenerator devices. However, the current energy and power densities of most generators are still not sufficient for prolonged operation and further improvements are still required for stretchability and sensing capabilities [19].

To maintain acceptable mechanical and sensing performances under complicated and changing working conditions, self-cleaning capability needs also to be introduced. This has been recently covered applying novel geometrical structure design. Conventionally, the self-cleaning ability is attributed to the ability of the hydrophobic hierarchical structure [110,167]. For example, super hydrophobic surfaces and self-cleaning capability were achieved by Kim et al. [110] with the gecko-inspired hierarchical structure design, as the high-aspect-ratio micropillars with spatula tips greatly increase the contact angle between various types of liquid droplets with the conductive dry adhesive surface. The hydrophobic performance was improved due to the increase of surface roughness in the triaxially post-buckling microstructure foam, and the stretchability, toughness, flexibility, energy absorbing ability, conductivity, piezoresistive sensitivity and crack resistance were also simultaneously improved [167]. In addition, by employing hydrophobic fluoropolymer as the encapsulation layer, a high-performance wearable electronic-bandage strain sensor based on CNT-silver nanoparticles (AgNP)/PDMS with sandwiched structure (Fig. 7C) was developed by Jeon et al. [168]. The bandage could be prevented from physical and chemical contact with the daily life conditions. Note that the hydrophobic property is critical for sensitivity maintenance as acuteness of the sensors tested at hydrous conditions will be very low [169].

Furthermore, for some special applications such as stretchable displays, human-skin attachable materials, and implantable sensing platforms, optical transparency is an important feature for conformal and instantaneous visualization for users. However, most reported stretchable strain sensors are nontransparent because of high loading of conventional nontransparent inorganic nanofillers or utilization of opaque materials. The lamination or sandwich-like [146] structure designed by using transparent active materials such as AgNWs [170], highly purified 99% metallic CNT [146], nanohybrids of CNTs and conductive elastomers [15], graphene/AgNWs hybrid structures [171] (Fig. 7D), single-layer graphene with serpentine-shaped pattern [172] as the force sensing element in conjunction with ultrathin and stretchable substrate enables conformal and transparent devices. More information about the advances in stretchable transparent thin-film electrodes especially based on in-plane structures can be obtained in the review of Kim et al. [141]. A review of materials and devices for transparent stretchable electronics is recently provided by Trung et al. [173].

In addition, especially for implantable sensing platforms in personalized healthcare applications, biocompatibility and biodegradability are quite critical design parameters. In this context, electronic systems entirely built with biocompatible and

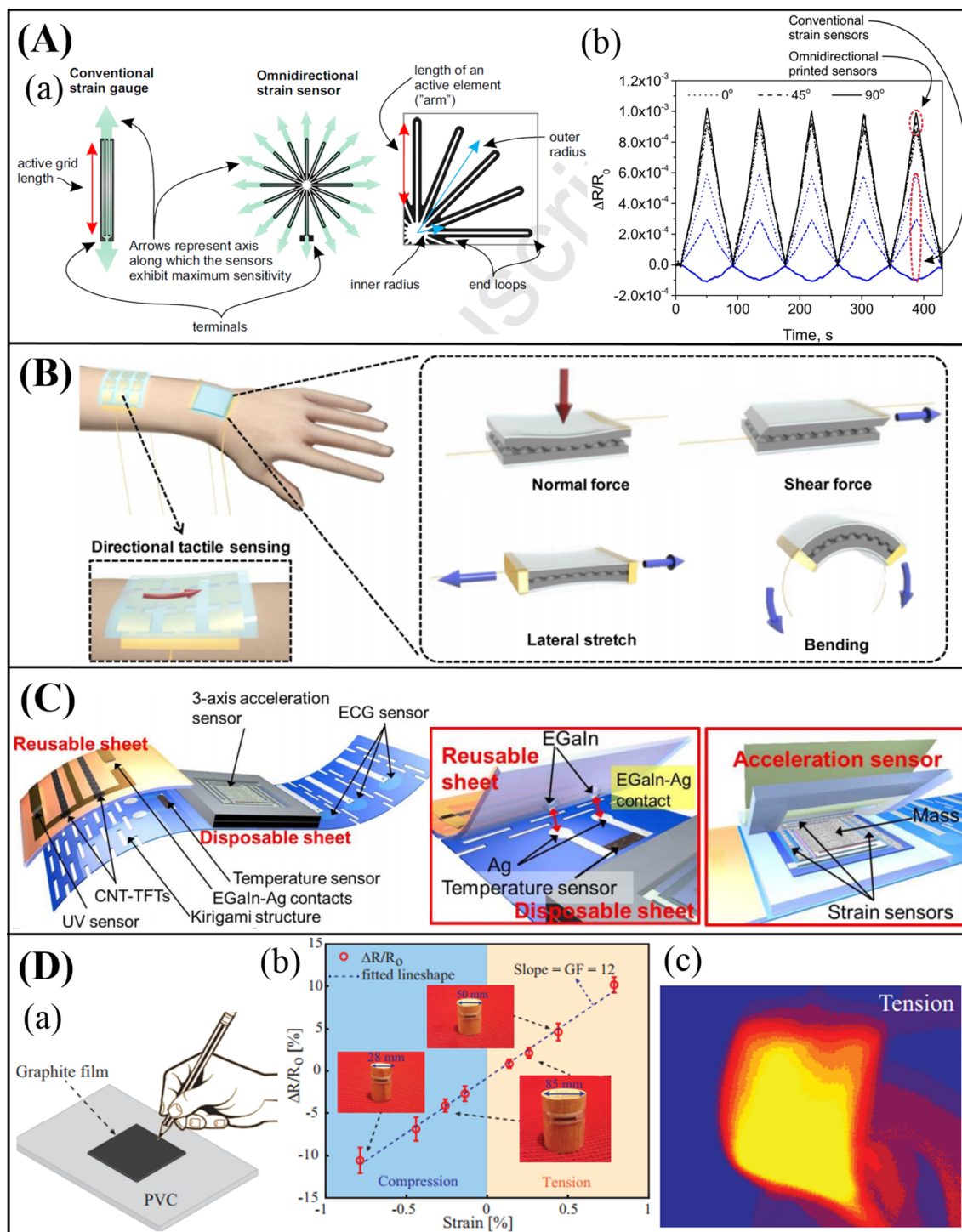


Fig. 8. Multifunctional sensing with (A) multidirectional strain sensing with (a) schematic design of conventional strain gauge (left) and the design of omnidirectional strain sensor (right); (b) relative change in resistance during dynamic strain measurements [175]. (B) Schematics of multi-mechanical stimuli (normal shear, stretching, bending, and twisting forces) sensing [108]. (C) Schematics of flexible multifunctional device for temperature, acceleration, and electrocardiograms monitoring [180]. (D) Flexible multifunctional electronics for human-motion and thermal therapy detection with (a) schematic diagram of graphite transfer to PVC using a pencil; (b) resistance changes under compression and tension; (c) infrared picture of the graphite-based flexible heater under tension [181].

Table 1
Summary and comparison of recently reported flexible strain sensors and their fabrication method details. The typical matrix materials and blending partners can also be distilled from this table.

Materials	Filler content	Gauge Factor (GF) ^a	Maximum strain under static stretching	Linearity	Cyclic stretching-releasing strain range	Fabrication process	Extra information
<i>PART A: Strain sensors fabricated via blending/ infiltrating/coating/transferring/filling process</i>							
<i>Matrix and one conductive functional component partner</i>							
SEBS/CB [56]	50 wt%	4–6.3 ($5\% \leq \epsilon \leq 50\%$)	50%	Nonlinear	Consistent (5%–10%, 15%–20%, 25%–30%, 35%–40%, 45%–50%, 5 cycles)	Torque rheometer mixing, capillary rheometer for sensor ribbon extrusion, and then pre-strained	
PDMS/CB [43]	8.11 vol%	1.58×10 ($\epsilon \leq 10\%$)	30%	Near linear ($\epsilon \leq 10\%$)	Consistent (0–10%, 100 cycles)	Solution mixing, curing	
Silicone rubber/CB grease [42]	N.A.	3.8 ($\epsilon \leq 100\%$) (Slope)	800%	Near linear ($\epsilon \leq 400\%$)	Consistent (0–100%, 5 cycles)	Embedded carbon-based resistive ink within an elastomeric matrix via 3D printing (filling process)	
NR/Graphene [59]	0.2 vol%	3.5×10 ($\epsilon = 700\%$)	~800%	Nonlinear	Consistent (5%–75%, 500 cycles)	Infuse liquid-exfoliated graphene into natural rubber	
PDMS/Ultrathin graphene films [204]	Volume of injected graphene dispersion: 0.8 mL (mass concentration of 1 mg mL ⁻¹)	$\sim 4.5 \times 10^2$ ($\epsilon = 0.5\%$); 1.04×10^3 ($\epsilon = 2\%$)	3.4% (failure strain)	Nonlinear	Consistent (0–2%, 5 cycles)	The assembled graphene films are derived rapidly at the liquid/air interface by Marangoni effect, transfer to PDMS	
TPU/MWCNT [285]	0.3 wt%; 1.0 wt%	22 ($\epsilon \leq 15\%$), 6395 ($\epsilon = 35\%$) (0.3 wt%); 7.0 ($\epsilon \leq 45\%$), 7935 ($\epsilon = 185\%$) (1.0 wt%)	185%	Near linear ($\epsilon \leq 15\%$ (0.3 wt %) and $\epsilon \leq 45\%$ (1.0 wt%))	Consistent (0–25%, 20 cycles, 0.3 wt%); hysteresis (0–50%, 20 cycles, 0.3 wt%)	Solution mixing, film casting	
PU/MWCNT [49]	Depending on the MWCNT network layer thickness	$\sim 6.9 \times 10$ ($\epsilon = 403\%$)	403%	Nonlinear	~Consistent ($\epsilon < 50\%$)	GNT suspension filtered via non-woven polyurethane filter membrane, compression molding	
Ecoflex/MWCNT [45]	Controlled by the amount and density of the sprayed solution	2.42 ($\epsilon \leq 100\%$) (Slope)	500%	Near linear ($\epsilon \leq 100\%$)	Consistent (0–500%, 5 cycles)	GNT film sandwiched between Ecoflex	
SEBS/PANI [286]	30 wt%	$1.5\text{--}2.4$ ($1\% \leq \epsilon \leq 10\%$)	10%	Near linear	Near consistent (0–1%, 10 cycles); hysteresis (0–10%, 10 cycles)	Solution mixing, film casting	
TPU-CB [293]	20 wt%	3.4×10^2 ($\epsilon = 90\%$)	90%	Nonlinear	Hysteresis (20%–40%, 40 cycles)	Extrusion compounding, annealing	
OBC-CB [293]	20 wt%	4.5×10^2 ($\epsilon = 150\%$)	150%	Nonlinear	Hysteresis (20%–40%, 40 cycles)	Extrusion compounding, annealing	
OBC-CB/TPU [293]	12 wt%	4.2×10^4 ($\epsilon = 85\%$)	85%	Nonlinear	Hysteresis (20%–40%, 40 cycles)	Extrusion compounding, annealing	
OBC-CB/TPU [294]	7 wt%	2.2×10^4 ($\epsilon = 52\%$)	52%	Nonlinear	Limited hysteresis (20%–40%, 40 cycles)	Extrusion compounding, annealing	

More conductive functional component partners

(continued on next page)

Table 1 (continued)

Materials	Filler content	Gauge Factor (GF) ^a	Maximum strain under static stretching	Linearity	Cyclic stretching-releasing strain range	Fabrication process	Extra information
SBS/AgNW-AgNP [287]	0.56 wt%	~15 ($\epsilon = 100\%$)	220%	Nonlinear	Consistent (0–20%, 40%, 60%, 80%, and 100%, 5 cycles); peak of the normalized resistance and baseline increase, stabilized after 600 cycles (0–10%, 1000 cycles)	AgNW-mixed SBS solution, wet spinning, Ag precursor adsorption and reduction	
Ecoflex/(rGO/DI conductive liquid) [288]	1 mg ml ⁻¹	2.5 ($0.1\% \leq \epsilon \leq 1\%$); 31.6 ($390\% \leq \epsilon \leq 400\%$)	400%	Nonlinear	Consistent (0–40%, 10,000 cycles)	Preparation of GO, preparation of rGO foams, rGO/DI conductive liquids injected into Ecoflex (filling process)	
PU/amino MWCNT/(graphene) [47]	0.8 vol% CNT; 0.5 vol% CNT and 0.1 vol % graphene	5.1 ($\epsilon = 5\%$), 3.21 × 10 ($\epsilon = 15\%$), 1.53 × 10 ² ($\epsilon = 30\%$) (0.8 vol% CNT); 3.58 ($\epsilon = 5\%$), 1.29 × 10 ($\epsilon = 15\%$), 3.58 × 10 ($\epsilon = 30\%$) (0.5 vol % CNT and 0.1 vol% graphene)	N.A.	Nonlinear	Hysteresis (0–5, 15, 30%, 20 cycles); consistent (0–5%, 5–20% or 0–15%, 20 cycles, after the pre-straining for about 24 h)	Solution mixing co-coagulation, compression molding	
PU/MWCNT/CB [46]	2 wt% MWCNT, 7 wt% CB and	~5 ($\epsilon = 0$); 1.4 × 10 ⁵ ($\epsilon = 220\%$)	220%	Nonlinear	Hysteresis (0–100%, 36 cycles)	Solution mixing, film casting	
PVDF/MWCNT/CB [65]	1 wt% MWCNT-COOH 0.5 wt% MWCNTs and 0.5 wt% CB	4R/R ₀ = 0.65 ($\epsilon = 10\%$)	10%	Nonlinear	N.A.	Twin screw microcompounder, compression molding	
PU/AgNW/PEDOT:PSS [73]	PEDOT:PSS/PU at 14/86	1.24 × 10 ($\epsilon < 6\%$)	100%	Nonlinear	Consistent (0–1.5–6%, 50 cycles per pulse) N.A.	Spin-coating solution of PEDOT:PSS/PU on AgNWs (PDMS as substrate)	
SBS-CNT/AgNP [55]	18.5 wt% CNT and 20.4 wt% AgNP	2.65 × 10 ⁴ ($\epsilon = 100\%$)	540% (break)	Nonlinear	N.A.	A series of processes including homogenizing-absorption-in-situ reduction technique	
TPU-CB/OBC [293]	10 wt% CB	1 × 10 ² ($\epsilon = 30\%$)	30%	Nonlinear	Hysteresis (20%–40%, 40 cycles)	extrusion-based; annealing	
OBC-CB/TPU [294]	7 wt% CB	2.2 × 10 ⁴ ($\epsilon = 52\%$)	52%	Nonlinear	Limited hysteresis (20%–40%, 40 cycles)	extrusion-based; annealing	
<i>PART B: Strain sensors with special structural design for the conductive functional component and/or substrate</i>							
CB@CNC/NR @ PU yarn [38]	CPC suspension: 8.5 vol %; Sensor: 50 LBL	3.89 × 10 ($\epsilon = 1\%$)	5%	Near linear ($\epsilon \leq 1\%$)	Consistent (0–1%, 10,000 cycles)	Solution mixing, dip coating	Sheath-core structure
Rubber core/(CNT/PP) [289]	CNT conductive ink diluted to 10 wt%	2.14 ($\epsilon \leq 280\%$); 6.14 ($\epsilon > 280\%$)	>200%	Linear ($\epsilon \leq 200\%$)	Consistent (0–0.5, 1, 2, 5, 10, 20, and 50%, 10 cycles; 0–10%, 20,000 cycles)	Immersed spring-like fiber substrates in the diluted CNT conductive ink	Spring-like fiber with helically double-leveled gaps
PDMS/SWCNT [290]	SWCNT solution, 0.5 mg ml ⁻¹	835 ($\epsilon \leq 15\%$); ~4694 ($\epsilon = 98\%$)	98%	Near linear ($\epsilon \leq 15\%$)	Consistent (0–15%, 2300 cycles; 0–30%, 2400 cycles, stable after 2200 cycles)	Fabrication auxetic mold, fabrication of substrate with auxetic frame, define hydrophilic area on substrate, drop SWCNT solution on hydrophilic area	Substrate with auxetic frame; microcracks

(continued on next page)

Table 1 (continued)

Materials	Filler content	Gauge Factor (GF) ^a	Maximum strain under static stretching	Linearity	Cyclic stretching-releasing strain range	Fabrication process	Extra information
PDMS/AgNW [291]	1 wt%	926 ($\epsilon = 9.6\%$; height ratio = 0.4)	–	Nonlinear	Hysteresis (0–30%, 100 cycles)	Creating a master for molding PDMS with a desired pitch, spin - coating PDMS precursor solution, AgNW coating, PDMS encapsulation	Substrate with relief-structure (trench)
Polycarbonate-urethane resin/MWCNT sheet [136]	Depending on the number of CNT web layers	1.05×10 ($\epsilon \leq 100\%$)	200%	Linear ($\epsilon \leq 100\%$)	Consistent, excellent repetition durability (5–30%, 180,000 cycles)	Millimeter-long MWCNTs are unidirectionally aligned and sandwiched between elastomer layers	Unidirectionally aligned MWCNT
PDMS/SWCNTs [41]	N.A.	1.61×10^2 ($\epsilon < 2\%$); 9.8 (Avg., $2\% < \epsilon < 15\%$); 5.8×10^{-1} ($\epsilon > 15\%$)	150%	Nonlinear	Consistent (0–60%, 100,000 cycles; 0–100%, 20,000 cycles)	Self-spinning process	Thickness-gradient SWCNTs film
NR/Graphene [72]	0.42 vol%	$\sim 1.39 \times 10^2$ ($\epsilon \sim 60\%$)	110%	Nonlinear	Hysteresis (0–30%, 400 cycles)	Suspension, freeze drying and reduction, compression molding	Segregated conductive network structure
SBR/NR/Graphene [58]	0.42 vol%	$\sim 8.25 \times 10$ ($\epsilon \sim 100\%$)	120%	Nonlinear	Hysteresis (0–30%, 300 cycles)	Latex electrostatic assembly, flocculation drying, vulcanization	Double-interconnected network structure
Ecoflex/Graphite [39]	Short microcracks; long microcracks	5.23×10^2 ($\epsilon = 50\%$) (short microcracks); 1.13×10^4 ($\epsilon = 50\%$) (long microcracks)	50%	Nonlinear	Consistent (0–0.5, 1.5, 10, 25, 50%, respectively, 50 cycles)	Graphite thin films coated on elastomer films	Parallel microcracks
PU/AgNW/Graphene [40]	$m_{AgNW}/m_{GO} = 4$	2×10 ($\epsilon < 0.3\%$); 10^3 ($0.3\% < \epsilon < 0.5\%$); 4×10^3 ($0.8\% < \epsilon < 1\%$) $\sim 10^7$ ($\epsilon = 120\%$)	1%	Nonlinear	Small hysteresis (0–0.6%, 1000 cycles)	Coprecipitation, reduction, vacuum filtration, casting, prestretching	Crack and overlap morphology
FGS/SBS/Ag [50]	N.A.	42.3	120% (break)	Nonlinear	Consistent (0–50%, 2000 cycles)	Synthesis of fragmented graphene sponges, infiltration of SBS matrix, absorption and reduction of Ag precursor	Crack and sponge-like structure
PDMS/gold [292]	N.A.	42.3	120% (decided by substrate)	Linear	Consistent (0–30%, 5000 cycles)	Fabrication of PDMS fibers, fabrication of beads onto the fibers, fabrication of gold film onto the fibers	Microbeads on PDMS fiber, microcracks

^a GF value as specified in reference, in worst case scenario: single-point value.

biodegradable materials are of growing interest for *in vivo* sensors [174]. Besides, the devices should be degraded and resorbed in the body, and therefore no further operation is needed.

3.6. Multifunctional sensing

Strain sensors that can detect the direction of potential failures in engineering structures under multi-directional or multi-plane deformations are highly desirable for applications such as structural health monitoring. However, the commercially available strain sensors can only effectively monitor the deformation in one specific direction, *i.e.* they are uniaxial [175]. Also, the dominant research work related to stretchable strain sensor development aimed at uniaxial sensing measurement.

One strategy to do allow for multidirectional sensing is to construct rosette-type strain gauges [176,177]. However, more inputs into the data acquisition system are required as three individual sensors are used to build the rosette configuration [175]. On the other hand, Zymelka et al. [175] recently demonstrated the concept of a single sensor structure that enables omnidirectional sensing capability. The strain sensor possesses symmetrical design with 16 active elements along eight different axes (Fig. 8A). The developed sensor device exhibited much more accurate measurements of both static and dynamic strain than conventional linear sensors [175]. Detailed optimization of the sensor structure and sensor performance, and exploration of applicability of this method for other materials and the corresponding sensing performance evaluation need to be still conducted.

More recently, multifunctional sensing platforms integrating strain with some other stimuli such as pressure [108,167,178], temperature [178–180], thermotherapy [181] (Fig. 8D), humidity [178], and biometric data [180] have drawn great attention due to their potential for simultaneous multi-stimuli detection capability. Generally, unique structure designs are employed to achieve multifunctionality. For instance, a device with a sensing film constructed from two parallel gold-nanoparticle strips with antiparallel sensitivity gradients can detect the load strain and discriminate the spatial position of the strain [182]. Similarly, a stretchable electronic skin with interlocked microstructures as for instance developed by Park et al. [108] can differentiate various mechanical stimuli, including normal shear, stretching, bending, and twisting forces (Fig. 8B). Due to the different levels of deformation of the arrays depending on the direction of applied forces, the flexibility and durability as a sensor are however limited.

Furthermore, Ho et al. [178] fabricated an all-graphene transparent conformable multifunctional electronic skin sensor through a simple lamination process by integrating humidity, temperature, and pressure sensors into a single unit with all sensors working simultaneously with an individual report. A printed, flexible multifunctional device equipped with a three-axis acceleration sensor was developed by Yamamoto et al. [180]. This multifunctional device can simultaneously monitor skin temperature, heart rate, and UV light exposure as well as physical movement and motion (Fig. 8C), which provided a proof-of-concept device that shows potential for healthcare monitoring combined with physical activity detection.

Additional descriptions related to the controlled design of device structures into bioinspired micro/nanostructures and 2/3D structures for the enhancement of multifunctional sensing properties of flexible electronic skins can be extracted from the review of Park et al. [19]. However, some significant challenges such as the possible signal crosstalk, discrimination of distinct external stimuli in particular the complicated structural engineering and integration process for most developed multifunctional sensing platforms, low-yielding, and issues for the adhesion interface still remain.

4. Material types

One of the most challenging steps in strain sensor development is the selection of the material types, as they define the final characteristics of the sensor to a great extent. In this section, the materials for flexible and/or stretchable strain sensors are summarized making a distinction between the matrix/substrate and the conductive materials. Along with the material types, the fabrication methods are discussed.

4.1. Flexible matrix or substrate

For materials expected to cover only tensile modes of deformation (*e.g.* stretching or bending), it is often sufficient to have a low tensile modulus and high crack-onset strain for the selected material. The most basic choice for supporting matrix/substrate is intrinsic stretchable materials (*e.g.* elastomers/rubbers), especially for large-scale deformation (see also first columns in Table 1). Elastomers can easily sustain dynamic strain (typically larger than 100%) for thousands of loading/unloading cycles [101]. Most of the substrate materials are currently silicone or polyurethane based.

The most commonly employed elastomer as flexible substrate is PDMS [41–43], due to its excellent elasticity, high thermal stability, transparency, chemical inertness, curability, non-toxicity, and biocompatibility [101,183]. Most of the reported skin-like stretchable sensors are based on conductive nanomaterials and (microstructured) PDMS films. A hydrophobic to hydrophilic surface modification is frequently utilized to control the interfacial adhesion between PDMS and conductive materials. Other elastomers such as Ecoflex [39,45], NR [57–59,72], SBR [58,60], and thermoplastic elastomer TPU [38,46–49], SBCs [50–56], and POE [61,62] are also used as matrix/substrate in systems that require higher stretchability than PDMS (maximum strain of 120–160%) [101]. Notably the sensitivity may change with temperature variation, creep, and material fatigue [102].

In addition to high stretchable elastomer/rubber, attention has also been paid to thermoplastics such as PP [63,64], PVDF [65,66,77,184], as well as epoxy [67,70] for high strength applications. However, if conductive fillers are incorporated, the ductility and toughness generally decreases. A small elastic region is therefore obtained, which can result in a relatively narrow strain sensing range [121]. A few percentage of strain may cause irreversible changes both in the substrate and in the conductive layer with

thermoplastics. Strains smaller than 1% are practically invisible for elastomers embedded with conductive materials. Hence, elastomers are more suitable for high strains monitoring (e.g. human motion detection with strain as much as 55% [157]) and thermoplastics are normally considered for structural health monitoring [65,66,184]. Next to these synthetic polymers, also silk fiber [160] and paper [185,186] have been used as substrates.

In all cases, the extensibility, *i.e.* the crack-onset strain, of the active material should be equal to or greater than that of the substrate, unless cracking itself is used to induce stretchability. For real applications, the ability to tune the sensitivity over a large

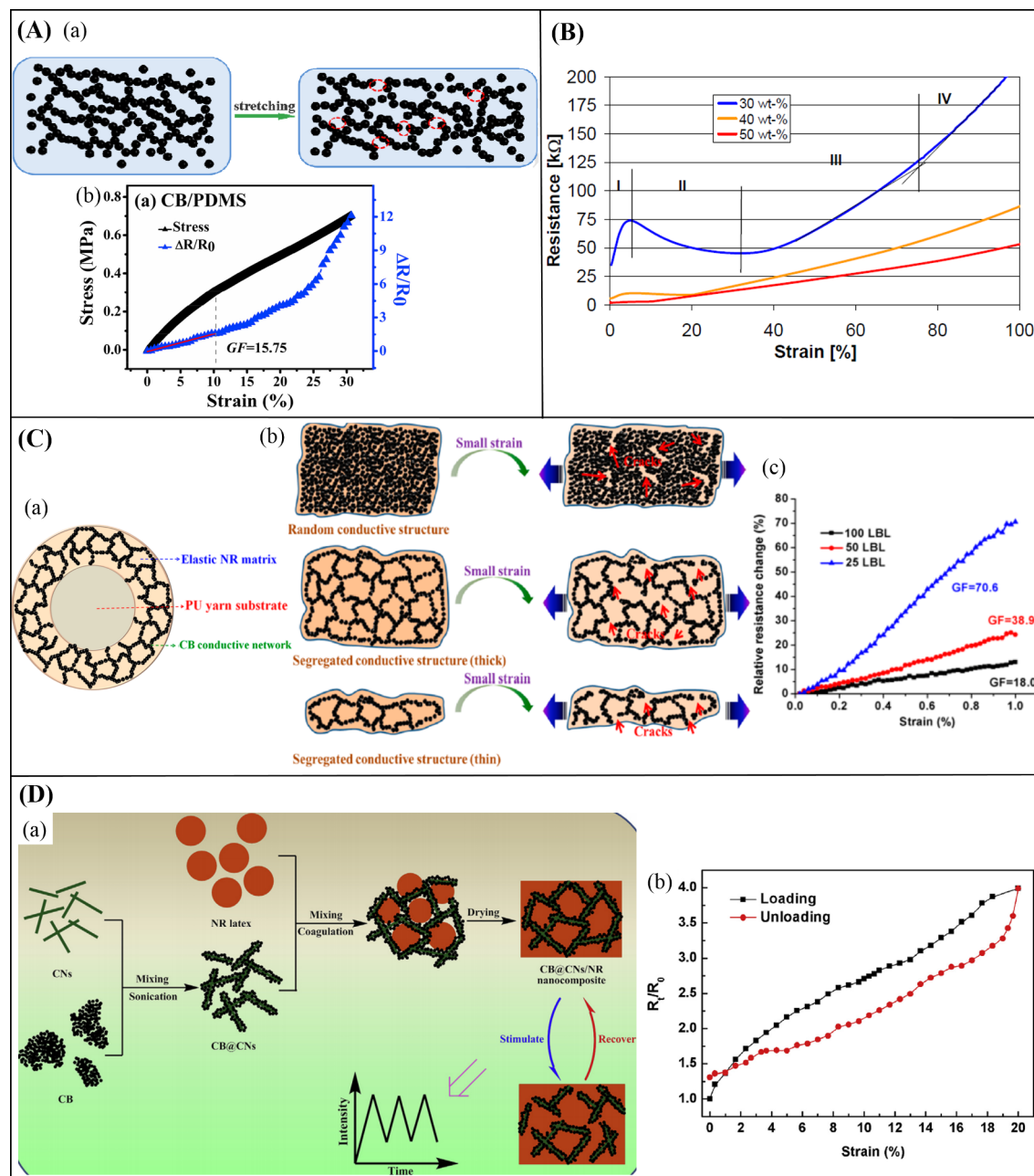


Fig. 9. Stretchable CB based strain sensors. (A) Random dispersed CB/PDMS strain sensor with (a) schematic illustrations of the morphology evolution during stretching for CB/PDMS; (b) normalized changes of resistance as a function of strain for CB/PDMS [43]. (B) Resistance change under stretching for random dispersed SEBS-CB strain sensor [54]. (C) CPC layer-decorated PU strain-sensitive yarn with (a) schematics of the cross section microstructure of the CPC layer-decorated PU yarn; (b) schematic illustrations of different conductive networks development under small strain; (c) relative resistance change of the CPC layer-decorated PU yarn with different LBL numbers [38]. (D) Cellulose nanowhisker modulated 3D hierarchical CB conductive structure with (a) schematic illustration for the fabrication of cellulose nanowhisker modulated 3D hierarchical CB conductive structure in NR matrix; (b) resistance change during a loading-unloading cycle [192].

range of strain should also be considered. Experimental and theoretical results show that increasing the Young's modulus of the nanocomposites can improve the sensing performance [32]. As the mechanical hysteresis of polymers leads to imperfect sensing performances and long response and recovery time, low-hysteretic matrix/substrates are preferable for strain sensor fabrication. However, the impact of matrix/substrate on the flexible sensors response is not yet fully understood and further research is required, as explained above.

4.2. Conductive materials

Diverse conductive materials, including carbon-based micro/nano phased materials (e.g. CNTs [46,47], CB [46,62], graphene [47,72], graphite [39], carbon fiber [187]), and some recently emerged carbonized materials [128,130,188], metallic nanoparticles [50,55,168] and nanowires [40,73,74,107,170] (e.g. AgNPs [168] and AgNWs [40,73,107,170]), conductive polymers (e.g. PEDOT:PSS [73], PANI [74]), IL [78,79], and their heterogeneous hybrids have been utilized to prepare flexible strain sensors (see also first columns in Table 1). Among them, so-called 1D nanomaterials (e.g. CNTs and metallic nanowires) have a high-aspect-ratio, which makes them easy for conductive percolation path formation. Most stretchable conductive composites have therefore been developed based on metal nanowires and CNTs as conductive fillers. CNTs and AgNWs are the most extensively studied 1D

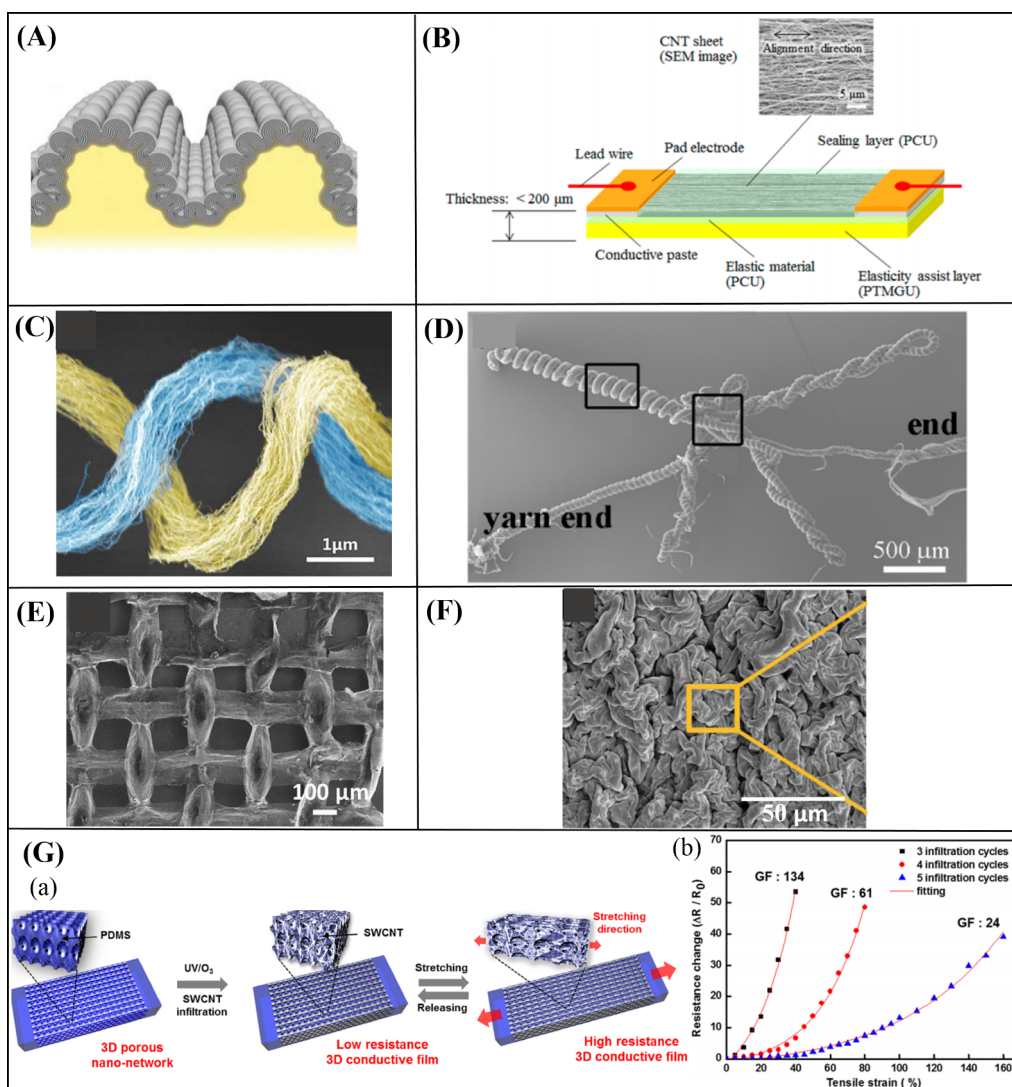


Fig. 10. Stretchable CNT based strain sensors with structural design. (A) Illustration of hierarchical buckling structure of sheath-core conducting fibers [85]. (B) Super aligned CNT film with structure of unidirectionally aligned and sandwiched MWCNT strain sensor [136]. (C) CNT-array double helices [84]. (D) SEM image of two CNT entanglements [197]. (E) SEM image of a CNT mesh after purification [139]. (F) SEM image of wrinkled CNT thin film on shrunken PS substrate [198]. (G) 3D continuous nanoporous conductive network structure with (a) schematic illustration of the fabrication procedure for the 3D continuous conductive nanostructure; (b) relative change of resistance as a function of strain [203].

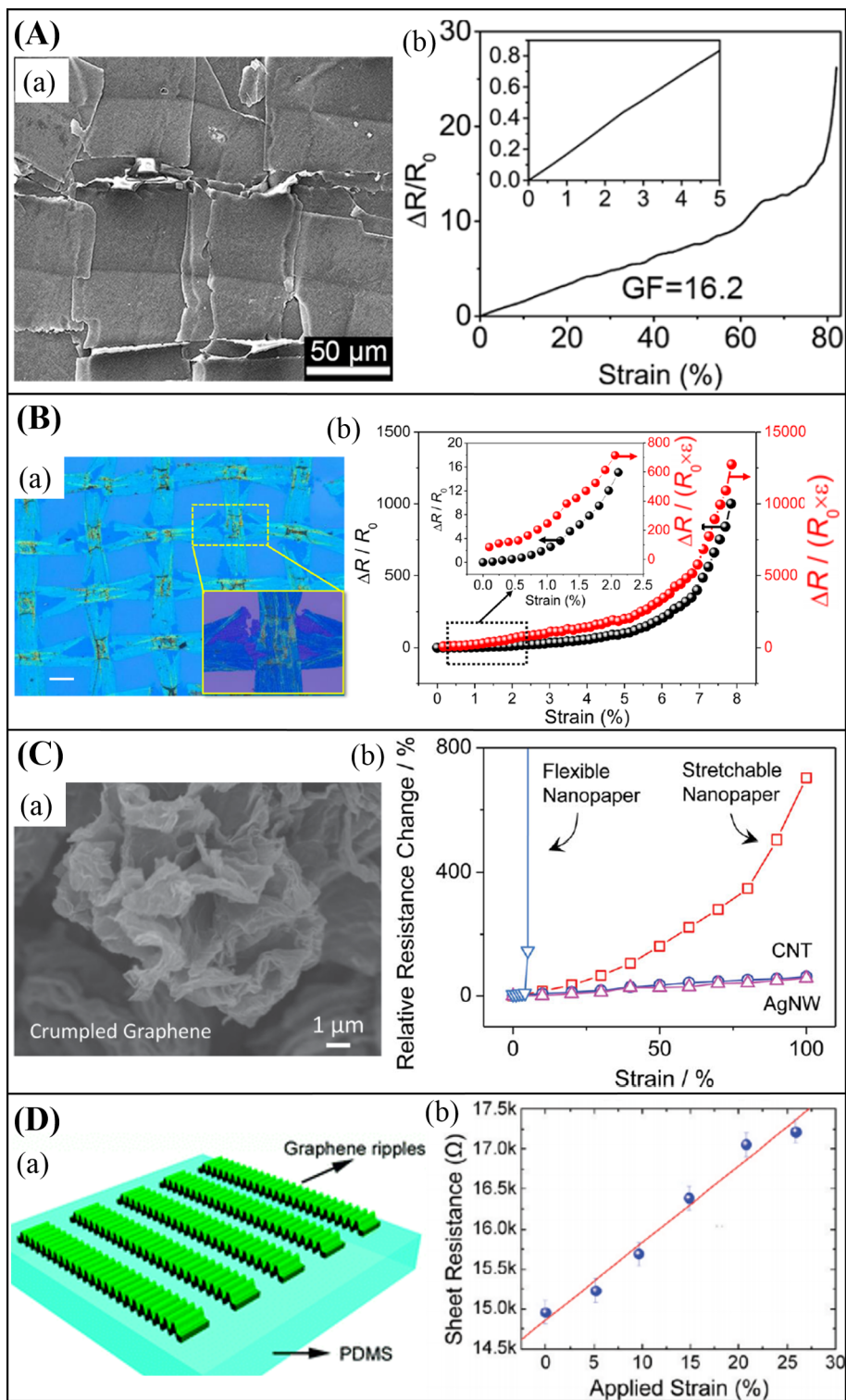


Fig. 11. Stretchable graphene based strain sensors with structural design. (A) Fish-scale-like graphene (FSG) layer with (a) top view SEM image of FSG strain sensor; (b) relative resistance-strain curve of a FSG strain sensor under stretching [7]. (B) Graphene woven fabric (GWF) with (a) top-view optical image of GWF; (b) relative resistances and gauge factors as a function of applied strain [208]. (C) Crumpled graphene nanopaper with (a) top view SEM image of macroporous structure based on crumpled graphene; (b) relative resistance change as a function of tensile strain [209]. (D) Buckled graphene film with (a) schematic diagram of the buckled graphene ribbon on PDMS substrate; (b) resistance change as a function of strain [86].

nanomaterial candidates for the fabrication of flexible and stretchable strain sensors. A number of reviews have already discussed the properties of the above conductive materials [102,134,189]. In what follows, the main important characteristics and limitations of these materials are highlighted, including an overview of more recent developments.

4.2.1. Carbon-based micro/nano materials

Carbon-based micro/nano materials are the most promising candidates for scalable production of strain sensors, with 0D CB, 1D CNT, and 2D graphene the most representative active materials for sensor fabrication. Compared to CNT and graphene, CB is much cheaper with excellent health and safety performance. To date, CB based sensors produced in bulk volume that can be used in a range of wearable products are fabricated via screen printing a composite of CB and silicon elastomer onto a fabric and connecting conductive yarns [190,191]. Strong aggregation of CB brings however difficulties to achieve good dispersion and usually a high loading is needed to obtain a satisfactory electrical conductivity due to their low aspect ratio. Until now, CB has been effectively employed with elastomers such as SBS [52,53], PDMS [43] (Fig. 9A), styrene-ethylene/butylene-styrene (SEBS) triblock copolymer [54,56] (Fig. 9B), and POE [62] for the fabrication of strain sensors.

Generally, with CB the sensitivities are relatively low for small or tiny strain detection. With microstructural design, a highly sensitive strain sensor has been developed by Wu et al. [38] by coating a CPC layer consisting of CB and NR on a PU yarn (Fig. 9C). This strain sensor exhibited high sensitivity (GF of 3.9×10) and a detection limit of 0.1% strain. The massive production feasibility and practical application still need to be further guaranteed. In addition, a unique 3D hierarchical CB conductive network structure has been constructed [192] by incorporating cellulose nanowhiskers via latex assembly technology (Fig. 9D). This unique conductive structure endowed the CB/NR nanocomposites with a very low electrical conductivity percolation threshold (1.65 vol%), and a nearly linear resistance-strain sensing performance. However, small hysteresis was observed under a cyclic loading process [192].

CNTs have been the most extensively studied conductive material used for strain sensor fabrication. Compared to SWCNTs, MWCNTs have relatively high purity and are more economical. MWCNTs based strain sensors exhibit exceptional sensing characteristics and are characterized by a larger working range. CNTs-based strain sensors are typically produced by dispersing CNTs into polymer matrix or directly depositing a CNT film or transferring CNT arrays with fine architectures onto flexible substrates. Generally, the sensitivity is tuned by controlling the filler loading [193] and filler functionalization [194], the dispersion [195], the fabrication process [51], the interaction between CNTs and polymers [46], and the network configurations [46]. Homogeneous dispersion and alignment of CNTs in the composites contribute to positive piezoresistive response with improved sensitivity and linearity. Despite the high stretchability, the GF of elastomeric polymer composite filled with CNTs is relatively low (< 5) under low strain. A linear piezoresistivity is usually obtained under low strains, followed by nonlinearity at larger strains. Moreover, elastomer-CNTs based strain sensors typically exhibit resistance hysteresis under a cyclic stretching/releasing profile [46–49,51], which indicates the irreversible conductive network change and deterioration of the CNT/polymer interface.

In addition to direct dispersion, many design and processing techniques have been developed to assemble CNTs with different architectures (buckled CNTs layers [85] (Fig. 10A), aligned and suspended CNTs [157], super-aligned CNT films [136,196] (Fig. 10B), spring-like CNT yarns [197] (Fig. 10C) and CNT-array double helices [84] (Fig. 10D), CNT meshes [139] (Fig. 10E), and wrinkled CNT thin film [198] (Fig. 10F)) onto flexible substrates. And generally, the fabrication of CNT with those well-defined architectures [84,136,139,157,197] involves chemical vapor deposition (CVD) [199–201] synthesized process of CNT and later transfer and assembly procedure. These network configurations can accommodate to high strain with low hysteresis, high durability, fast response [136] due to the compact and a nearly-intact intertube network composed of a high ratio of CNTs. On the other hand, the sensitivity is relatively low. The structural stability is critical and many strategies have been adopted to resist the destruction induced by buckling and bundling of CNT network during cyclic deformation [202]. In order to avoid segregation or agglomeration, highly porous 3D network [203] (Fig. 10G) has been fabricated before integration into elastomeric polymers. Despite the excellent performance and advancement of CNT based strain sensors in prototypes, there are still numerous challenges to be addressed to fulfill the large scale utilization, such as the elevated cost of high purity CNTs and their scalable controlled dispersions, as well as hazardous concerns.

As a 2D material, graphene exhibits extraordinary electrical and mechanical properties, and is also non-toxic. Generally, graphene has been assembled to various types of nanostructures through different fabrication strategies. For example, Liu et al. [7] developed a high-performance strain sensor with fish-scale-like configuration (Fig. 11A) by stretching/releasing the graphene films on elastic tapes. The strain sensor could detect strain up to 82% and ultralow limit strain ($< 0.1\%$), showing high sensitivity (GF of 1.62×10 in the strain range of 0–60 % and 1.5×10^2 at strain $> 60\%$) with excellent reliability and stability (> 5000 cycles). Inspired by this work, Li et al. [204] developed large-area ultrathin graphene film with “fish scale” like structure for a highly sensitive flexible strain sensor via a novel self-assembled technique based on the so-called Marangoni effect [205–207], and the strain sensor possessed a GF of 1.0×10^3 at 2% strain with high transparency (94%–86% at 550 nm). Graphene woven fabrics fabricated by Yang et al. [208] through chemical vapor deposition using a copper mesh also showed ultrahigh GFs of 5×10^2 under 2% strain and 10^4 over 8% strain due to the synergistic effect of the formation of position-controllable, locally oriented zigzag cracks and large interfacial resistance between the interlaced ribbons. Similar research work related to highly sensitive graphene woven fabric based strain sensors has also been recently reported by Liu et al. [133].

Moreover, some research groups developed graphene [40] (Fig. 2A) or similarly graphite [39] (Fig. 4B) crack-assisted strain sensors, which exhibit ultrahigh piezoresistive sensitivity under small strains (cf. Section 3.1). In general, the piezoresistivity of the above high performance graphene-based strain sensors originates from the breaking of contacts, the change of spacing, and overlapping area upon stretching. Although these strain sensors exhibit ultrahigh GFs, the repeatability of the resistance signals needs to be further investigated. In addition to sensitivity increment, some other structural designs such as patterned graphene mesh [142]

(Fig. 4B), crumpled [209] (Fig. 11C), or buckled [86] (Fig. 11D) structure can help to increase the working strain range. Besides good electrical property, graphene is highly stretchable and almost transparent [210], which helps achieve strain sensors with good transparency [171,172]. Despite much advancement of using graphene for strain sensor fabrication, a critical problem lies however in the preparation of high-quality and well-defined graphene in bulk quantities [210].

4.2.2. Metallic nanoparticles and nanowires

Metallic nanoparticles and nanowires possess a very high conductivity. A particularly attractive research venue for metallic nanoparticles is to develop micro/nano-crack assisted strain sensors (Figs. 1C, 2B–C) with ultrahigh GFs (especially for tiny strain detection) through printing [81], sputtering [111], or depositing [112] on flexible substrates. However, the disconnections between nanoparticles under high strain can lead to the formation of irreversible inter-particle gaps/cracks, and the devices can only be operated within a limited strain range. Increasing the diameter of the nanoparticles results in a higher disorder within the constituent nanoparticle assemblies, which results in a GF and hysteresis increase [211]. For high strain detection, serpentine design is employed to prevent the materials delamination and/or cracking [134,212].

AgNPs-based conductive inks have been developed to enable large area printing of stretchable strain sensors. However, limitations such as small sensing range, reduced sensitivity, nonlinear behavior under certain degree of mechanical deformations may appear due to the weak interparticle connectivity, which is ascribed to their simple spherical architecture [189]. Metallic nanowires have excellent mechanical compliance, which makes them very promising candidates for stretchable strain sensor fabrication. This can be explained by the high conductivity and stretchability in nanowire percolation network, and the high resistance to oxidation and corrosion. AgNWs have been widely used to fabricate transparent, flexible, and stretchable strain sensors via embedding in the elastomeric substrate [40,73,107]. For instance, highly stretchable and sensitive strain sensors based on sandwiched PDMS/AgNWs/PDMS composite was developed by Amjadi et al. [107]. The sandwiched structure contributed to high linearity and negligible hysteresis upon comparison with a simple AgNWs/PDMS layer structure. In addition to a 2D film-based layout, hierarchical 3D assemblies [213] for stable electromechanical performance and 1D-fiber-based structures [214] for high stretchability have also been reported. However, AgNWs are relatively expensive and based on a nonabundant metal.

Copper nanowires (CuNWs) are a promising alternative due to their merits such as being inexpensive, high availability, and also high electrical conductivity. On the other hand, CuNWs are extremely prone to oxidation, which requires further approaches to alleviate or prevent the oxidation. For example, Zhu et al. [215] developed a strain sensor with a hybrid conductive film by embedding CuNWs into water-dispersible modified graphene sheets. The hybrid film exhibited excellent anti-oxidation stability even after exposure in air for 8 weeks.

On an overall basis it can be concluded that despite the performance and advancement issues such as roughness, structure and performance stability, high cost, and low abundance still hinder the scalable utilization of metallic nanoparticles/nanowires in industry.

4.2.3. Conductive polymers and analogues

Most conductive polymers are composed of rigid π -conjugated chains in highly aggregated morphologies, which are responsible for charge transport and also render these materials stiffness and brittleness. PANI [216,217], PPy [76], and PEDOT:PSS [15] are the most explored conductive polymers up to date. Generally, the original conductive polymers are insoluble and non-fusible, as well as exhibit unsatisfying conductivity and sensitivity [44]. Normally, in-situ polymerization [216–218] is adopted for the fabrication of functional composites based on conductive polymers or a doping process [217] is needed to increase the conductivity and solution processability.

PEDOT imbedded in PSS forms the water-based PEDOT: PSS complex, which receives the most attention in strain sensor fabrication due to its high conductivity, low density, high flexibility, and processability. For instance, sandwich-like stacked piezoresistive nanohybrid films based on PU-PEDOT:PSS and SWNT layers have been developed by Roh et al. [15]. The patchable strain sensor possessed a high GF of 6.2×10 and stretchability up to 100%. However, the conductive polymers are sensitive to moisture, and their semi-conducting transport mechanism can imply an exponential drop in conductivity with decreasing temperature [219]. The environmental stability [44] and processing routes therefore still limit the utilization of conductive polymers for scalable sensor production.

In addition, IIs [78,79] and liquid metals [80], which are other conductive materials than polymers, have also been used for strain sensor fabrication. Specifically, microfluidic strain sensors [79,220] fabricated by employing IIs or liquid metals show eligible hysteresis and allow accurate sensing up to the strain limits of the encapsulating elastomers, which are quite promising for the fabrication of strain sensors with excellent stretchability and self-healability [79,221]. Generally, the sensing performance of the microfluidic strain sensors depends on the fluid type, cross-section geometry, depth, and relative lateral position of the embedded channel [102]. However, the repeatability improvement requirement, the relatively complicated and time-consuming fabrication process, the low GF, as well as the high cost still limit the processing scalability.

4.2.4. Hybrid materials

Each material has its own strengths and weaknesses for a specific application. To compensate for the disadvantage of a single material, numerous researches have focused on hybrid nanomaterials of 0D/1D [46], 1D/1D [222] and 1D/2D [202] combinations, as also briefly highlighted above. For example, compared to other graphene and CNT strain sensors, strain sensors based on graphene hybridized CNTs films developed by Shi et al. [202] depicted advantages of high linearity and reproducibility under cyclic tensile strains up to 20%. This was ascribed to the strong interaction and effective load transfer within the hybridized films that effectively

resisted the buckling deformation of CNTs.

Another usefulness of hybrid conductive fillers is to tune the piezoresistive sensitivity of CPCs based strain sensors. For instance, the incorporation of CB reduced the entanglement in the MWCNT conductive network, which increased the resistivity-strain sensitivity [46]. Similarly, CPCs with high sensitivity, high repeatability, and electrical stability under fatigue cycles have been reported in the work of Ning et al. [223], which was ascribed to the synergistic effect of a dual conductive network of CNT arrays and CB.

In summary, hybrid fillers exhibit advantages for the fabrication of piezoresistive CPCs due to their diverse connections or contacts among fillers with different geometries, which also contributes to the electrical conductivity improvement through a synergistic effect.

5. Fabrication and design methods

As highlighted above, one of the common methods to obtain flexible and stretchable strain sensors is to disperse conductive fillers

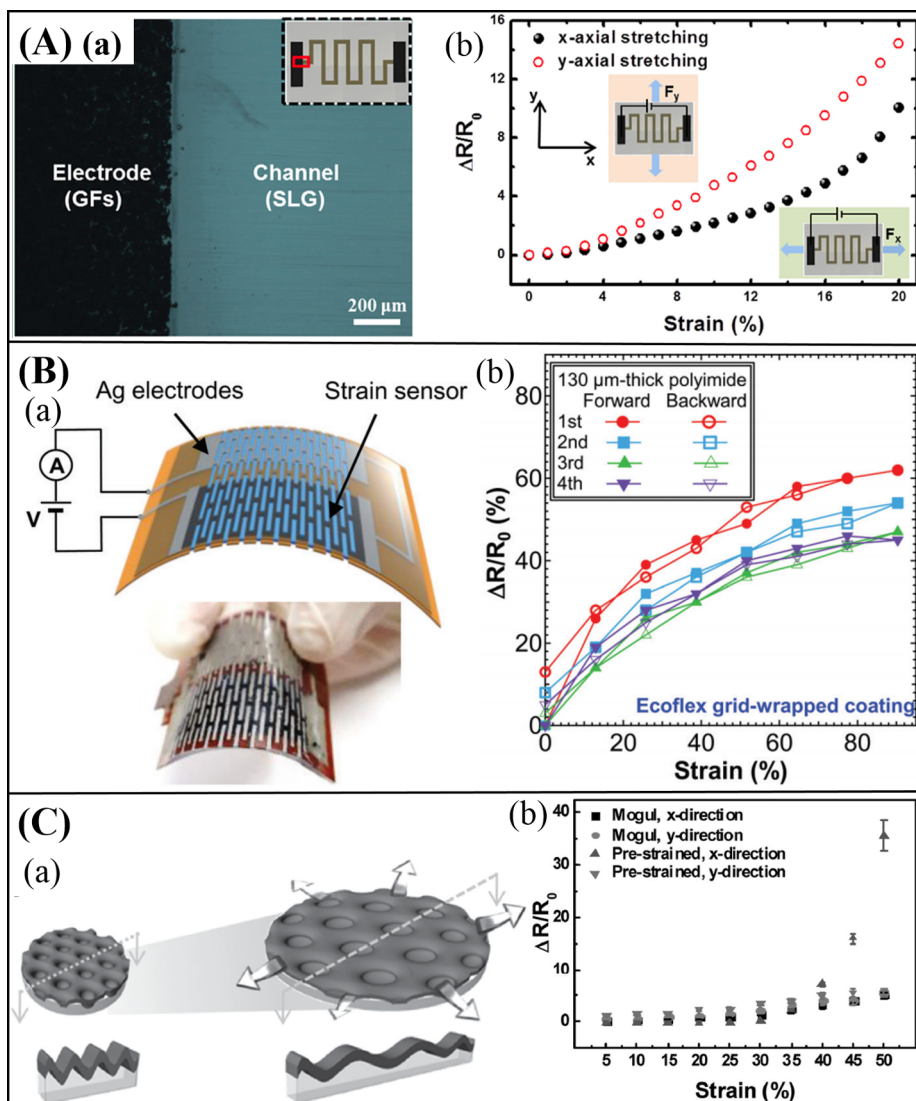


Fig. 12. Illustration of strain relief structures for stretchability. (A) Strain sensor with serpentine pattern with (a) optical image of the boundary between the single-layer graphene channel and the graphene flake electrode. The red square in the insets describing the sensor schematic indicates each part of the optical image in the entire graphene sensor device; (b) the resistance changes with tensile strain for the all-graphene strain sensor [172]. (B) kirigami-structured stretchable strain sensor with (a) schematic of an integrated device with printed electrodes; (b) normalized resistance change ratio of ecoflex grid-wrapped device with 130 μm -thick polyimide [228]. (C) Mogul-patterned stretchable electrode with (a) schematic of the substrate with a mogul pattern under stretching; (b) average value of relative resistance change at each strain of the Au layer on a mogul-patterned stretchable substrate [229]. (For interpretation of the references to colour in this figure legend, the reader is referred to the web version of this article.)

in an elastomer polymer matrix. In general, the most commonly used dispersing techniques include shear mixing [64,193], solution mixing [43], and in-situ polymerization [77]. In case of solution dispersion, surface functionalization or incorporation of surfactants is adopted to achieve a more uniform dispersion. Each method has its own advantages and disadvantages. More details can be found in for instance following review [119].

Depending on the final morphology and shape of the composites, further processing is possible by extrusion [224], compression molding [47,51,65], film casting [3,46,51,82,154,161,194], and spinning [225]. The piezoresistivity of these CPCs can be tuned by controlling the concentration of the conductive fillers [225,226], the interaction between the fillers and matrix [46,194], and the conductive network morphology [47,65,161,202,227]. Normally, a compromise between sensitivity, conductivity, mechanical stretchability, and stability is required through the optimization of the filler loading and conductive network morphology. This approach has some significant inherent advantages, such as simple fabrication processes, low cost, and high structural integrity. However, the sensing performance and mechanical integrity may deteriorate under long-term large cyclic mechanical deformation.

Strain sensors can also be produced by assembling conductive material layers on or embedded in flexible substrates. Typically, the fabrication methods are classified into two categories. The first category relies on the conductive materials layers deposited on top of the flexible substrate through direct coating (e.g. drop-casting [50], dip-coating [38], Meyer rod coating [160], spray coating [45], bar coating [39], spin coating [15], transferring [139], infiltration [40], or printing [42]). The strain sensors with layered structure are generally fabricated on or embedded in stretchable substrate like PDMS [41], Ecoflex [45], due to their appropriate flexibility and strength for flexible electronics. Such strain sensors can be used for both integral measurement on a certain surface or local measurement at a certain position depending on the sensor geometry. However, some limitations still exist, including that the solution-based process is not environmentally friendly, the uniformity of the nanomaterials film is hard to control, as well as the bonding interaction between nanomaterials layers and elastomeric substrate is weak, which may lead to delamination and/or buckling of the conductive layers. The second category relies on conductive materials encapsulated within the flexible substrate, which is suitable for fabricating conductive networks with relatively large thickness [101].

Another method for realizing stretchable strain sensors is based on structural design of strain absorbing interconnections, such as wrinkled [82] (Fig. 10F) and buckling [85] (Fig. 10A) structures, wavy [87] (Fig. 6A) and serpentine [172] (Fig. 12A) patterns, open-mesh geometry [139] (Fig. 4D), and Kirigami-like structure [228] (Fig. 12B). Next to stretchable electrode making, a mogul-patterned stretchable substrate [229] (Fig. 12C) also offers a possible strategy for stretchability enhancement for layer structured strain sensor. These strain-relief structures permit the use of metallic films and semiconductor nanoribbons. For example, multiscale wrinkled microstructures have been built through coating AgNWs/waterborne polyurethane composite layers on the surface of pre-strained commercial PU fibers [82]. The wrinkled microstructures inside the piezoresistive fibers made contributions to the elimination of the viscoelastic delay of polymer composites [82]. Similarly, highly stretchable (up to 1320%) sheath-core conducting fibers have been fabricated by Liu et al. [85] through wrapping carbon sheets oriented in the fiber direction on stretched rubber fiber cores. The resulting structure exhibited a distinct short and long-period sheath buckling structure. The pre-strain process is however not preferable for large-scale manufacturing. Alternative approaches are being developed for the fabrication. More information can be found in following review [44].

The anisotropic property of wrinkled and buckling structures can also be used to discriminate strains of different directions, which enables the sensors precise monitoring of movement and surface conditions of targeting objects. In contrast, these conductive fibers exhibit a very small resistance change even under large strain [82,85]. Fabricating the substrate into a wavy shape largely improves the stretchability of the whole system. Serpentine structures [172,230] are 2D or 3D arrays of a repeating horseshoe-shaped unit, which might be selected if digital patterning and low cost are more important considerations than complex function or high-performance operation. Current research on this topic is focused on new material and specialized structure design. As for the structured strain sensors, it should be noted that the adhesion between the conductive layer and the substrate should be strong enough to remain the structural integrity. Otherwise, the use of inherently rigid materials can lead to cracks and fractures during long-term use.

By specific structure design, the strain sensors can be very sensitive to detect very small mechanical motions. Some bio-inspired micro/nanostructures such as interlocked microdomes [108] (Fig. 3A) or nanofiber arrays [109], whisker arrays [126,127] (Fig. 3B), and silk-molded microstructures [129] (Fig. 3C) are efficient ways for improving the sensitivity or obtaining multiple sensing capabilities or enhanced interfacial adhesion [231]. Piezoresistive strain sensors based on elastomer/rubber filled with conductive fillers normally show slow response and high hysteresis. However, the structured strain sensor with interlocked microdome arrays [108] shows fast response with a minimal dependence on temperature. On the other hand, the stretchability of these materials is low. In addition, while these strategic structural design are effective for creating sensors, they often need complex, multistep, and time-consuming microfabrication processes, which normally requires elaborate adjustment of the experimental conditions. They also still need to confirm their long-term reliability, economic feasibility and possibility for a high yield.

To further reflect the current status of the field, the last two columns in Table 1 summarize the fabrication process and special structural design, experimental GFs and hysteresis behavior extracted for more recently reported flexible and stretchable strain sensors. A distinction is made between strain sensors fabricated based on mainly blending of two or more components, including also processes such as infiltration, coating, transfer and filling (Part A) and strain sensors fabricated via multi-steps, which may involve the above mentioned or other processes employing special structural design for the conductive functional component and/or substrate (Part B). It is again shown that each approach has its own advantages and disadvantages (e.g. contributing to high sensitivity [39,40,50] or low hysteresis [39,59,136] while involving a multi-step process [39,40,50,59,73,136], or offering a simple fabrication route while showing less satisfied sensing performances [42,46,48]). The proper selection of matrix/substrate and conductive materials is therefore crucial for optimum performance achievement, while the preparation and formulation methods have even stronger impact on the final performance [48,136]. A more practical, cost-effective, mass-producible, faster and easier way to fabricate

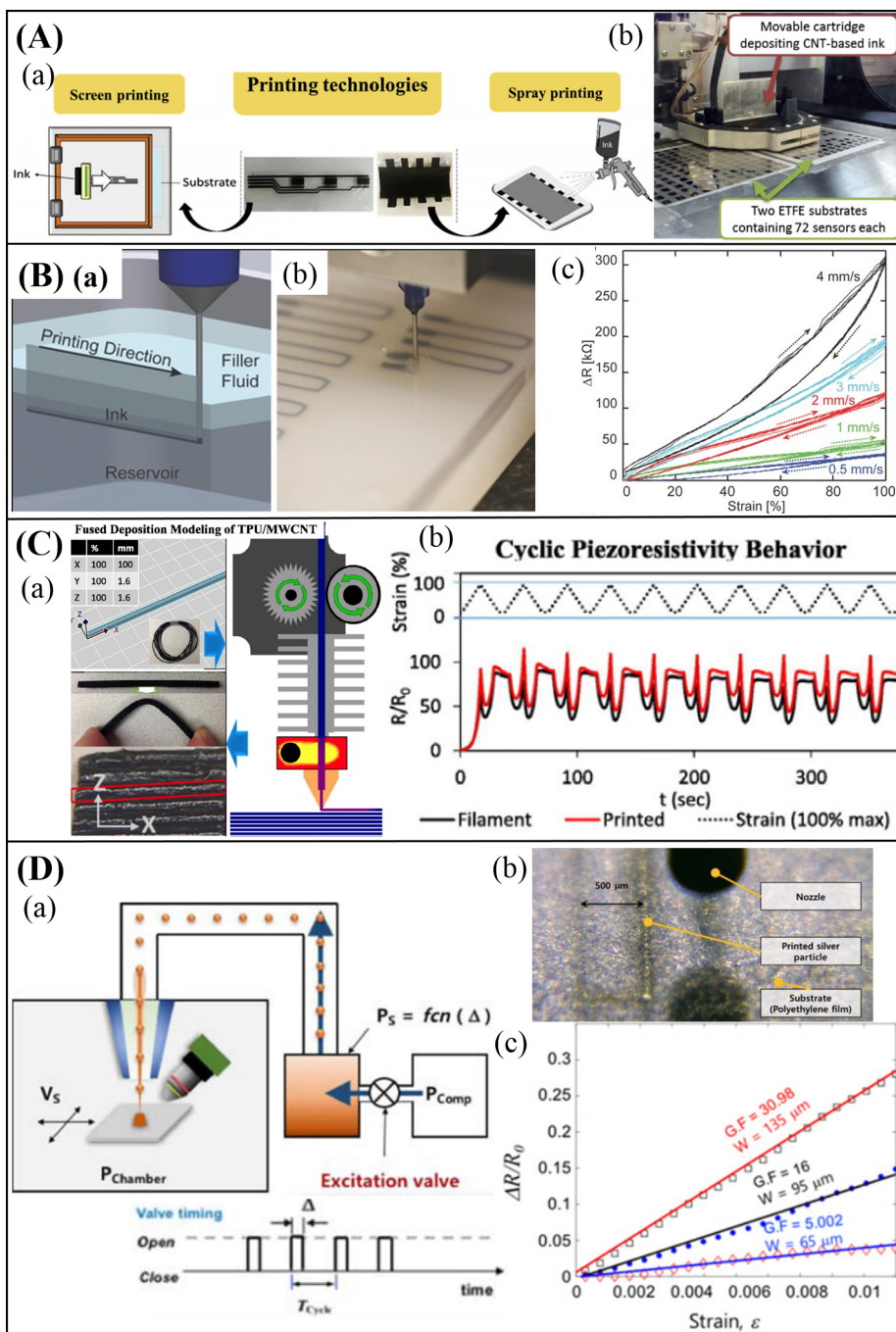


Fig. 13. Summary of printing techniques for strain sensor fabrication. (A) Non-digital printing with (a) screen printing and spray printing [226]; (b) inkjet printing [235]. (B) Conductive ink based 3D printing with (a) schematic illustration of the embedded 3D (e-3DP) printing process; (b) photograph of e-3DP for a planar array of soft strain sensor; (c) electrical resistance change as a function of elongation for sensors subjected to cyclic deformation [42]. (C) Fused deposition modelling with (a) TPU/MWCNT fused deposition modelling process; (b) relative resistance change under cyclic strain [248]. (D) Aerodynamically focused nanoparticle (AFN) printing with (a) a simplified schematic illustration of the AFN printer; (b) in-situ image captures silver nanoparticle printing; (c) relative resistance change as a function of strain of the printed strain sensor [246].

flexible and stretchable strain sensor with high sensitivity, high stretchability, low hysteresis, and long-term durability still needs to be developed.

6. Scale-up potential

Numerous strategies have been adopted to fabricate flexible and stretchable strain sensors, ranging from lab scale approaches (see Section 5) to scalable extrusion-based processing [64] and printing [42,230,232] techniques. The lab scale methods are normally employed for exploratory studies, involving either new materials or new applications for established materials, or performance optimization. The majority of current lab scale manufactured strain sensors are one-off prototypes. They lack manufacturing extensibility and scalability, as mass production is required for practical applications. Printing technology is a quite promising candidate for large-scale manufacturing. This is due to the large-area and high-throughput production capabilities, and the ability to create complex conductive geometries on a single printing platform that cannot be easily achieved by previous and non-automated approaches. It also does not require a mold [28,230]. Also, printing technology is more efficient and cost-effective [36,224,230,233].

Key components for printed flexible and stretchable strain sensors are flexible substrate or monitored structural parts [234] and conductive materials such as conductive inks [42,235]. It is crucial to use an elastomer that can be easily printed and has no impact on the subsequent process. The choice of the base elastomer should be optimized on the hardness and elasticity. Silicon rubbers [28,42] (e.g. PDMS, Ecoflex) are considered to be the best choice as substrate with remarkable stretchability and flexibility [36]. Conductive materials such as graphite [236], graphene [237], CNTs [235], PEDOT:PSS [238], and silver [234,238,239] in pure form or in the form of composites with elastomers and in general polymers [240] have been employed to fabricate printed strain sensors. Generally, nanoparticle-based inks possess the ability to create precise patterns, while 1D and 2D materials are difficult to pattern with good electrical properties [36]. CNT inks are widely used for printed flexible strain sensors [42,147,235]. Except conductive inks, some kinds of 3D printing filaments infused with CNTs and graphene are already commercially available [241].

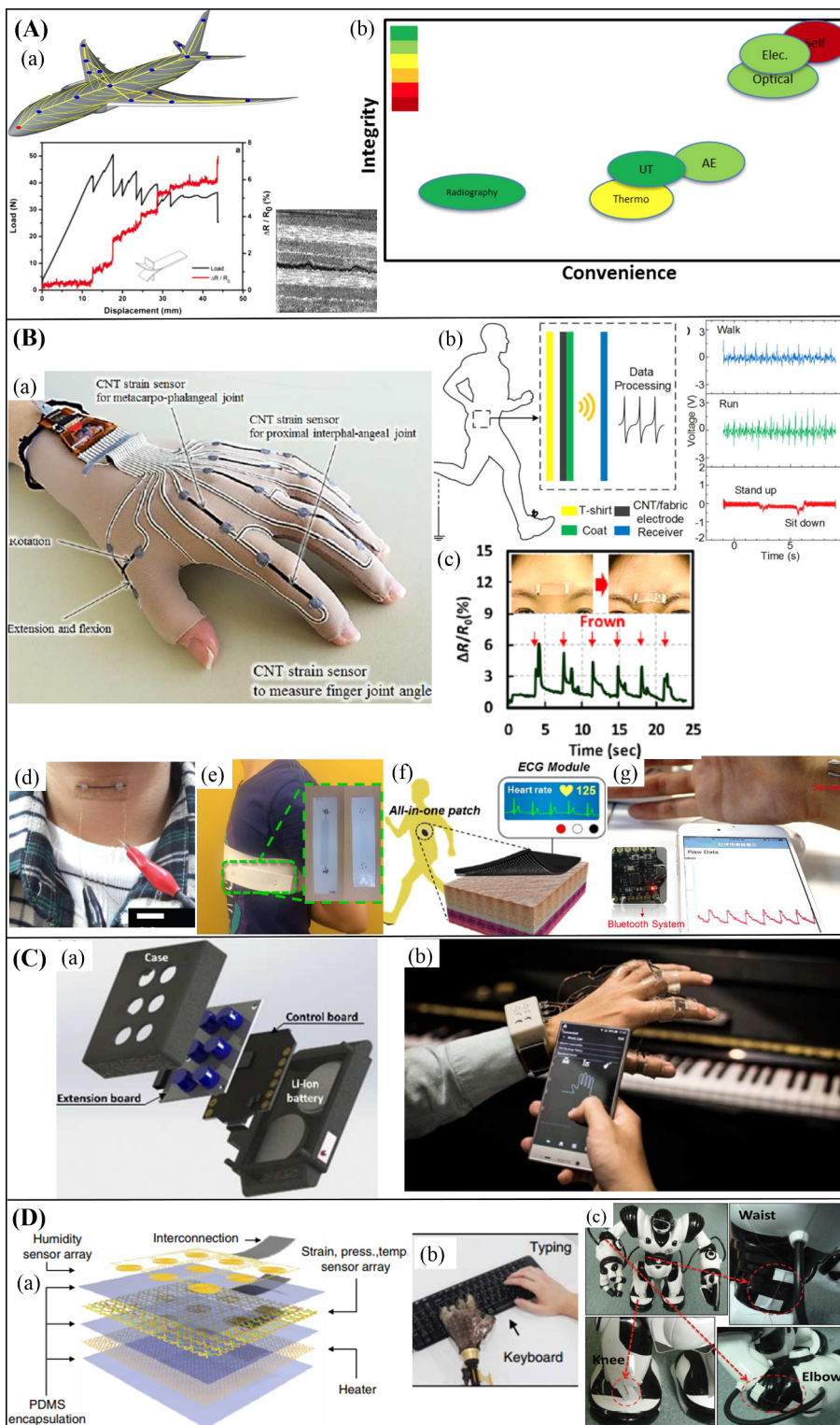
Printing techniques are sub-divided into two categories: (i) master printing and (ii) digital printing [37]. A pre-patterned printing plate as a master is required for the master-printing techniques, which include flexography, gravure printing, offset printing, and screen printing. These techniques are suitable for applications without high complexity and superfine resolution requirement [101]. Digital printing technique is “master free” and based on the relative motion between substrates and the printing head or nozzle [37]. The digital printing techniques encompass inkjet printing, direct ink writing, and laser patterning, which are more attractive due to their easily controlled programmable fabrication process [37] and architecture [227]. Generally, the printed flexible and stretchable strain sensors are fabricated by screen printing [126,224,226,239,242,243] (Fig. 13A (a)), inkjet printing [224,235,238] (Fig. 13A (b)), and three-dimensional (3D) printing [42,232,244] (Fig. 13B and C), which has drawn much attention for directly realizing complex objects [36].

Among all-printing techniques, screen and inkjet printing are well suited for smaller-scale prototyping and have drawn much interest due to their maturity of printing procedures and availability of compatible inks and substrates [234]. The variation in characteristics of printed sensors is especially large in manual screen printing, which makes digital printing more attractive [234]. Inkjet printing shows great advantages of high spatial precision of ink droplet and feature design for personalized electronics, while it is only appropriate for application scales ranging from device prototyping up to medium-scale production throughputs, due to its serial printing nature [233]. The rheological properties of inks, in terms of surface tension and viscosity may although bring problems for inkjet printing process. Besides, the wetting and adhesion between substrate and conductive inks, the substrate swelling, thermal hardening, and thermal expansion [101] may inhibit the printing process. Moreover, cracking and low stretchability may be the resulting issues found in the printed stretchable devices. Additional information related to recent advances in inks, and strategies about inkjet printing can be found in following reviews [101,245]. More recently, the aerodynamically focused nanoparticle (AFN) printer (Fig. 13D) was utilized for strain sensor printing of for instance silver nanoparticles [246]. Compared to inkjet printing, this method is solvent-free, room temperature adaptable, and has some advantages for flexibility and compatibility [246].

While further exploration and improvement of dynamic strain sensing performance are still required, 3D printing technology is increasingly been used for directly printing sensing components [42,230,232,247,248]. For example, Muth et al. [42] fabricated a flexible and stretchable strain sensor with conformal and extensible elastomeric matrices by embedded 3D printing (e-3DP) technology (Fig. 13B). A viscoelastic ink made of carbon conductive grease was directly printed into an elastomeric reservoir. Different finger gestures can be monitored by resistance variations. The GF for all sensors collapsed to a single value of 3.8, while significant hysteresis was observed during cyclic stretching. Alternate inks are needed for the optimization of sensor performances [42]. Besides conductive ink printing, multidirectional embedded strain sensors based on pure TPU and TPU/MWCNT nanocomposites were recently fabricated by Christ et al. [232,248] through 3D printing in tandem using a low-cost multi-material fused deposition modeling (FDM) printer (Fig. 13C). The printed sensors showed strong piezoresistive response to strain as high as 100% in both the axial and transverse directions [232]. The strain sensor depicted possesses low sensitivity and evidenced hysteresis [232,248], which is observed for the majority MWCNT-elastomer based CPCs strain sensors. CNTs as an additive incorporated into filaments for FDM are relatively new [241], as the difficulties in mixed material filament production and especially the additional problems associated with the rheology and flux during FDM extrusion are still needed to be properly addressed. Moreover, maintaining uniform performance during the printing process is challenging [102]. In addition, 3D printing technologies involve some inevitable problems such as the requirement of expensive machines, limited printable materials, intellectual property rights and legal ethics problems, as well as low mass production efficiency [244].

Overall, low-cost printing methods potentially enable the medium and large scale volume production of flexible electronics, while some problems still exist. For example, inks used for printing strain gauges are sensitive to temperature variations [234]. Also, the

prepared ink is not solvent free [235] and rheological properties should be tailored to meet the printing requirements [42,147]. Moreover, several criteria must be fulfilled to achieve successful device fabrication [42], which inevitably limit the printing adaptability for most materials. To promote widespread adoption of printing technology by industry, the printing process should be



(caption on next page)

Fig. 14. Diagram of some applications of flexible and stretchable strain sensors. (A) Structural health monitoring/damage detection with (a) illustration of a “smart aircraft” with fully embedded sensory network for damage detection; (b) comparisons between various structural health monitoring methods and their possibility of in situ damage detection in composites [4]. (B) Human motion detection and healthcare with (a) data glove with CNT strain sensors for finger joint motion detection [136]; (b) smart patch for human motion (walking, running, standing) state detection [97]; motion detection induced by (c) human emotions [146]; (d) muscle movement of trachea and esophagus [149]; (e) respiration [99]; (f) heartbeat [110]; and (g) wrist pulse [150]. (C) Human machine interface with (a) layout of wearable device; (b) schematic illustration of a wearable wireless music instrument based on GWF/PDMS woven fabric strain sensor [133]. (D) Electronic skins with (a) an exploded view of artificial skin for prosthetic; (b) an image of the prosthetic limb tapping keyboard and the corresponding resistance change versus time [138]; (c) images of a robot wears fiber sensors at movable joints [281].

further optimized to produce printable devices with more uniform performances and high resolution [233]. Also, in order to achieve robust and reproducible devices by reducing or avoiding the influence of surrounding changes, further exploration is demanded for practical system-packing solutions. For extremely large scale and high-throughput application, roll-to-roll printing methods are although more applicable [233]. The top-down approach with roll-to-roll techniques has seen remarkable success for CNT-based electronics due to their compatibility with batch fabrication. However, it is challenging to realize large-scale manufacturing of nanowire-based electronics because of their large-scale synthesis methods and bottom-up assembly methods through which it is difficult to achieve the same level of precision, uniformity, and scalability. Except the printing process optimization, an emerging trend is also to develop all-printed sensor devices [224,249] with full integration systems [36,250] without any external processing. Issues here are still the fabrication of flexible circuits, batteries, protecting layers by printing methods and/or comparable low-cost fabrication strategies for seamlessly structural integration [126].

In recent years, fiber or fiber assemblies (textile/fabric structures) have been utilized to prepare flexible strain sensors via add-on or built-in approaches, which make it possible to develop large-area electronic systems for wearable devices. Generally, the approaches for the fabrication of fiber-based flexible and wearable electronics are divided into two categories. The first category is the single fiber type, which is made from conductive polymer, metallic nanoparticles/nanowires, carbon-based micro/nano materials, or conventional fibers/yarns surface modified with conductive materials. A good example is the sheath-core structured strain sensors by using ultrafine graphite flakes as the sheath and single silk fibers as the core through a Meyer rod coating strategy [160]. The second category is the fabric type with electronic functions imparted through coating, printing or a lamination process on the surface of the fabrics [251]. The flexibility and comfort of the fabric may be compromised when using rigid components, thus, imparting electronic functions at the fiber level is more desirable [251]. Fabric-based sensors have been not only demonstrated as prototypes but also used in real applications [96,251]. More information about fiber/fabric-based strain sensors can be found in following review [251].

Some explorations for scalable fabrication of flexible and stretchable strain sensors based on fabrics or off-the-shelf materials are emerging. For example, a flexible conductive cotton fabric used as strain sensor has been fabricated through vacuum filtration of graphene oxide solution, which is now readily available on the market, and a hot press reduction method. The as-prepared strain sensors showed reproducible sensing characteristics [252]. Wang et al. [128] fabricated wearable strain sensors that can be stretched up to 500% with high sensitivity (GF of 9.6 for strain within 250% and 3.8×10 for strain of 250–500%) by utilizing carbonized plain-weave silk fabric (Fig. 3C) as sensing elements embedded in Ecoflex. Similar strain sensors based on cotton have also been developed [130]. They exhibit a GF (slope) of 2.5×10 and 6.4×10 under strain of 0%–80% and 80%–140%, separately, and superior capability for detecting subtle strain as low as 0.02%, inconspicuous drift, and long-term stability. The high performances are attributed to the reversible contact and separation of tentacle-like cotton fibers [130]. Similarly, Shi et al. [253] have fabricated high performance composite strain sensors with tunable GFs of 2.8×10 – 1.7×10^2 by pressing graphene platelets on a medical tap. The sensors also presented fast response, ideal linearity and reproducibility to tensile strains. As sensors from ordinary textile fabrics have relatively small strain range and low long-term stability, Cai et al. [254] developed a fabric strain sensor by dip-coating graphene oxide on elastic nylon/PU fabrics and then conducting a reduction process. The strain sensor showed high sensitivity, fast response, and great stability with a working range up to 30%. The aforementioned methods are thus promising for cost-effective and scalable fabrication. However, the performance stability after a prolonged period of wearing or repeated deformation cycles needs to be still guaranteed as most reported fabric-based sensors suffer from deterioration upon application [251].

Despite the progress described above, some issues or disadvantages such as the need for a high temperature heat treatment process [128,130], the use of non-abundant active materials [252], performance uniformity, and structural robustness still need to be addressed before the actual implementation of large scale production. Hence, more research efforts are critically needed for developing simple, reliable, low-cost, and large-scale manufacturing strategies.

7. Applications

The low working voltage and energy consumption make resistive-type devices ideal for wearable/portable electronic systems. Promising applications of flexible and stretchable strain sensors include structural health/damage monitoring [1–5], human motion detection [6,7,136], personal healthcare [6,8–13], human-machine interfaces [14–17], and electronic skin [18–20]. Since there are several recent and detailed reviews [14,102,104] summarizing the application potential of flexible strain sensors in the present contribution only three major application fields are covered.

7.1. Structural damage and health monitoring

Cracking or damage monitoring in large structures such as maritime applications, airplanes, bridges, and buildings requires typically high GFs and large strain measurement capability. With the increasing demand of fiber-reinforced composites (e.g. carbon fiber reinforced composites [255,256]) in e.g. the aerospace, marine, and automobile industry, a significant safety and reliability concern is to monitor the structural integrity of such materials. Especially for laminated composites (Fig. 14A), whose out-of-plane properties are weak compared to their excellent in-plane properties, this monitoring is highly recommended [4].

Existing solutions are using combinations of FBGs and ultrasonic sensors to track the displacement evolution and crack propagations in the composite [5]. However, the complicated method requires expensive instrumentation for signal analysis. Also as FBGs are sensitive to moisture and chemicals, a protected polymer sheath is needed, so that the diameter becomes at least ten times larger than that of reinforcement fibers, possibly leading to localized weak points in the composite part. Additionally, the production costs for large parts can be too high. If damage or cracks occur at different locations without crossing one of the FBG sensors, there is also a lack of performance [5].

An electrical resistance measurement strategy can be seen as an effective approach with advantages in price and simplicity. The self-sensing of carbon fibers [2,255,257–259] or CNTs [2,4,5,67,148,260,261] has been utilized to detect internal damage and failures in composites, taking into account the intrinsic electrical conductive nature. However, due to the anisotropic structure and complex failure pathway, the majority of damage and fractures dominated by the matrix is hardly to be monitored with conductive fibers [5]. Carbon fiber laminates are comparatively less sensitive to matrix damage [262]. Compared with traditional carbon fibers, CNTs are smaller and have an outstanding reinforcement efficiency in both mechanical and electrical properties [68]. A great potential for isotropic reinforcement and damage self-sensing thus arises. The modification of the polymer matrix with CNTs provides also opportunity to increase damage sensitivity [262]. In any case, one still needs to control the initial resistance of the developed sensors as a too high values imply difficult signal processing and reading. In this respect promising are multicomponent mixtures based on basic conductive fillers that upon design of the formulation variables can cover a wide range of initial resistances [293–295].

It should be put forward that fiber-reinforced polymer composites are still an important class of engineering materials in case fiber breakage is not an issue [263]. As for this aspect, in-situ structural health monitoring has been recently pushed forward by transferring the conductive network from the matrix to the interface of fiber-reinforced polymer composites [264]. Generally, the conductive network within the interphases is built up by incorporating CNTs [260,263,265–268] or graphene [266,269], onto the reinforcing fiber surface (e.g. glass fiber [263,265,267,269], carbon fiber [260]) via coating [265,269] or a deposition process [260,263,266,267]. Electrophoresis, and in-situ growth of the CNTs (e.g. by chemical vapor deposition [267]) on the surface of the fibers have allowed improving interlaminar properties and increasing through-thickness conductivity for carbon, glass and alumina fibers [219]. A major benefit is that the diameter is smaller or comparable with those of the reinforcing fibers of the composite unlike FBGs which are much thicker [264]. Due to their small size, CNTs are able to create electrically conductive networks surrounding structural fibers [270] and are adopted in most cases [260,263,265–268,270]. Composites with MWCNT-modified fibers show great potential for in-situ fiber- and fiber/matrix interface damage sensing [263], or localized structural health monitoring by controlled CNT deposition into damage prone zones [263,265]. Furthermore, CNTs in the relevant interphase or designed region have the advantage to reduce the weight usage [265,268] and flow distances [219], exclude structure distortions of the composites owing to their early warning ability [268], and avoid nanofiller drawbacks such as filtering or increased resin viscosity [219,260,265].

Producing highly conductive hierarchical composites of nanofiller/macroscopic fiber/polymer matrix is although still a challenge [219]. Despite the huge potential of CNT loaded composites [2,4,5,67,148,261] or CNT interface modified fiber reinforced composites [268] for structural health monitoring, numerous challenges relating to processing, integrity of the structure, cost, safety, and environmental issues are still relevant in view of real industrial application [4]. In addition, precisely detecting and locating cracks in structural components and joints that have specific densities are still challenging problems and demands sensors with much higher sensitivity [271].

7.2. Human motion detection and healthcare

As the mechanical properties of flexible and stretchable electronics resemble those of human tissues and their functional behavior can be similar to conventional rigid sensing electronics, these sensors can be used to measure and quantify electrical signals generated by human activities. In other words they can be considered for human-motion detection and personal healthcare (Fig. 14B).

Generally, flexible and stretchable strain sensors are utilized in skin-mountable [73,136] (Fig. 14B (a, c, e, f)), fabric wearable [96,97] (Fig. 14B (b)), or implantable forms [9]. The detection of human motions ranges from large strain (e.g. bending strain of joints [94,95] of fingers [42,98,136] (Fig. 14B (a)), hands [220], and knees [98] induced by movements such as grasping, walking, and running [97] (Fig. 14B (b)) to small strain motions (e.g. tiny skin motion induced by facial expression [15,146] (Fig. 14B (c)), phonation [149] (Fig. 14B (d)), respiration [99], and heartbeat [100,110]). By mounting the strain sensors in different parts of the human body, the sensing signal can be used for real-time movement and load measurements of athletes [272]. A problem that persists in the current research field is that many of the human activities are still not addressed for monitoring purposes [169]. On the other hand, the real-time tracking of physiological signals, such as respiration rate [99] (Fig. 14B (e)), heart-beat rate [110] (Fig. 14B (f)) or pulse rate [150] (Fig. 14B (g)) provides a convenient and non-invasive way for disease diagnoses and health assessments.

Currently sensors have been placed mostly on the trunk, upper arm, the forearm, the wrist, and the finger to measure the kinematics and/or posture [273]. Sensors are typically attached rather than embedded in wearable devices and garments [273]. For

wearable devices, smart textiles have been predicted to be the future of wearable technologies [169]. Typical functions of smart textiles are sensing and reacting, possibly also energy supply, data processing, and communication [274]. Conductive textiles have been developed with the purpose of health monitoring [169,274,275] as strain gauge sensors as well as for detection and monitoring posture, position of body segments, and body motion [169]. The most important progress in textile sensors for health monitoring is in the area of heart beats sensing [169,274,275].

For these particular applications, however, various challenges exist for practical usage. For example, to distinguish different body movements and/or to extract other physiological information, the precision, sensitivity, long-term stability, and biocompatibility of devices must be improved to meet the standard requirements. Robust interfacial adhesion between the devices and tissues is also demanded for high measurement quality. Additionally, cost-effective, reproducible fabrication strategies are required for mass-production and commercialization.

Printing and 3D printing electronic technology are promising in this respect. However, there still exists the problem that the flexible printed sensors used for health monitoring are not of the optimum quality which affects the long-term sensitivity. This has been ascribed to the design and fabrication procedure of the sensor [169]. In addition, miniaturization and simplicity of configuration of the devices, as well as decreasing power consumption are still considerable challenges. Self-powered sensing devices have been developed to meet the power demands of wearable health monitoring systems [216–219], while the power generation efficiency and power capacity should be further improved to satisfy the practical long-time application. Except the performance optimization, multifunctionality, long-term sustainability, and multifunction integration of wearable healthcare devices have attracted increasing attention [19]. For a more detailed description on the flexible and stretchable strain sensors for human motion detection and healthcare applications, the reader is referred to the following references [8–11,19,276].

7.3. Human machine interfaces and electronic skins

For human machine interfaces, flexible and stretchable strain sensors are capable to integrate with curved surfaces [15,16]. This allows to detect the contact force and location, physical activities, health status, and the surrounding environment, and to send the monitored data to the integrated smart systems [15,17]. A good example is the recent work from Liu et al. [133] with a highly flexible and sensitive strain sensor based on graphene woven fabric (GWF)/PDMS composite integrated with wearable interface and wireless communications into a musical instrument, which can convert human body motions to controllable music (Fig. 14C) [133]. The sensors can be also potentially used as electronic skin [19,20] (Fig. 14D) in prosthetics [138,277,278] and robotics [279,280]. The flexible, soft and compliant strain sensors can be used as prosthetic skins (Fig. 14D (a)) to mimic the real-skin and transmit the stimuli-responsive electrical signals to specific peripheral nerves for nerve stimulation [138]. This allows patients to comfortably use their devices during intimate interactions [278]. To fully mimic the natural properties of skin, it is important to implement materials with low elastic moduli and good stretchability [278].

For robotics applications, the electronic skins can be used to monitor complicated robotic movements in real time [281], to remote control [74] and to actuate the smart robots [280], to detect the environment, and to interact with surrounding objects [279], or to perceive tactile [282]. Additional information about the human-machine interface and electronic skins can be found in following reviews [14,18–20]. The integration of flexible and stretchable sensors into wearable platforms is in the form of skin patch [15,98,129], wrist band [56,133], neck band [73,215], data glove [95,136], belt [190], and strap [283]. More information about the advances in wearable sensing systems and representative examples of integrated sensor devices are included in a recent review from Lee et al. [189].

7.4. Common challenges

Despite the intense research in the above application fields, the development of flexible and stretchable strain sensors for practical usage is still at the early stage. Sensing systems that are used for monitoring are of high technical complexity [169]. The integration of sensors with power, data analysis, data processing, wireless data transmission, as well as display and operation systems [102] in a soft and compact device with robustness, high reliability, and long-term monitoring potential has not yet been achieved.

Most studies are proof of concept [249]. Several fundamental and technical challenges still remain to be addressed, including rational sensing platform and device configuration design for a specific application, simple, economical and macroscale fabrication, and full integration of all components. Considering scalability and costs, fully printed artificial devices are more attractive for the future sensing platforms. Supplying self-sustainable power is another important requirement. In addition, further development of advanced techniques for seamless integration [284] will make it possible to bring the developed physical sensing platforms closer to reality.

8. Conclusions

The present contribution highlights that the working principle of piezoresistive strain sensors, which translate strain alternations into resistance changes, is fundamentally based on a tunneling effect, a disconnection mechanism or a crack propagation mechanism. In view of maximization of the sensor performance the rational selection of the conductive materials and the matrix/substrate, the control over interfacial interaction, and in particular delicate assembly of conductive fillers and unique structural features are crucial.

The main design variables are the sensitivity or gauge factor, the stretchability, the linearity, and the hysteresis. More novel variables are self-healing, self-powering, self-cleaning, transparency, biocompatibility, and biodegradability. The sensitivity can be

optimized by conductive network morphological control strategies and by adopting processing thus manufacturing procedures. Stretchability can be increased by adapting the stretchable materials or through structural conversion. Linearity can be most easily quantified by the coefficient of determination and a switch to non-linearity is ascribed to an alternation from a (quasi-)homogeneous to a more heterogeneous morphology. Hysteresis is in turn explained by the competition of network breakdown and reformation during cyclic loading.

Despite that strain sensing performances have been significantly improved and progress has been made for the development of more basic fabrication techniques and material structural engineering, most piezoresistive strain sensors developed to date are still one-off prototypes and many challenges still exist. For scale-up, main focus has been on extrusion-based processing and printing techniques. The latter techniques are promising due to the large-area and high-throughput production possibilities, in particular for more complex geometries. Disadvantages for large-scale production are performance uniformity and structural robustness. A challenge is also to guarantee the comparable advantages of capacitive stretch strain sensors. Here focus should be put on the minimization of electrical and mechanical hysteresis, which cause slow response due to relaxation time of the conductor, and low sensitivity under small strain. In addition, the viscoelastic nature of the rubber/elastomer may suffer from a relatively late response time, which prevents its use in high-frequency applications. Another challenge for piezoresistive strain sensors is their electrical and structural stability, especially under large stretching with possible irrevocable collapse of the structure.

Major challenges and research opportunities from an application point of view also originate from the rational sensing device design and elegant integration of flexible strain sensors with other critical components such as power, data processing, analysis, and transmission. For multiple stimuli monitoring, strain sensors should be effectively integrated with other transducers. It is further challenging to achieve integrated devices with diminishing size and weight. At the same time, the corresponding fabrication techniques, software, and protective and packaging techniques should be further improved.

Hence, it can be concluded that more comprehensive property control of piezoresistive strain sensors is still needed to enable real monitoring beyond lab scale application demonstration and commercialization. As the predominant motivation for stretchable and flexible strain sensor is for complicated human motion or other 3D objectives deformation capture/monitoring, research for reasonable multidirectional and geometrical design of such strain sensors should also be conducted to a larger extent.

Acknowledgments

L.D. appreciates funding from the China Scholarship Council (grant 201506240217) for the Ph.D. study at Ghent university. D.R.D acknowledges the Fund for Scientific Research Flanders (FWO) through a postdoctoral fellowship.

Declaration of Competing Interest

The authors declared that there is no conflict of interest.

Contributors

All three authors contributed to the writing of the manuscript. The structure of the article was proposed by three authors, with the detailed aspects covered in a first instance by L.D. and further adapted by D.R.D. and L.C. All authors have approved the final article.

References

- [1] Vertuccio L, Guadagno L, Spinelli G, Lamberti P, Tucci V, Russo S. Piezoresistive properties of resin reinforced with carbon nanotubes for health-monitoring of aircraft primary structures. *Compos Part B Eng* 2016;107:192–202.
- [2] Naghashpour A, Hoa SV. A technique for real-time detecting, locating, and quantifying damage in large polymer composite structures made of carbon fibers and carbon nanotube networks. *Struct Health Monit Int J* 2014;14:35–45.
- [3] Zha J-W, Zhang B, Li RKY, Dang Z-M. High-performance strain sensors based on functionalized graphene nanoplates for damage monitoring. *Compos Sci Technol* 2016;123:32–8.
- [4] Zhang H, Bilotti E, Peijs T. The use of carbon nanotubes for damage sensing and structural health monitoring in laminated composites: a review. *Nanocomposites* 2015;1:177–94.
- [5] Nag-Chowdhury S, Bellegou H, Pillin I, Castro M, Longrais P, Feller JF. Non-intrusive health monitoring of infused composites with embedded carbon quantum piezo-resistive sensors. *Compos Sci Technol* 2016;123:286–94.
- [6] Trung TQ, Lee NE. Flexible and stretchable physical sensor integrated platforms for wearable human-activity monitoring and personal healthcare. *Adv Mater* 2016;28:4338–72.
- [7] Liu Q, Chen J, Li Y, Shi G. High-performance strain sensors with fish-scale-like graphene-sensing layers for full-range detection of human motions. *ACS Nano* 2016;10:7901–6.
- [8] Wang X, Liu Z, Zhang T. Flexible sensing electronics for wearable/attachable health monitoring. *Small* 2017;13:1602790.
- [9] Choi C, Choi MK, Hyeon T, Kim D-H. Nanomaterial-based soft electronics for healthcare applications. *ChemNanoMat* 2016;2:1006–17.
- [10] Jin H, Abu-Raya YS, Haick H. Advanced materials for health monitoring with skin-based wearable devices. *Adv Healthc Mater* 2017;6:1700024.
- [11] Kenry YJC, Lim CT. Emerging flexible and wearable physical sensing platforms for healthcare and biomedical applications. *Microsystems Nanoeng* 2016;2:16043.
- [12] Chen M, Ma Y, Song J, Lai C-F, Hu B. Smart clothing: connecting human with clouds and big data for sustainable health monitoring. *Mob Networks Appl* 2016;21:825–45.
- [13] Andreu-Perez J, Leff DR, Ip HM, Yang GZ. From wearable sensors to smart implants-toward pervasive and personalized healthcare. *IEEE Trans Biomed Eng* 2015;62:2750–62.
- [14] Wang H, Ma X, Hao Y. Electronic devices for human-machine interfaces. *Adv Mater Interfaces* 2017;4:1600709.
- [15] Roh E, Hwang B-U, Kim D, Kim B-Y, Lee N-E. Stretchable, transparent, ultrasensitive, and patchable strain sensor for human-machine interfaces comprising a

- nanohybrid of carbon nanotubes and conductive elastomers. *ACS Nano* 2015;9:6252–61.
- [16] Lim S, Son D, Kim J, Lee YB, Song J-K, Choi S, et al. Transparent and stretchable interactive human machine interface based on patterned graphene heterostructures. *Adv Funct Mater* 2015;25:375–83.
- [17] Lee H, Kwon D, Cho H, Park I, Kim J. Soft nanocomposite based multi-point, multi-directional strain mapping sensor using anisotropic electrical impedance tomography. *Sci Rep* 2017;7:39837.
- [18] Zhao Y, Huang X. Mechanisms and materials of flexible and stretchable skin sensors. *Micromachines* 2017;8:69.
- [19] Park J, Lee Y, Ha M, Cho S, Ko H. Micro/nanostructured surfaces for self-powered and multifunctional electronic skins. *J Mater Chem B* 2016;4:2999–3018.
- [20] Case J, Yuen M, Mohammed M, Kramer R. Sensor skins: an overview. *Stretchable bioelectronics for medical devices and systems*. Springer; 2016. p. 173–91.
- [21] Lee C, Kim M, Kim YJ, Hong N, Ryu S, Kim HJ, et al. Soft robot review. *Int J Control Autom Syst* 2017;15:3–15.
- [22] Alamusi, Hu N, Fukunaga H, Atobe S, Liu Y, Li J. Piezoresistive strain sensors made from carbon nanotubes based polymer nanocomposites. *Sensors (Basel)* 2011;11:10691–723.
- [23] Atalay A, Sanchez V, Atalay O, Vogt DM, Haufe F, Wood RJ, et al. Batch fabrication of customizable silicone-textile composite capacitive strain sensors for human motion tracking. *Adv Mater Technol* 2017;2:1700136.
- [24] Sha F, Cheng X, Li S, Xu D, Huang S, Liu R, et al. Nondestructive evaluation on strain sensing capability of piezoelectric sensors for structural health monitoring. *Res Nondestruct Eval* 2017;28:61–75.
- [25] Kanaparthi S, Badhulika S. Solvent-free fabrication of a biodegradable all-carbon paper based field effect transistor for human motion detection through strain sensing. *Green Chem* 2016;18:3640–6.
- [26] Růžička M, Dvořák M, Schmidová N, Šašek L, Štěpánek M. Health and usage monitoring system for the small aircraft composite structure. *AIP Conf Proc*. 1858. AIP Publishing; 2017. p. 20007.
- [27] Lei Z, Wang Y, Qin F, Qiu W, Bai R, Chen X. Multi-fiber strains measured by micro-Raman spectroscopy: principles and experiments. *Opt Lasers Eng* 2016;77:8–17.
- [28] Mohammed MG, Kramer R. All-printed flexible and stretchable electronics. *Adv Mater* 2017;29.
- [29] Zheng Q, Shi B, Li Z, Wang ZL. Recent progress on piezoelectric and triboelectric energy harvesters in biomedical systems. *Adv Sci* 2017;4:1700029.
- [30] Shieh J, Huber JE, Fleck NA, Ashby MF. The selection of sensors. *Prog Mater Sci* 2001;46:461–504.
- [31] Dobie WB, Isaac PCG, Gale GO. Electrical resistance strain gauges. *Am J Phys* 1950;18:117–8.
- [32] Kanoun O, Muller C, Benchirouf A, Sanli A, Dinh TN, Al-Hamry A, et al. Flexible carbon nanotube films for high performance strain sensors. *Sensors (Basel)* 2014;14:10042–71.
- [33] Obitayo W, Liu T. A review: carbon nanotube-based piezoresistive strain sensors. *J Sensors* 2012;2012:1–15.
- [34] Coiai S, Passaglia E, Pucci A, Ruggeri G. Nanocomposites based on thermoplastic polymers and functional nanofiller for sensor applications. *Materials (Basel)* 2015;8:3377–427.
- [35] Noh J-S. Conductive elastomers for stretchable electronics, sensors and energy harvesters. *Polymer (Basel)* 2016;8:123.
- [36] Rim YS, Bae SH, Chen H, De Marco N, Yang Y. Recent progress in materials and devices toward printable and flexible sensors. *Adv Mater* 2016;28:4415–40.
- [37] Harris KD, Elias AL, Chung H-J. Flexible electronics under strain: a review of mechanical characterization and durability enhancement strategies. *J Mater Sci* 2016;51:2771–805.
- [38] Wu X, Han Y, Zhang X, Lu C. Highly sensitive, stretchable, and wash-durable strain sensor based on ultrathin conductive layer@polyurethane yarn for tiny motion monitoring. *ACS Appl Mater Interfaces* 2016;8:9936–45.
- [39] Amjadi M, Turan M, Clementson CP, Sitti M. Parallel microcracks-based ultrasensitive and highly stretchable strain sensors. *ACS Appl Mater Interfaces* 2016;8:5618–26.
- [40] Chen S, Wei Y, Wei S, Lin Y, Liu L. Ultrasensitive cracking-assisted strain sensors based on silver nanowires/graphene hybrid particles. *ACS Appl Mater Interfaces* 2016;8:25563–70.
- [41] Liu Z, Qi D, Guo P, Liu Y, Zhu B, Yang H, et al. Thickness-gradient films for high gauge factor stretchable strain sensors. *Adv Mater* 2015;27:6230–7.
- [42] Muth JT, Vogt DM, Truby RL, Menguc Y, Kolesky DB, Wood RJ, et al. Embedded 3D printing of strain sensors within highly stretchable elastomers. *Adv Mater* 2014;26:6307–12.
- [43] Zheng Y, Li Y, Li Z, Wang Y, Dai K, Zheng G, et al. The effect of filler dimensionality on the electromechanical performance of polydimethylsiloxane based conductive nanocomposites for flexible strain sensors. *Compos Sci Technol* 2017;139:64–73.
- [44] Zhao S, Li J, Cao D, Zhang G, Li J, Li K, et al. Recent advancements in flexible and stretchable electrodes for electromechanical sensors: strategies, materials, and features. *ACS Appl Mater Interfaces* 2017;9:12147–64.
- [45] Amjadi M, Yoon YJ, Park I. Ultra-stretchable and skin-mountable strain sensors using carbon nanotubes-Ecoflex nanocomposites. *Nanotechnology* 2015;26:375501.
- [46] Lin L, Liu S, Zhang Q, Li X, Ji M, Deng H, et al. Towards tunable sensitivity of electrical property to strain for conductive polymer composites based on thermoplastic elastomer. *ACS Appl Mater Interfaces* 2013;5:5815–24.
- [47] Liu H, Gao J, Huang W, Dai K, Zheng G, Liu C, et al. Electrically conductive strain sensing polyurethane nanocomposites with synergistic carbon nanotubes and graphene bifillers. *Nanoscale* 2016;8:12977–89.
- [48] Lin L, Deng H, Gao X, Zhang S, Bilotti E, Peijs T, et al. Modified resistivity-strain behavior through the incorporation of metallic particles in conductive polymer composite fibers containing carbon nanotubes. *Polym Int* 2013;62:134–40.
- [49] Slobodian P, Riha P, Saha P. A highly-deformable composite composed of an entangled network of electrically-conductive carbon-nanotubes embedded in elastic polyurethane. *Carbon* 2012;50:3446–53.
- [50] Zhao S, Guo L, Li J, Li N, Zhang G, Gao Y, et al. Binary synergistic sensitivity strengthening of bioinspired hierarchical architectures based on fragmented reduced graphene oxide sponge and silver nanoparticles for strain sensors and beyond. *Small* 2017;13:1700944.
- [51] Duan L, Fu S, Deng H, Zhang Q, Wang K, Chen F, et al. The resistivity–strain behavior of conductive polymer composites: stability and sensitivity. *J Mater Chem A* 2014;2:17085–98.
- [52] Cochrane C, Koncar V, Lewandowski M, Dufour C. Design and development of a flexible strain sensor for textile structures based on a conductive polymer composite. *Sensors* 2007;7:473–92.
- [53] Cochrane C, Lewandowski M, Koncar V. A flexible strain sensor based on a conductive polymer pomposite for in situ measurement of parachute canopy deformation. *Sensors (Basel)* 2010;10:8291–303.
- [54] Mattmann C, Clemens F, Troster G. Sensor for measuring strain in textile. *Sensors (Basel)* 2008;8:3719–32.
- [55] Zhao S, Li J, Cao D, Gao Y, Huang W, Zhang G, et al. Percolation threshold-inspired design of hierarchical multiscale hybrid architectures based on carbon nanotubes and silver nanoparticles for stretchable and printable electronics. *J Mater Chem C* 2016;4:6666–74.
- [56] Melnykowycz M, Tschudin M, Clemens F. Piezoresistive soft condensed matter sensor for body-mounted vital function applications. *Sensors* 2016;16:326.
- [57] Natarajan TS, Eshwaran SB, Stockelhuber KW, Wiessner S, Potschke P, Heinrich G, et al. Strong strain sensing performance of natural rubber nanocomposites. *ACS Appl Mater Interfaces* 2017;9:4860–72.
- [58] Lin Y, Liu S, Chen S, Wei Y, Dong X, Liu L. A highly stretchable and sensitive strain sensor based on graphene–elastomer composites with a novel double-interconnected network. *J Mater Chem C* 2016;4:6345–52.
- [59] Boland CS, Khan U, Backes C, O'Neill A, McCauley J, Duane S, et al. Sensitive, high-strain, high-rate bodily motion sensors based on graphene–rubber composites. *ACS Nano* 2014;8:8819–30.
- [60] Georgousis G, Pandis C, Chatzimanolis-Moustakas C, Kyritsis A, Kontou E, Pissis P, et al. Study of the reinforcing mechanism and strain sensing in a carbon black filled elastomer. *Compos Part B Eng* 2015;80:20–6.
- [61] Ma Z, Su B, Gong S, Wang Y, Yap LW, Simon GP, et al. Liquid-wetting-solid strategy to fabricate stretchable sensors for human-motion detection. *ACS Sensors* 2016;1:303–11.

- [62] Flandin L, Hiltner A, Baer E. Interrelationships between electrical and mechanical properties of a carbon black-filled ethylene–octene elastomer. *Polymer* 2001;42:827–38.
- [63] Qu Y, Dai K, Zhao J, Zheng G, Liu C, Chen J, et al. The strain-sensing behaviors of carbon black/polypropylene and carbon nanotubes/polypropylene conductive composites prepared by the vacuum-assisted hot compression. *Colloid Polym Sci* 2014;292:945–51.
- [64] Cravanzola S, Haznedar G, Scarano D, Zecchina A, Cesano F. Carbon-based piezoresistive polymer composites: structure and electrical properties. *Carbon* 2013;62:270–7.
- [65] Ke K, Potschke P, Wiegand N, Krause B, Voit B. Tuning the network structure in poly(vinylidene fluoride)/carbon nanotube nanocomposites using carbon black to: toward improvements of conductivity and piezoresistive sensitivity. *ACS Appl Mater Interfaces* 2016;8:14190–9.
- [66] Zeng Z, Liu M, Xu H, Liao Y, Duan F, Zhou L-m, et al. Ultra-broadband frequency responsive sensor based on lightweight and flexible carbon nanostructured polymeric nanocomposites. *Carbon* 2017;121:490–501.
- [67] Sánchez-Romate XF, Moriche R, Jiménez-Suárez A, Sánchez M, Prolongo SG, Güemes A, et al. Highly sensitive strain gauges with carbon nanotubes: from bulk nanocomposites to multifunctional coatings for damage sensing. *Appl Surf Sci* 2017;424:213–21.
- [68] He D, Salem D, Cinquin J, Piau G-P, Bai J. Impact of the spatial distribution of high content of carbon nanotubes on the electrical conductivity of glass fiber fabrics/epoxy composites fabricated by RTM technique. *Compos Sci Technol* 2017;147:107–15.
- [69] Cao X, Wei X, Li G, Hu C, Dai K, Guo J, et al. Strain sensing behaviors of epoxy nanocomposites with carbon nanotubes under cyclic deformation. *Polymer* 2017;112:1–9.
- [70] Bouhamed A, Al-Hamry A, Müller C, Choura S, Kanoun O. Assessing the electrical behaviour of MWCNTs/epoxy nanocomposite for strain sensing. *Compos Part B Eng* 2017;128:91–9.
- [71] Sanli A, Benchirouf A, Müller C, Kanoun O. Piezoresistive performance characterization of strain sensitive multi-walled carbon nanotube-epoxy nanocomposites. *Sensors Actuators A Phys* 2017;254:61–8.
- [72] Lin Y, Dong X, Liu S, Chen S, Wei Y, Liu L. Graphene-elastomer composites with segregated nanostructured network for liquid and strain sensing application. *ACS Appl Mater Interfaces* 2016;8:24143–51.
- [73] Hwang B-U, Lee J-H, Trung TQ, Roh E, Kim D-I, Kim S-W, et al. Transparent stretchable self-powered patchable sensor platform with ultrasensitive recognition of human activities. *ACS Nano* 2015;9:8801–10.
- [74] Gong S, Lai DT, Wang Y, Yap LW, Si KJ, Shi Q, et al. Tattolike polyaniline microparticle-doped gold nanowire patches as highly durable wearable sensors. *ACS Appl Mater Interfaces* 2015;7:19700–8.
- [75] Lim G-H, Lee N-E, Lim B. Highly sensitive, tunable, and durable gold nanosheet strain sensors for human motion detection. *J Mater Chem C* 2016;4:5642–7.
- [76] Niu H, Zhou H, Wang H, Lin T. Polypyrrole-coated PDMS fibrous membrane: flexible strain sensor with distinctive resistance responses at different strain ranges. *Macromol Mater Eng* 2016;301:707–13.
- [77] Yu GF, Yan X, Yu M, Jia MY, Pan W, He XX, et al. Patterned, highly stretchable and conductive nanofibrous PANI/PVDF strain sensors based on electrospinning and in situ polymerization. *Nanoscale* 2016;8:2944–50.
- [78] Choi DY, Kim MH, Oh YS, Jung SH, Jung JH, Sung HJ, et al. Highly stretchable, hysteresis-free ionic liquid-based strain sensor for precise human motion monitoring. *ACS Appl Mater Interfaces* 2017;9:1770–80.
- [79] Yoon SG, Park BJ, Chang ST. Highly sensitive microfluidic strain sensors with low hysteresis using a binary mixture of ionic liquid and ethylene glycol. *Sensors Actuators A Phys* 2017;254:1–8.
- [80] Jiao Y, Young CW, Yang S, Oren S, Ceylan H, Kim S, et al. Wearable graphene sensors with microfluidic liquid metal wiring for structural health monitoring and human body motion sensing. *IEEE Sens J* 2016;16:7870–5.
- [81] Hoang PT, Salazar N, Porokka TN, Joshi K, Liu T, Dickens TJ, et al. Engineering crack formation in carbon nanotube-silver nanoparticle composite films for sensitive and durable piezoresistive sensors. *Nanoscale Res Lett* 2016;11:422.
- [82] Wei Y, Chen S, Yuan X, Wang P, Liu L. Multiscale wrinkled microstructures for piezoresistive fibers. *Adv Funct Mater* 2016;26:5078–85.
- [83] Mu J, Hou C, Wang G, Wang X, Zhang Q, Li Y, et al. An elastic transparent conductor based on hierarchically wrinkled reduced graphene oxide for artificial muscles and sensors. *Adv Mater* 2016;28:9491–7.
- [84] Li C, Cui YL, Tian GL, Shu Y, Wang XF, Tian H, et al. Flexible CNT-array double helices Strain Sensor with high stretchability for Motion Capture. *Sci Rep* 2015;5:15554.
- [85] Liu ZF, Fang S, Moura FA, Ding JN, Jiang N, Di J, et al. Hierarchically buckled sheath-core fibers for superelastic electronics, sensors, and muscles. *Science* 2015;349:400–4.
- [86] Wang Y, Yang R, Shi Z, Zhang L, Shi D, Wang E, et al. Super-elastic graphene ripples for flexible strain sensors. *ACS Nano* 2011;5:3645–50.
- [87] Xu J, Chen J, Zhang M, Hong J-D, Shi G. Highly conductive stretchable electrodes prepared by in situ reduction of wavy graphene oxide films coated on elastic tapes. *Adv Electron Mater* 2016;2:1600022.
- [88] Shin MK, Oh J, Lima M, Kozlov ME, Kim SJ, Baughman RH. Elastomeric conductive composites based on carbon nanotube forests. *Adv Mater* 2010;22:2663–7.
- [89] Shang Y, He X, Li Y, Zhang L, Li Z, Ji C, et al. Super-stretchable spring-like carbon nanotube ropes. *Adv Mater* 2012;24:2896–900.
- [90] Lu N, Lu C, Yang S, Rogers J. Highly sensitive skin-mountable strain gauges based entirely on elastomers. *Adv Funct Mater* 2012;22:4044–50.
- [91] Guo CF, Sun T, Liu Q, Suo Z, Ren Z. Highly stretchable and transparent nanomesh electrodes made by grain boundary lithography. *Nat Commun* 2014;5:3121.
- [92] Chen M, Zhang L, Duan S, Jing S, Jiang H, Li C. Highly stretchable conductors integrated with a conductive carbon nanotube/graphene network and 3D porous poly(dimethylsiloxane). *Adv Funct Mater* 2014;24:7548–56.
- [93] Wang S, Huang Y, Rogers JA. Mechanical designs for inorganic stretchable circuits in soft electronics. *IEEE Trans Compon Packag Manuf Technol* 2015;5:1201–18.
- [94] Nakamoto H, Ootaka H, Tada M, Hirata I, Kobayashi F, Kojima F. Stretchable strain sensor with anisotropy and application for joint angle measurement. *IEEE Sens J* 2016;16:3572–9.
- [95] Zhu H, Wang X, Liang J, Lv H, Tong H, Ma L, et al. Versatile electronic skins for motion detection of joints enabled by aligned few-walled carbon nanotubes in flexible polymer composites. *Adv Funct Mater* 2017;27:1606604.
- [96] Yetisen AK, Qu H, Manbachi A, Butt H, Dokmeci MR, Hinestroza JP, et al. Nanotechnology in textiles. *ACS Nano* 2016;10:3042–68.
- [97] Shi M, Wu H, Zhang J, Han M, Meng B, Zhang H. Self-powered wireless smart patch for healthcare monitoring. *Nano Energy* 2017;32:479–87.
- [98] Wang C, Zhao J, Ma C, Sun J, Tian L, Li X, et al. Detection of non-joint areas tiny strain and anti-interference voice recognition by micro-cracked metal thin film. *Nano Energy* 2017;34:578–90.
- [99] Wang L, Loh KJ. Wearable carbon nanotube-based fabric sensors for monitoring human physiological performance. *Smart Mater Struct* 2017;26:055018.
- [100] Nassar JM, Mishra K, Lau K, Aguirre-Pablo AA, Hussain MM. Recyclable nonfunctionalized paper-based ultralow-cost wearable health monitoring system. *Adv Mater Technol* 2017;2:1600228.
- [101] Yu X, Mahajan B, Shou W, Pan H. Materials, mechanics, and patterning techniques for elastomer-based stretchable conductors. *Micromachines* 2016;8:7.
- [102] Yang T, Xie D, Li Z, Zhu H. Recent advances in wearable tactile sensors: materials, sensing mechanisms, and device performance. *Mater Sci Eng R Reports* 2017;115:1–37.
- [103] Rolnick H. Tension coefficient of resistance of metals. *Phys Rev* 1930;36:506–12.
- [104] Amjadi M, Kyung K-U, Park I, Sitti M. Stretchable, skin-mountable, and wearable strain sensors and their potential applications: a review. *Adv Funct Mater* 2016;26:1678–98.
- [105] Oliva-Avilés AI, Avilés F, Seidel GD, Sosa V. On the contribution of carbon nanotube deformation to piezoresistivity of carbon nanotube/polymer composites. *Compos Part B Eng* 2013;47:200–6.
- [106] Hu N, Karube Y, Arai M, Watanabe T, Yan C, Li Y, et al. Investigation on sensitivity of a polymer/carbon nanotube composite strain sensor. *Carbon* 2010;48:680–7.
- [107] Amjadi M, Pichitpajongkit A, Lee S, Ryu S, Park I. Highly stretchable and sensitive strain sensor based on silver nanowire-elastomer nanocomposite. *ACS Nano*

- 2014;8:5154–63.
- [108] Park J, Lee Y, Hong J, Lee Y, Ha M, Jung Y, et al. Tactile-direction-sensitive and stretchable electronic skins based on human-skin-inspired interlocked microstructures. *ACS Nano* 2014;8:12020–9.
- [109] Pang C, Lee GY, Kim TI, Kim SM, Kim HN, Ahn SH, et al. A flexible and highly sensitive strain-gauge sensor using reversible interlocking of nanofibres. *Nat Mater* 2012;11:795–801.
- [110] Kim T, Park J, Sohn J, Cho D, Jeon S. Bioinspired, highly stretchable, and conductive dry adhesives based on 1D–2D hybrid carbon nanocomposites for all-in-one ECG electrodes. *ACS Nano* 2016;10:4770–8.
- [111] Kang D, Pikhitsa PV, Choi YW, Lee C, Shin SS, Piao L, et al. Ultrasensitive mechanical crack-based sensor inspired by the spider sensory system. *Nature* 2014;516:222–6.
- [112] Park B, Kim J, Kang D, Jeong C, Kim KS, Kim JU, et al. Dramatically enhanced mechanosensitivity and signal-to-noise ratio of nanoscale crack-based sensors: effect of crack depth. *Adv Mater* 2016;28:8130–7.
- [113] Lee CJ, Park KH, Han CJ, Oh MS, You B, Kim YS, et al. Crack-induced Ag nanowire networks for transparent, stretchable, and highly sensitive strain sensors. *Sci Rep* 2017;7:7959.
- [114] Zhou J, Yu H, Xu X, Han F, Lubineau G. Ultrasensitive, stretchable strain sensors based on fragmented carbon nanotube papers. *ACS Appl Mater Interfaces* 2017;9:4835–42.
- [115] Liao X, Zhang Z, Kang Z, Gao F, Liao Q, Zhang Y. Ultrasensitive and stretchable resistive strain sensors designed for wearable electronics. *Mater Horiz* 2017;4:502–10.
- [116] Valentine AD, Busbee TA, Boley JW, Raney JR, Chortos A, Kotikian A, et al. Hybrid 3D printing of soft electronics. *Adv Mater* 2017;29:1703817.
- [117] Moriche R, Sánchez M, Jiménez-Suárez A, Prolongo SG, Ureña A. Strain monitoring mechanisms of sensors based on the addition of graphene nanoplatelets into an epoxy matrix. *Compos Sci Technol* 2016;123:65–70.
- [118] Li S, Park JG, Wang S, Liang R, Zhang C, Wang B. Working mechanisms of strain sensors utilizing aligned carbon nanotube network and aerosol jet printed electrodes. *Carbon* 2014;73:303–9.
- [119] Deng H, Lin L, Ji M, Zhang S, Yang M, Fu Q. Progress on the morphological control of conductive network in conductive polymer composites and the use as electroactive multifunctional materials. *Prog Polym Sci* 2014;39:627–55.
- [120] Ma L-F, Bao R-Y, Dou R, Zheng S-D, Liu Z-Y, Zhang R-Y, et al. Conductive thermoplastic vulcanizates (TPVs) based on polypropylene (PP)/ethylene-propylene-diene rubber (EPDM) blend: from strain sensor to highly stretchable conductor. *Compos Sci Technol* 2016;128:176–84.
- [121] Ke K, Potschke P, Gao S, Voit B. An ionic liquid as interface linker for tuning piezoresistive sensitivity and toughness in poly(vinylidene fluoride)/carbon nanotube composites. *ACS Appl Mater Interfaces* 2017;9:5437–46.
- [122] Kang D, Shin Y-E, Jo HJ, Ko H, Shin HS. Mechanical properties of poly(dopamine)-coated graphene oxide and poly(vinyl alcohol) composite fibers coated with reduced graphene oxide and their use for piezoresistive sensing. *Part Part Syst Charact* 2017;34:1600382.
- [123] Kim M, Kim DJ, Ha D, Kim T. Cracking-assisted fabrication of nanoscale patterns for micro/nanotechnological applications. *Nanoscale* 2016;8:9461–79.
- [124] Wang DY, Tao LQ, Liu Y, Zhang TY, Pang Y, Wang Q, et al. High performance flexible strain sensor based on self-locked overlapping graphene sheets. *Nanoscale* 2016;8:20090–5.
- [125] Liu Z, Wang X, Qi D, Xu C, Yu J, Liu Y, et al. High-adhesion stretchable electrodes based on nanopile interlocking. *Adv Mater* 2017;29:1603382.
- [126] Harada S, Honda W, Arie T, Akita S, Takei K. Fully printed, highly sensitive multifunctional artificial electronic whisker arrays integrated with strain and temperature sensors. *ACS Nano* 2014;8:3921–7.
- [127] Hua Q, Liu H, Zhao J, Peng D, Yang X, Gu L, et al. Bioinspired electronic whisker arrays by pencil-drawn paper for adaptive tactile sensing. *Adv Electron Mater* 2016;2:1600093.
- [128] Wang C, Li X, Gao E, Jian M, Xia K, Wang Q, et al. Carbonized silk fabric for ultrastretchable, highly sensitive, and wearable strain sensors. *Adv Mater* 2016;28:6640–8.
- [129] Wang X, Gu Y, Xiong Z, Cui Z, Zhang T. Silk-molded flexible, ultrasensitive, and highly stable electronic skin for monitoring human physiological signals. *Adv Mater* 2014;26:1336–42.
- [130] Zhang M, Wang C, Wang H, Jian M, Hao X, Zhang Y. Carbonized cotton fabric for high-performance wearable strain sensors. *Adv Funct Mater* 2017;27:1604795.
- [131] Li J, Zhao S, Zeng X, Huang W, Gong Z, Zhang G, et al. Highly stretchable and sensitive strain sensor based on facilely prepared three-dimensional graphene foam composite. *ACS Appl Mater Interfaces* 2016;8:18954–61.
- [132] Nakamura A, Hamanishi T, Kawakami S, Takeda M. A piezo-resistive graphene strain sensor with a hollow cylindrical geometry. *Mater Sci Eng B* 2017;219:20–7.
- [133] Liu X, Tang C, Du X, Xiong S, Xi S, Liu Y, et al. A highly sensitive graphene woven fabric strain sensor for wearable wireless musical instruments. *Mater Horizons* 2017;4:477–86.
- [134] Gong S, Cheng W. One-dimensional nanomaterials for soft electronics. *Adv Electron Mater* 2017;3:1600314.
- [135] Jang H, Park YJ, Chen X, Das T, Kim MS, Ahn JH. Graphene-based flexible and stretchable electronics. *Adv Mater* 2016;28:4184–202.
- [136] Suzuki K, Yataka K, Okumiya Y, Sakakibara S, Sako K, Mimura H, et al. Rapid-response, widely stretchable sensor of aligned MWCNT/elastomer composites for human motion detection. *ACS Sensors* 2016;1:817–25.
- [137] Trung TQ, Lee NE. Recent progress on stretchable electronic devices with intrinsically stretchable components. *Adv Mater* 2017;29.
- [138] Kim J, Lee M, Shim HJ, Ghaffari R, Cho HR, Son D, et al. Stretchable silicon nanoribbon electronics for skin prosthesis. *Nat Commun* 2014;5:5747.
- [139] Guo FM, Cui X, Wang KL, Wei JQ. Stretchable and compressible strain sensors based on carbon nanotube meshes. *Nanoscale* 2016;8:19352–8.
- [140] Li X, Zhang R, Yu W, Wang K, Wei J, Wu D, et al. Stretchable and highly sensitive graphene-on-polymer strain sensors. *Sci Rep* 2012;2:870.
- [141] Kim K, Kim J, Hyun BG, Ji S, Kim SY, Kim S, et al. Stretchable and transparent electrodes based on in-plane structures. *Nanoscale* 2015;7:14577–94.
- [142] Tao L-Q, Wang D-Y, Tian H, Ju Z-Y, Liu Y, Pang Y, et al. Self-adapted and tunable graphene strain sensors for detecting both subtle and large human motions. *Nanoscale* 2017;9:8266–73.
- [143] Li X, Hua T, Xu B. Electromechanical properties of a yarn strain sensor with graphene-sheath/polyurethane-core. *Carbon* 2017;118:686–98.
- [144] Tadakaluru S, Thongsuwan W, Singjai P. Stretchable and flexible high-strain sensors made using carbon nanotubes and graphite films on natural rubber. *Sensors (Basel)* 2014;14:868–76.
- [145] Selvan NT, Eshwaran SB, Das A, Stöckelhuber KW, Wießner S, Pötschke P, et al. Piezoresistive natural rubber-multiwall carbon nanotube nanocomposite for sensor applications. *Sensors Actuators A Phys* 2016;239:102–13.
- [146] Lee J, Lim M, Yoon J, Kim MS, Choi B, Kim DM, et al. Transparent, flexible strain sensor based on a solution-processed carbon nanotube network. *ACS Appl Mater Interfaces* 2017;9:26279–85.
- [147] Giffney T, Benjanin E, Kurian AS, Travas-Sejdic J, Aw K. Highly stretchable printed strain sensors using multi-walled carbon nanotube/silicone rubber composites. *Sensors Actuators A Phys* 2017;259:44–9.
- [148] Sanli A, Müller C, Kanoun O, Elibol C, Wagner MFX. Piezoresistive characterization of multi-walled carbon nanotube-epoxy based flexible strain sensitive films by impedance spectroscopy. *Compos Sci Technol* 2016;122:18–26.
- [149] Kim JY, Ji S, Jung S, Ryu B-H, Kim H-S, Lee SS, et al. 3D printable composite dough for stretchable, ultrasensitive and body-patchable strain sensors. *Nanoscale* 2017;9:11035–46.
- [150] Yang T, Jiang X, Zhong Y, Zhao X, Lin S, Li J, et al. A wearable and highly sensitive graphene strain sensor for precise home-based pulse wave monitoring. *ACS Sensors* 2017;2:967–74.
- [151] Wang R, Jiang N, Su J, Yin Q, Zhang Y, Liu Z, et al. A bi-sheath fiber sensor for giant tensile and torsional displacements. *Adv Funct Mater* 2017;27:1702134.
- [152] Benchirouf A, Muller C, Kanoun O. Electromechanical behavior of chemically reduced graphene oxide and multi-walled carbon nanotube hybrid material. *Nanoscale Res Lett* 2016;11:4.

- [153] Xin Y, Zhou J, Xu X, Lubineau G. Laser-engraved carbon nanotube paper for instilling high sensitivity, high stretchability, and high linearity in strain sensors. *Nanoscale* 2017;9:10897–905.
- [154] Lozano-Pérez C, Cauch-Rodríguez JV, Avilés F. Influence of rigid segment and carbon nanotube concentration on the cyclic piezoresistive and hysteretic behavior of multiwall carbon nanotube/segmented polyurethane composites. *Compos Sci Technol* 2016;128:25–32.
- [155] Liu H, Li Y, Dai K, Zheng G, Liu C, Shen C, et al. Electrically conductive thermoplastic elastomer nanocomposites at ultralow graphene loading levels for strain sensor applications. *J Mater Chem C* 2016;4:157–66.
- [156] Hu C, Li Z, Wang Y, Gao J, Dai K, Zheng G, et al. Comparative assessment of the strain-sensing behaviors of polylactic acid nanocomposites: reduced graphene oxide or carbon nanotubes. *J Mater Chem C* 2017;5:2318–28.
- [157] Yamada T, Hayamizu Y, Yamamoto Y, Yomogida Y, Izadi-Najafabadi A, Futaba DN, et al. A stretchable carbon nanotube strain sensor for human-motion detection. *Nat Nanotechnol* 2011;6:296–301.
- [158] Song H, Zhang J, Chen D, Wang K, Niu S, Han Z, et al. Superfast and high-sensitivity printable strain sensors with bioinspired micron-scale cracks. *Nanoscale* 2017;9:1166–73.
- [159] Foroughi J, Spinks GM, Aziz S, Mirabedini A, Jeiranikhameneh A, Wallace GG, et al. Knitted carbon-nanotube-sheath/spandex-core elastomeric yarns for artificial muscles and strain sensing. *ACS Nano* 2016;10:9129–35.
- [160] Zhang M, Wang C, Wang Q, Jian M, Zhang Y. Sheath-core graphite/silk fiber made by dry-meyer-rod-coating for wearable strain sensors. *ACS Appl Mater Interfaces* 2016;8:20894–9.
- [161] Wang Z, Huang Y, Sun J, Huang Y, Hu H, Jiang R, et al. Polyurethane/cotton/carbon nanotubes core-spun yarn as high reliability stretchable strain sensor for human motion detection. *ACS Appl Mater Interfaces* 2016;8:24837–43.
- [162] Flandin L, Chang A, Nazareno S, Hiltner A, Baer E. Effect of strain on the properties of an ethylene-octene elastomer with conductive carbon fillers. *J Appl Polym Sci* 2000;76:894–905.
- [163] Zhao J, Dai K, Liu C, Zheng G, Wang B, Liu C, et al. A comparison between strain sensing behaviors of carbon black/polypropylene and carbon nanotubes/polypropylene electrically conductive composites. *Compos Part A Appl Sci Manuf* 2013;48:129–36.
- [164] Liu S, Lin Y, Wei Y, Chen S, Zhu J, Liu L. A high performance self-healing strain sensor with synergetic networks of poly (ϵ -caprolactone) microspheres, graphene and silver nanowires. *Compos Sci Technol* 2017;146:110–8.
- [165] Wang Y, Wang Y, Yang Y. Graphene-polymer nanocomposite-based redox-induced electricity for flexible self-powered strain sensors. *Adv Energy Mater* 2018;8:1800961.
- [166] Zhang SL, Lai Y-C, He X, Liu R, Zi Y, Wang ZL. Auxetic foam-based contact-mode triboelectric nanogenerator with highly sensitive self-powered strain sensing capabilities to monitor human body movement. *Adv Funct Mater* 2017:1606695.
- [167] Dai Z, Weng C, Liu L, Hou Y, Zhao X, Kuang J, et al. Multifunctional polymer-based graphene foams with buckled structure and negative Poisson's ratio. *Sci Rep* 2016;6:32989.
- [168] Jeon JY, Ha TJ. Waterproof electronic-bandage with tunable sensitivity for wearable strain sensors. *ACS Appl Mater Interfaces* 2016;8:2866–71.
- [169] Postolache OA, Mukhopadhyay SC, Jayasundera KP, Swain AK. Sensors for everyday life: healthcare settings. Springer; 2016.
- [170] Mun S, Zhai L, Min S-K, Yun Y, Kim J. Flexible and transparent strain sensor made with silver nanowire-coated cellulose. *J Intell Mater Syst Struct* 2016;27:1011–8.
- [171] Li Q, Ullah Z, Li W, Guo Y, Xu J, Wang R, et al. Wide-range strain sensors based on highly transparent and supremely stretchable graphene/Ag-nanowires hybrid structures. *Small* 2016;12:5058–65.
- [172] Chun S, Choi Y, Park W. All-graphene strain sensor on soft substrate. *Carbon* 2017;116:753–9.
- [173] Trung TQ, Lee N-E. Materials and devices for transparent stretchable electronics. *J Mater Chem C* 2017;5:2202–22.
- [174] Liu Y, Chakrabartty S, Gkinosatis DS, Mohanty AK, Lajnef N. Multi-walled carbon nanotubes/poly (l-lactide) nanocomposite strain sensor for biomechanical implants. *Biomedical circuits and systems conference (IEEE BIOCAS 2007)*. IEEE; 2007. p. 119–22.
- [175] Zymelka D, Yamashita T, Takamatsu S, Itoh T, Kobayashi T. Thin-film flexible sensor for omnidirectional strain measurements. *Sensors Actuators A Phys* 2017;263:391–7.
- [176] Bae S-H, Lee Y, Sharma BK, Lee H-J, Kim J-H, Ahn J-H. Graphene-based transparent strain sensor. *Carbon* 2013;51:236–42.
- [177] Kong J-H, Jang N-S, Kim S-H, Kim J-M. Simple and rapid micropatterning of conductive carbon composites and its application to elastic strain sensors. *Carbon* 2014;77:199–207.
- [178] Ho DH, Sun Q, Kim SY, Han JT, Kim Do H, Cho JH. Stretchable and multimodal all graphene electronic skin. *Adv Mater* 2016;28:2601–8.
- [179] Liao X, Liao Q, Zhang Z, Yan X, Liang Q, Wang Q, et al. A highly stretchable ZnO@fiber-based multifunctional nanosensor for strain/temperature/UV detection. *Adv Funct Mater* 2016;26:3074–81.
- [180] Yamamoto Y, Harada S, Yamamoto D, Honda W, Arie T, Akita S, et al. Printed multifunctional flexible device with an integrated motion sensor for health care monitoring. *Sci Adv* 2016;2:e1601473.
- [181] Dinh T, Phan H-P, Qamar A, Nguyen N-T, Dao DV. Flexible and multifunctional electronics fabricated by a solvent-free and user-friendly method. *RSC Adv* 2016;6:77267–74.
- [182] Segev-Bar M, Konvalina G, Haick H. High-resolution unipixelated smart patches with antiparallel thickness gradients of nanoparticles. *Adv Mater* 2015;27:1779–84.
- [183] Mata A, Fleischman AJ, Roy S. Characterization of polydimethylsiloxane (PDMS) properties for biomedical micro/nanosystems. *Biomed Microdevices* 2005;7:281–93.
- [184] Zeng Z, Liu M, Xu H, Liu W, Liao Y, Jin H, et al. A coatable, light-weight, fast-response nanocomposite sensor for their situ acquisition of dynamic elastic disturbance: from structural vibration to ultrasonic waves. *Smart Mater Struct* 2016;25:065005.
- [185] Li Y, Samad YA, Taha T, Cai G, Fu S-Y, Liao K. Highly flexible strain sensor from tissue paper for wearable electronics. *ACS Sustain Chem Eng* 2016;4:4288–95.
- [186] Liu H, Qing H, Li Z, Han YL, Lin M, Yang H, et al. Paper: A promising material for human-friendly functional wearable electronics. *Mater Sci Eng R Reports* 2017;112:1–22.
- [187] Tallman TN, Gungor S, Wang KW, Bakis CE. Tactile imaging and distributed strain sensing in highly flexible carbon nanofiber/polyurethane nanocomposites. *Carbon* 2015;95:485–93.
- [188] Ren J, Du X, Zhang W, Xu M. From wheat bran derived carbonaceous materials to a highly stretchable and durable strain sensor. *RSC Adv* 2017;7:22619–26.
- [189] Lee Y, Kim J, Joo H, Raj MS, Ghaffari R, Kim DH. Wearable sensing systems with mechanically soft assemblies of nanoscale materials. *Adv Mater Technol* 2017;2:1700053.
- [190] Wang X, Tao X, So RCH, Shu L, Yang B, Li Y. Monitoring elbow isometric contraction by novel wearable fabric sensing device. *Smart Mater Struct* 2016;25:125022.
- [191] Wang F, Liu S, Shu L, Tao X-M. Low-dimensional carbon based sensors and sensing network for wearable health and environmental monitoring. *Carbon* 2017;121:353–67.
- [192] Wu X, Lu C, Han Y, Zhou Z, Yuan G, Zhang X. Cellulose nanowhisker modulated 3D hierarchical conductive structure of carbon black/natural rubber nanocomposites for liquid and strain sensing application. *Compos Sci Technol* 2016;124:44–51.
- [193] Costa P, Silvia C, Viana JC, Lanceros Mendez S. Extruded thermoplastic elastomers styrene-butadiene-styrene/carbon nanotubes composites for strain sensor applications. *Compos B Eng* 2014;57:242–9.
- [194] Costa P, Silva J, Anson-Casaos A, Martinez MT, Abad MJ, Viana J, et al. Effect of carbon nanotube type and functionalization on the electrical, thermal, mechanical and electromechanical properties of carbon nanotube/styrene-butadiene-styrene composites for large strain sensor applications. *Compos B Eng* 2014;61:136–46.
- [195] Deng H, Ji M, Yan D, Fu S, Duan L, Zhang M, et al. Towards tunable resistivity-strain behavior through construction of oriented and selectively distributed conductive networks in conductive polymer composites. *J Mater Chem A* 2014;2:10048–58.

- [196] Yu Y, Luo Y, Guo A, Yan L, Wu Y, Jiang K, et al. Flexible and transparent strain sensors based on super-aligned carbon nanotube films. *Nanoscale* 2017;9:6716–23.
- [197] Li Y, Shang Y, He X, Peng Q, Du S, Shi E, et al. Overtwisted, resolvable carbon nanotube yarn entanglement as strain sensors and rotational actuators. *ACS Nano* 2013;7:8128–35.
- [198] Park SJ, Kim J, Chu M, Khine M. Highly flexible wrinkled carbon nanotube thin film strain sensor to monitor human movement. *Adv Mater Technol* 2016;1:1600053.
- [199] Gorrasi G, Milone C, Piperopoulos E, Pantani R. Preparation, processing and analysis of physical properties of calcium ferrite-CNTs/PET nano-composite. *Compos Part B Eng* 2015;81:44–52.
- [200] Gorrasi G, D'Ambrosio S, Patimo G, Pantani R. Hybrid clay-carbon nanotube/PET composites: preparation, processing, and analysis of physical properties. *J Appl Polym Sci* 2014;131:40441.
- [201] Sarno M, Tamburrano A, Arurault L, Fontorbes S, Pantani R, Datas L, et al. Electrical conductivity of carbon nanotubes grown inside a mesoporous anodic aluminium oxide membrane. *Carbon* 2013;55:10–22.
- [202] Shi J, Li X, Cheng H, Liu Z, Zhao L, Yang T, et al. Graphene reinforced carbon nanotube networks for wearable strain sensors. *Adv Funct Mater* 2016;26:2078–84.
- [203] Cho D, Park J, Kim J, Kim T, Kim J, Park I, et al. Three-dimensional continuous conductive nanostructure for highly sensitive and stretchable strain sensor. *ACS Appl Mater Interfaces* 2017;9:17369–78.
- [204] Li X, Yang T, Yang Y, Zhu J, Li L, Alam FE, et al. Large-area ultrathin graphene films by single-step marangoni self-assembly for highly sensitive strain sensing application. *Adv Funct Mater* 2016;26:1322–9.
- [205] Park Y, Shim J, Jeong S, Yi GR, Chae H, Bae JW, et al. Microtopography-guided conductive patterns of liquid-driven graphene nanoplatelet networks for stretchable and skin-conformal sensor array. *Adv Mater* 2017;29:1606453.
- [206] Shim J, Yun JM, Yun T, Kim P, Lee KE, Lee WJ, et al. Two-minute assembly of pristine large-area graphene based films. *Nano Lett* 2014;14:1388–93.
- [207] Velarde MG, Zeytounian RK. Interfacial phenomena and the Marangoni effect. Springer; 2002. p. 283.
- [208] Yang T, Wang W, Zhang H, Li X, Shi J, He Y, et al. Tactile sensing system based on arrays of graphene woven microfabrics: electromechanical behavior and electronic skin application. *ACS Nano* 2015;9:10867–75.
- [209] Yan C, Wang J, Kang W, Cui M, Wang X, Foo CY, et al. Highly stretchable piezoresistive graphene-nanocellulose nanopaper for strain sensors. *Adv Mater* 2014;26:2022–7.
- [210] Papageorgiou DG, Kinloch IA, Young RJ. Mechanical properties of graphene and graphene-based nanocomposites. *Prog Mater Sci* 2017;90:75–127.
- [211] Sangeetha NM, Decorde N, Viallet B, Viau G, Ressler L. Nanoparticle-based strain gauges fabricated by convective self assembly: strain sensitivity and hysteresis with respect to nanoparticle sizes. *J Phys Chem C* 2013;117:1935–40.
- [212] Rogers JA, Someya T, Huang Y. Materials and mechanics for stretchable electronics. *Science* 2010;327:1603–7.
- [213] Gao HL, Xu L, Long F, Pan Z, Du YX, Lu Y, et al. Macroscopic free-standing hierarchical 3D architectures assembled from silver nanowires by ice templating. *Angew Chem Int Ed Engl* 2014;53:4561–6.
- [214] Ge J, Sun L, Zhang FR, Zhang Y, Shi LA, Zhao HY, et al. A stretchable electronic fabric artificial skin with pressure-, lateral strain-, and flexion-sensitive properties. *Adv Mater* 2016;28:722–8.
- [215] Zhu Y, Hu Y, Zhu P, Zhao T, Liang X, Sun R, et al. Enhanced oxidation resistance and electrical conductivity copper nanowires-graphene hybrid films for flexible strain sensors. *New J Chem* 2017;41:4950–8.
- [216] Tian M, Wang Y, Qu L, Zhu S, Han G, Zhang X, et al. Electromechanical deformation sensors based on polyurethane/polyaniline electrospinning nanofibrous mats. *Synth Met* 2016;219:11–9.
- [217] Hong J, Pan Z, ZheWang YM, Chen J, Zhang Y. A large-strain weft-knitted sensor fabricated by conductive UHMWPE/PANI composite yarns. *Sensors Actuators A Phys* 2016;238:307–16.
- [218] Razak SIA, Azmi NS, Fakhruddin K, Dahli FN, Wahab IF, Sharif NFA, et al. Coating of conducting polymers on natural cellulosic fibers. *Conducting polymers. InTech*; 2016.
- [219] González C, Vilatela JJ, Molina-Aldareguía JM, Lopes CS, Llorca J. Structural composites for multifunctional applications: current challenges and future trends. *Prog Mater Sci* 2017;89:194–251.
- [220] Chossat J-B, Tao Y, Duchaine V, Park Y-L. Wearable soft artificial skin for hand motion detection with embedded microfluidic strain sensing. *Robot Autom (ICRA), 2015 IEEE Int Conf. IEEE*; 2015. p. 2568–73.
- [221] Yoon SG, Koo HJ, Chang ST. Highly stretchable and transparent microfluidic strain sensors for monitoring human body motions. *ACS Appl Mater Interfaces* 2015;7:27562–70.
- [222] Takei K, Yu Z, Zheng M, Ota H, Takahashi T, Javey A. Highly sensitive electronic whiskers based on patterned carbon nanotube and silver nanoparticle composite films. *Proc Natl Acad Sci* 2014;111:1703–7.
- [223] Ning N, Wang S, Zhang L, Lu Y, Tian M, Chan T. Synchronously tailoring strain sensitivity and electrical stability of silicone elastomer composites by the synergistic effect of a dual conductive network. *Polymers (Basel)* 2016;8:100.
- [224] Zhang Y, Anderson N, Bland S, Nutt S, Jursich G, Joshi S. All-printed strain sensors: building blocks of the aircraft structural health monitoring system. *Sensors Actuators A Phys* 2017;253:165–72.
- [225] Bautista-Quijano JR, Pötschke P, Brünig H, Heinrich G. Strain sensing, electrical and mechanical properties of polycarbonate/multiwall carbon nanotube monofilament fibers fabricated by melt spinning. *Polymer* 2016;82:181–9.
- [226] Gonçalves BF, Oliveira J, Costa P, Correia V, Martins P, Botelho G, et al. Development of water-based printable piezoresistive sensors for large strain applications. *Compos Part B Eng* 2017;112:344–52.
- [227] Truby RL, Lewis JA. Printing soft matter in three dimensions. *Nature* 2016;540:371–8.
- [228] Xu K, Lu Y, Honda S, Arie T, Akita S. Takei KJJoMCC. Highly stable kirigami-structured stretchable strain sensors for perdurable wearable electronics. *J Mater Chem C* 2019;7:9609–17.
- [229] Lee HB, Bae CW, Duy le T, Sohn IY, Kim DI, Song YJ, et al. Mogul-patterned elastomeric substrate for stretchable electronics. *Adv Mater* 2016;28:3069–77.
- [230] Wei H, Li K, Liu WG, Meng H, Zhang PX, Yan CY. 3D Printing of free-standing stretchable electrodes with tunable structure and stretchability. *Adv Eng Mater* 2017;19:1700341.
- [231] Drotlef DM, Amjadi M, Yunusa M, Sitti M. Bioinspired composite microfibers for skin adhesion and signal amplification of wearable sensors. *Adv Mater* 2017;29:1701753.
- [232] Christ JF, Hohimer CJ, Aliheidari N, Ameli A, Mo C, Pötschke P. 3D printing of highly elastic strain sensors using polyurethane/multiwall carbon nanotube composites. Sensors and smart structures technologies for civil, mechanical, and aerospace systems 2017. 10168. SPIE-Int Soc Optical Engineering; 2017. p. 101680E.
- [233] Chen K, Gao W, Emaminejad S, Kiriya D, Ota H, Nyein HY, et al. Printed carbon nanotube electronics and sensor systems. *Adv Mater* 2016;28:4397–414.
- [234] Joshi S, Bland S, DeMott R, Anderson N, Jursich G. Challenges and the state of the technology for printed sensor arrays for structural monitoring. Industrial and commercial applications of smart structures technologies. 10166. SPIE-Int Soc Optical Engineering; 2017. p. 101660H.
- [235] Michelis F, Bodelot L, Bonnassieux Y, Lebental B. Highly reproducible, hysteresis-free, flexible strain sensors by inkjet printing of carbon nanotubes. *Carbon* 2015;95:1020–6.
- [236] Bessonov A, Kirikova M, Haque S, Gartsev I, Bailey MJA. Highly reproducible printable graphite strain gauges for flexible devices. *Sensors Actuators A Phys* 2014;206:75–80.
- [237] Kim JH, Chang WS, Kim D, Yang JR, Han JT, Lee GW, et al. 3D printing of reduced graphene oxide nanowires. *Adv Mater* 2015;27:157–61.
- [238] Borghetti M, Serpelloni M, Sardini E, Pandini S. Mechanical behavior of strain sensors based on PEDOT:PSS and silver nanoparticles inks deposited on polymer substrate by inkjet printing. *Sensors Actuators A Phys* 2016;243:71–80.

- [239] Li CY, Liao YC. Adhesive stretchable printed conductive thin film patterns on PDMS surface with an atmospheric plasma treatment. *ACS Appl Mater Interfaces* 2016;8:11868–74.
- [240] Bessonov AA, Kirikova MN. Flexible and printable sensors. *Nanotechnologies Russ* 2015;10:165–80.
- [241] Acquah SF, Leonhardt BE, Nowotarski MS, Magi JM, Chambliss KA, Venzel TE, et al. Carbon nanotubes and graphene as additives in 3D printing. *Carbon nanotubes-current progress of their polymer composites*. InTech; 2016.
- [242] Zymelka D, Yamashita T, Takamatsu S, Itoh T, Kobayashi T. Printed strain sensor with temperature compensation and its evaluation with an example of applications in structural health monitoring. *Jpn J Appl Phys* 2017;56:05EC02.
- [243] Zymelka D, Togashi K, Yamashita T, Kobayashi T, Takamatsu S, Itoh T. Printed carbon-based sensors array for measuring 2D dynamic strain distribution and application in structural health monitoring. *SENSORS*, 2016 IEEE. IEEE; 2016. p. 1–3.
- [244] Ni Y, Ji R, Long K, Bu T, Chen K, Zhuang S. A review of 3D-printed sensors. *Appl Spectrosc Rev* 2017;52:623–52.
- [245] Gao M, Li L, Song Y. Inkjet printing wearable electronic devices. *J Mater Chem C* 2017;5:2971–93.
- [246] Lee G-Y, Kim M-S, Yoon H-S, Yang J, Ihn J-B, Ahn S-H. Direct printing of strain sensors via nanoparticle printer for the applications to composite structural health monitoring. *Procedia CIRP* 2017;66:238–42.
- [247] Lee J, Faruk Emon MO, Vatani M, Choi J-W. Effect of degree of crosslinking and polymerization of 3D printable polymer/ionic liquid composites on performance of stretchable piezoresistive sensors. *Smart Mater Struct* 2017;26:035043.
- [248] Christ JF, Aliheidari N, Ameli A, Pötschke P. 3D printed highly elastic strain sensors of multiwalled carbon nanotube/thermoplastic polyurethane nanocomposites. *Mater Des* 2017;131:394–401.
- [249] Yamamoto D, Nakata S, Kanao K, Arie T, Akita S, Takei K. A planar, multisensing wearable health monitoring device integrated with acceleration, temperature, and electrocardiogram sensors. *Adv Mater Technol* 2017;2:1700057.
- [250] Sundaram S, Jiang Z, Sitthi-Amorn P, Kim DS, Baldo MA, Matusik W. 3D-printed autonomous sensory composites. *Adv Mater Technol* 2017;2:1600257.
- [251] Zeng W, Shu L, Li Q, Chen S, Wang F, Tao XM. Fiber-based wearable electronics: a review of materials, fabrication, devices, and applications. *Adv Mater* 2014;26:5310–36.
- [252] Ren J, Wang C, Zhang X, Carey T, Chen K, Yin Y, et al. Environmentally-friendly conductive cotton fabric as flexible strain sensor based on hot press reduced graphene oxide. *Carbon* 2017;111:622–30.
- [253] Shi G, Zhao Z, Pai J-H, Lee I, Zhang L, Stevenson C, et al. Highly sensitive, wearable, durable strain sensors and stretchable conductors using graphene/silicon rubber composites. *Adv Funct Mater* 2016;26:7614–25.
- [254] Cai G, Yang M, Xu Z, Liu J, Tang B, Wang X. Flexible and wearable strain sensing fabrics. *Chem Eng J* 2017;325:396–403.
- [255] Salvado R, Lopes C, Szojda L, Araujo P, Gorski M, Velez FJ, et al. Carbon fiber epoxy composites for both strengthening and health monitoring of structures. *Sensors (Basel)* 2015;15:10753–70.
- [256] Park JM, Kwon DJ, Shin PS, Kim JH, DeVries KL. New sensing method of dispersion and damage detection of carbon fiber/polypropylene-polyamide composites via two-dimensional electrical resistance mapping. 10165. *SPIE-INT Soc Optical Engineering*; 2017. p. 101650M.
- [257] Park J-M, Kwon D-J, Wang Z-J, DeVries KL. Review of self-sensing of damage and interfacial evaluation using electrical resistance measurements in nano/micro carbon materials-reinforced composites. *Adv Compos Mater* 2014;24:197–219.
- [258] Kwon D-J, Shin P-S, Kim J-H, Wang Z-J, DeVries KL, Park J-M. Detection of damage in cylindrical parts of carbon fiber/epoxy composites using electrical resistance (ER) measurements. *Compos Part B Eng* 2016;99:528–32.
- [259] Bowland CC, Wang Y, Naskar AK. Development of nanoparticle embedded sizing for enhanced structural health monitoring of carbon fiber composites. 10169. *Int Soc Optics Photonics*; 2017. p. 1–7.
- [260] Zhang H, Liu Y, Huang M, Bilotti E, Peijs T. Dissolvable thermoplastic interleaves for carbon nanotube localization in carbon/epoxy laminates with integrated damage sensing capabilities. *Struct Health Monit* 2018;17:59–66.
- [261] Vertuccio L, Vittoria V, Guadagno L, De Santis F. Strain and damage monitoring in carbon-nanotube-based composite under cyclic strain. *Compos Part A Appl Sci Manuf* 2015;71:9–16.
- [262] Gallo GJ, Thostenson ET. Electrical characterization and modeling of carbon nanotube and carbon fiber self-sensing composites for enhanced sensing of microcracks. *Mater Today Commun* 2015;3:17–26.
- [263] de Jesus Ku-Herrera J, La Saponara V, Avilés F. Selective damage sensing in multiscale hierarchical composites by tailoring the location of carbon nanotubes. *J Intell Mater Syst Struct* 2018;29:553–62.
- [264] Karger-Kocsis J, Mahmood H, Pegoretti A. Recent advances in fiber/matrix interphase engineering for polymer composites. *Prog Mater Sci* 2015;73:1–43.
- [265] Zhang H, Kuwata M, Bilotti E, Peijs T. Integrated damage sensing in fibre-reinforced composites with extremely low carbon nanotube loadings. *J Nanomater* 2015;2015:1–7.
- [266] Hao B, Ma Q, Yang S, Mäder E, Ma P-C. Comparative study on monitoring structural damage in fiber-reinforced polymers using glass fibers with carbon nanotubes and graphene coating. *Compos Sci Technol* 2016;129:38–45.
- [267] He D, Fan B, Zhao H, Lu X, Yang M, Liu Y, et al. Design of electrically conductive structural composites by modulating aligned CVD-grown carbon nanotube length on glass fibers. *ACS Appl Mater Interfaces* 2017;9:2948–58.
- [268] Wiegand N, Mäder E. Multifunctional interphases: percolation behavior, interphase modification, and electro-mechanical response of carbon nanotubes in glass fiber polypropylene composites. *Adv Eng Mater* 2016;18:376–84.
- [269] Moriche R, Jiménez-Suárez A, Sánchez M, Prolongo SG, Ureña A. Graphene nanoplatelets coated glass fibre fabrics as strain sensors. *Compos Sci Technol* 2017;146:59–64.
- [270] Gallo GJ, Thostenson ET. Spatial damage detection in electrically anisotropic fiber-reinforced composites using carbon nanotube networks. *Compos Struct* 2016;141:14–23.
- [271] Segev-Bar M, Haick H. Flexible sensors based on nanoparticles. *ACS Nano* 2013;7:8366–78.
- [272] Seshadri DR, Drummond C, Craker J, Rowbottom JR, Voos JE. Wearable devices for sports: new integrated technologies allow coaches, physicians, and trainers to better understand the physical demands of athletes in real time. *IEEE Pulse* 2017;8:38–43.
- [273] Wang Q, Markopoulos P, Yu B, Chen W, Timmermans A. Interactive wearable systems for upper body rehabilitation: a systematic review. *J Neuroeng Rehabil* 2017;14:20.
- [274] Van Langenhove L. Smart textiles: past, present, and future. *Handbook of Smart Textiles*. Springer; 2015. p. 1035–58.
- [275] van Langenhove L. *Advances in smart medical textiles: treatments and health monitoring*. Woodhead Publishing; 2015.
- [276] Choi S, Lee H, Ghaffari R, Hyeon T, Kim DH. Recent advances in flexible and stretchable bio-electronic devices integrated with nanomaterials. *Adv Mater* 2016;28:4203–18.
- [277] Yildiz SK, Mutlu R, Alici G. Fabrication and characterisation of highly stretchable elastomeric strain sensors for prosthetic hand applications. *Sensors Actuators A Phys* 2016;247:514–21.
- [278] Chortos A, Liu J, Bao Z. Pursuing prosthetic electronic skin. *Nat Mater* 2016;15:937–50.
- [279] McEvoy MA, Correll N. Materials that couple sensing, actuation, computation, and communication. *Science* 2015;347:1261689.
- [280] Yeo JC, Yap HK, Xi W, Wang Z, Yeow C-H, Lim CT. Flexible and stretchable strain sensing actuator for wearable soft robotic applications. *Adv Mater Technol* 2016;1:1600018.
- [281] Cheng Y, Wang R, Sun J, Gao L. A Stretchable and highly sensitive graphene-based fiber for sensing tensile strain, bending, and torsion. *Adv Mater* 2015;27:7365–71.
- [282] Yeo JC, Liu Z, Zhang Z-Q, Zhang P, Wang Z, Lim CT. Wearable mechanotransduced tactile sensor for haptic perception. *Adv Mater Technol* 2017;2:1700006.
- [283] Borghetti M, Serpelloni M, Sardini E, Casas O. Multisensor system for analyzing the thigh movement during walking. *IEEE Sens J* 2017;17:4953–61.
- [284] Bartlett MD, Markvicka EJ, Majidi C. Rapid fabrication of soft, multilayered electronics for wearable biomonitoring. *Adv Funct Mater* 2016;26:8496–504.
- [285] Kumar S, Gupta TK, Varadarajan KM. Strong stretchable and ultrasensitive MWCNT/TPU nanocomposites for piezoresistive strain sensing. *Compos Part B Eng*

- 2019;177:107285.
- [286] Costa P, Oliveira J, Horta-Romaris L, Abad M-J, Moreira JA, Zapiran I, et al. Piezoresistive polymer blends for electromechanical sensor applications. *Compos Sci Technol* 2018;168:353–62.
- [287] Lee S, Shin S, Lee S, Seo J, Lee J, Son S, et al. Ag nanowire reinforced highly stretchable conductive fibers for wearable electronics. *Adv Funct Mater* 2015;25:3114–21.
- [288] Xu M, Qi J, Li F, Zhang Y. Highly stretchable strain sensors with reduced graphene oxide sensing liquids for wearable electronics. *Nanoscale* 2018;10:5264–71.
- [289] Lu L, Zhou Y, Pan J, Chen T, Hu Y, Zheng G, et al. Design of helically double-leveled gaps for stretchable fiber strain sensor with ultralow detection limit, broad sensing range, and high repeatability. *ACS Appl Mater Interfaces* 2019;11:4345–52.
- [290] Jiang Y, Liu Z, Matsuhisa N, Qi D, Leow WR, Yang H, et al. Auxetic mechanical metamaterials to enhance sensitivity of stretchable strain sensors. *Adv Mater* 2018;30:1706589.
- [291] Heo Y, Hwang Y, Jung HS, Choa SH, Ko HC. Secondary sensitivity control of silver-nanowire-based resistive-type strain sensors by geometric modulation of the elastomer substrate. *Small* 2017;13:1700070.
- [292] Liu Z, Qi D, Hu G, Wang H, Jiang Y, Chen G, et al. Surface strain redistribution on structured microfibers to enhance sensitivity of fiber-shaped stretchable strain sensors. *Adv Mater* 2018;30:1704229.
- [293] Duan L, D'hooge DR, Spoerk M, Cornillie P, Cardon L. Facile and low-cost route for sensitive stretchable sensors by controlling kinetic and thermodynamic conductive network regulating strategies. *ACS Appl Mater Interfaces* 2018;10:22678–91.
- [294] Duan L, Spoerk M, Wieme T, Cornillie P, Xia H, Zhang J, et al. Designing formulation variables for extrusion-based manufacturing of carbon black conductive polymer composites for piezoresistive sensing. *Compos Sci Technol* 2019;171:78–85.
- [295] Sang Z, Guo H, Ke K, Manas-Zloczower I. Effect of solvent on segregated network morphology in elastomer composites for tunable piezoresistivity. *Macromol Mater Eng* 2019;304:1900278.

Lingyan Duan received her B.S. degree in polymer science and engineering and her M.S. degree in materials science from Sichuan University, Chengdu, China, in 2012 and 2015, respectively. She received her Ph.D. degree in materials engineering from Ghent University, Gent, Belgium, in November 2019 under the supervision of Prof. Dagmar R. D'hooge and Prof. Ludwig Cardon. Her present research interests mainly focus on flexible/wearable sensors.

Dagmar R. D'hooge (1983) is Associate Professor at Ghent University and focuses in his research on the design of polymerization and polymer processing techniques. The functional material design and related process intensification is performed up to the industrial scale, using advanced in-house developed multi-scale modeling tools in combination with experimental validation. He is currently coauthor of 90 peer-reviewed full length research articles, 2 book chapters, 1 book, and 1 patent. He was a postdoctoral researcher in the Matyjaszewski Polymer Group (Carnegie Mellon University, USA) in 2011 and in the Macromolecular Architectures Research Team (Karlsruhe Institute of Technology, Germany) in 2013. He is also a former postdoctoral researcher of the Fund for Scientific Research Flanders. Since 2017 he is a visiting Associate Professor at Stanford University.

Prof. Ludwig Cardon is the head of the Centre for Polymer and Material Technologies CPMT. His field of expertise is Characterization and 3D Processing of Polymers and Composites, including technologies such as injection moulding, (co-)extrusion, and 3D Printing. He is and has been project leader of numerous national and EU projects related to polymer processing, product design and 3D printing. He currently works on design/construction/processing of extrusion-based additive manufacturing for a wide range of virgin and filled polymers and composites.